Integrated Sequence Stratigraphic and Geochemical Resource Characterization of the Lower Mancos Shale, Uinta Basin, Utah

by Donna S. Anderson and Nicholas B. Harris

Open-File Report 483
Utah Geological Survey
a division of
Utah Department of Natural Resources
2006

Integrated Sequence Stratigraphic and Geochemical Resource Characterization of the Lower Mancos Shale, Uinta Basin, Utah

Donna S. Anderson
Department of Geology and Geological Engineering
Colorado School of Mines
Golden, Colorado 80401
303-273-3284
dsanders@mines.edu

Nicholas B. Harris
Department of Geology and Geological Engineering
Colorado School of Mines
Golden, Colorado 80401
303-273-3854
nbharris@mines.edu

This open-file report was prepared by the authors under contract to the Utah Department of Natural Resources, Utah Geological Survey. The report has not undergone the full UGS review process, and may not necessarily conform to UGS technical, editorial, or policy standards. Therefore, it may be premature for an individual or group to take action based on its content.

The Utah Department of Natural Resources, Utah Geological Survey, makes no warranty, expressed or implied, regarding the suitability of this product for a particular use. The Utah Department of Natural Resources, Utah Geological Survey, shall not be liable under any circumstances for any direct, indirect, special, incidental, or consequential damages with respect to claims by users of this product.

Open-File Report 483
Utah Geological Survey
a division of
Utah Department of Natural Resources
2006

Table of Contents

Executive Summary 6
Introduction 7
  Scope 7
  Acknowledgments 7
Westwater Outcrop Study 8
  Methods 8
    Field Description 8
    Outcrop Gamma Ray 9
    Laboratory Analyses 9
  Lithofacies 9
    Carbonate Lithofacies 10
    Mudrock Lithofacies 10
    Sandstone Lithofacies 11
  Biostratigraphic and Sequence Stratigraphic Interpretation 12
    Ammonite biostratigraphy 12
    Sequence Stratigraphy 13
  Summary 15
Larsen State-1 Well Cuttings 15
  Analyses of Cuttings Samples 16
    Rock-Eval / TOC 16
    Vitrinite Reflectance / Visual Kerogen Analysis 17
    Carbon / Oxygen Isotopes 18
    Mineralogy / Clay Mineralogy 18
    Palynological Analyses 19
    Sample Group from 473-804 ft MD 19
    Sample Group from 804-880 ft MD 20
    Sample Group from 900-1087 ft MD 20
    Sample Group from 1100-1105 ft MD 20
  Summary 21
Correlation 21
  Correlation of Westwater Measured Section to Larsen State-1 and other Subsurface Wells 22
  Database Tops 23
    Hiatus at the Base of the Lower Mancos (MTUNC) 23
    Condensed Sections 23
    Sequence boundaries 24
  Summary 24
Isochore Maps 24
  Dakota Silt 25
  Organic-rich interval FJ1 to FJLM 25
  Organic-rich shale at base of the F3 to FJL Interval 26
  Thin Sandstone at base of F2 to F3 Interval 26
  Summary 26
Burial History and Basin Modeling 27
Summary and Conclusions 28
References Cited 31

List of Tables

Table 1. Lithofacies for Westwater section.

Table 2. Westwater measured section intervals and facies successions.

Table 3. Results of Rock-Eval and Total Organic Carbon Analysis.

Table 4. Results of vitrinite reflectance / visual kerogen analysis of Mancos Shale samples, Larsen State-1 well.

Table 5. Results of carbon and oxygen isotopic analysis of Mancos Shale samples, Larsen State-1 well.

Table 6. Qualitative results of X-Ray diffraction analysis of Mancos Shale samples, Larsen State-1 well.

List of Figures

Figure 1. Study area.

Figure 2. Stratigraphic columns.

Figure 3. Westwater measured section.

Figure 4. Westwater field area.

Figure 5. Carbonate, bentonite and shale facies.

Figure 6. Sandstone facies.

Figure 7. Carter Larsen State-1 cuttings description.

Figure 8. Log stretch in Larsen State-1.

Figure 9. Larsen State-1: Total Organic Carbon data.

Figure 10. Larsen State-1: Hydrogen Index (from Rock-Eval analysis) data.

Figure 11. Larsen State-1: Cross-plot of hydrogen index and oxygen index (from Rock-Eval analysis) data.

Figure 12. Larsen State-1: Cross-plot of Total organic carbon and hydrogen index data.

Figure 13. Larsen State-1: Vitrinite reflectance profile in Mancos Formation.

Figure 14. Larsen State-1: Oxygen isotopic composition of carbonate in Mancos Formation. Values are in per mil notation, with respect to PDB standard.

Figure 15. Larsen State-1: Carbon isotopic composition of carbonate in Mancos Formation. Values are in per mil notation, with respect to PDB standard.

Figure 16. Larsen State-1: Cross-plot of carbon and oxygen isotopic compositions of carbonate from the Mancos formation.

Figure 17. Larsen State-1: Calcite content of lower Mancos shale samples; qualitative determination from X-ray diffraction analysis.

Figure 18. Larsen State-1: Dolomite content of lower Mancos shale samples; qualitative determination from X-ray diffraction analysis.

Figure 19. Larsen State-1: Kaolinite content of lower Mancos shale samples; qualitative determination from X-ray diffraction analysis.

Figure 20. Larsen State-1: Orthoclase content of lower Mancos shale samples; qualitative determination from X-ray diffraction analysis.

Figure 21. Larsen State-1: Plagioclase content of lower Mancos shale samples; qualitative determination from X-ray diffraction analysis.

Figure 22. Larsen State-1: Pyrite content of lower Mancos shale samples; qualitative determination from X-ray diffraction analysis.

Figure 23. Correlation of Westwater section to Larsen State-1 and adjacent wells.

Figure 24. A) BENT_38 to MTUNC isochore map. B) Coon Spring Sandstone Bed net sandstone Isochore map.

Figure 25. Southwest to northeast stratigraphic cross section of Dakota Silt interval (BENT_38 to MTUNC), showing net sandstone of Coon Spring Sandstone Bed (yellow bars).

Figure 26. A) Isochore map of organic-rich interval FJ1 to FJLM. B) Isochore map of condensed section directly above the FJLM marker.

Figure 27. Northwest to southeast stratigraphic cross section of the FJ1 to FJLM and adjacent intervals, showing "net shale" of the condensed sections immediately overlying the FJLM (orange bars) and the FJL (pink bars) markers.

Figure 28. A) Isochore map of F3 to FJL interval. B) Isochore map of condensed interval directly above the FJL marker.

Figure 29. A) Isochore map of F2 to F3 interval. B) Isochore map of widespread, thin sandstone interval above F3 marker.

Figure 30. Burial history model for the Mancos and underlying section in the Westwater Canyon area.

Figure 31. Calculated thermal maturity profile for the Mancos and underlying section in the Westwater Canyon / Larsen State-1 area.

Figure 32. Oil generation and expulsion model for the Mancos Formation in the Westwater Canyon / Larsen State-1 area.

Figure 33. Gas generation and expulsion for the Mancos Formation in the Westwater Canyon / Larsen State-1 area.

List of Appendices

Appendix A. Westwater measured section, raw log sheets, raw GPS data, shapefiles.

Appendix B. Outcrop gamma ray raw data.

Appendix C. Palynological Report for Larsen State-1 cuttings by Dr. G. Waanders.

Appendix D. Digital tops and "pay zones" database (on CD).

Executive Summary

This study characterizes the lateral and vertical distributions of shale facies within a sequence stratigraphic framework and integrates depositional facies with geochemical analysis as a basis for assessing the shale-gas potential of the lower Mancos Shale in the south-central Uinta basin. It also evaluates the potential for sandstone reservoirs that may be interbedded with lower Mancos mudrocks.

Eleven condensed sections form a correlation framework for a 650-ft thick interval of the lower Mancos Shale in the southern and southeastern Uinta basin study area. Two of these condensed sections, represented by the FJLM and FJL tops, are important for source-rock characterization and are widely distributed across the study area. A major switch from a southwest to a northwest source during deposition of the Ferron-Frontier (FE_SB_1 to F2 markers) may have created an embayment along the western margin of the Cretaceous Seaway that led to more anoxic conditions favorable to the accumulation of more organic-rich condensed sections. Three sequence boundaries within the lower Mancos are associated with sandstone units that are probably the fully marine equivalents of deltaic lowstands and are postulated to have turbidite depositional origins, based on facies relationships and map distribution patterns. These are potential reservoirs and include the Coon Springs Sandstone Bed, between the CS_SB_1 and BENT_38 markers, and a thin sandstone interval at the base of the F2-F3 isochore.

Organic geochemical analysis of cuttings in the Larsen State-1 well indicates that two main intervals have source-rock potential: the highest quality and thickest is present between 820 to 890 ft MD in sequence 4 and the other is more limited in thickness, from 787 to 789 ft MD above the FJL marker in or above sequence 5. The organic rich section in sequence 4 has the highest TOC, hydrogen index values, and tracks the Type II kerogen trend, indicating the presence of good-quality oil-prone organic matter. Vitrinite reflectance, TAI, and Tmax values from the Larsen State-1 cuttings place the lower Mancos section at the Larsen well in the upper part of the oil window.

Basin modeling shows that the Mancos section in the Westwater Canyon area is in the oil window and has generated significant amounts of oil and some gas at the base of Mancos interval. With deeper burial conditions north of the Westwater area, in the subsurface of the south-central Uinta basin, higher maturity levels would be expected, yielding conditions favorable for dominantly gas generation within the organic-rich intervals of the lower Mancos Shale. Sandstone intervals in close juxtaposition to the organic-rich shales also could be charged under the right burial/maturity conditions.

Deliverables for this study include: 1) a digital correlation database consisting of 13 tops representing a sequence stratigraphic framework for 216 wells; 2) description of a 93m- thick measured section near Westwater, Utah that contains 79m (259 ft) of lower Mancos Shale and 14m of underlying Dakota Sandstone; 3) an outcrop gamma-ray log and associated LAS file for the measured section; 4) cuttings description combined with palynological and geochemical analyses for 73 samples over a 632-ft (192m) interval in the Carter Larsen State-1 well near Westwater, Utah; and 5) this final report.

Introduction

This study develops an outcrop-based and subsurface wireline log sequence-stratigraphic framework integrated with organic geochemistry for the lower Mancos Shale of the southern and eastern Uinta basin of Utah (Figure 1). The framework forms a basis for the characterization of the distribution and geochemistry of mudrocks, and distribution of intervening reservoir sandstones. It provides a step for assessing the lower Mancos Shale in the Uinta basin as an unconventional shale-gas resource play.

Scope

The study integrates organic geochemistry, x-ray diffraction (XRD) and carbon-oxygen isotope analyses of lower Mancos cuttings in the Carter Larsen State-1 well near Westwater, Utah with stratigraphic analysis of a measured section, also near Westwater. It correlates the same stratigraphic interval in 216 wells across the southern and eastern Uinta basin of Utah (Figure 1), encompassing an area of approximately 7000 square miles. Although the Mancos Shale crops out along the entire length of the Book Cliffs, the highly weathered outcrops generally are not conducive to detailed outcrop study with exceptions such as that near Westwater (Figure 1). The outcrop data correlate directly to several wells within an 10-mile radius, including the Carter Larsen State-1 well, that in turn correlate regionally to 40 wells that penetrate the Mancos outcrop belt south of the Book Cliffs, 177 wells north of the Book Cliffs, and three outcrop sections (Figure 1) studied by Molenaar and Cobban (1991): two on the eastern San Rafael Swell and one northeast of Rangely, Colorado, near the Utah-Colorado state border.

The lower Mancos Shale includes several members (Willis et al. 1996) mapped at Westwater, Utah (Figure 2). From oldest to youngest they are: Tununk Shale, with the Coon Springs Sandstone Bed, Ferron Sandstone (correlated to the Juana Lopez Member by Molenaar and Cobban, 1991), and the lower Blue Gate Shale (Figure 2). Molenaar and Cobban (1991) defined the same gross interval as the Tununk Member containing the Coon Springs Sandstone Bed, the Juana Lopez Member, and the "main body of the lower Mancos Shale," similar to the units of Willis et al. (1996), but differing in the naming of the Ferron Sandstone versus the Juana Lopez members. The corresponding sequences interpreted by Gardner (1995) on the east side of the San Rafael Swell include, from oldest to youngest, the Mytiloides, Woollgari, Hyatti, and Juana Lopez sequences, largely named for the ammonite biozones characterizing each sequence, and corresponding to the units defined by Molenaar and Cobban (1991). A series of stratigraphic "tops" that correspond to these various units were correlated in well logs that penetrate the lower Mancos interval across the study area.

Acknowledgments

This study was funded by the Utah Geological Survey. Ryan Fisher and Larry Anderson provided invaluable field assistance in October 2005 and March 2006, respectively. Software used in the study was provided by GeoPlus Petra™, Neuralog™, ESRI (ArcView™ and ArcMap™) and Platte River Associates (BasinMod 1D). Raster well-log images were provided by the Utah Division of Oil, Gas and Mining website and A2D. John D. Humphrey at Colorado School of Mines (CSM) measured carbon and oxygen isotopes. Rick Wendlandt at CSM performed XRD analyses. Humble Geochemical performed RockEval™ pyrolysis, vitrinite reflectance and visual kerogen analyses. Gerald Waanders, Consulting Palynologist, analyzed

pollen biostratigraphy from well cuttings, funded separately by the Utah Geological Survey. William A. Cobban, USGS emeritus, identified the ammonite at the Westwater outcrop. Conversations with Michael Lewan, Mark Kirschbaum, Richard Grauch, and Bridget Ball, all of the USGS in Denver, Colorado, Gerald Waanders, Consulting Palynologist, and Mary McPherson of McPherson Geologic Consulting in Vernal, Utah, were invaluable.

Westwater Outcrop Study

The 93-m thick "Westwater section" (Figures 1, 3, Appendix A) was measured near Westwater, Utah in section 33, Township 19E, Range 24S (Figure 4), where the Mancos Shale crops out in a series of low hills along the gently west-dipping (< 3°) flank of the Harley Dome and Bitter Creek anticlines of Willis et al. (1996). The measured section covers 14m of Dakota Sandstone and 79m of Mancos Shale, including the Tununk Shale Member, Coon Springs Sandstone Bed, and Ferron Sandstone Member of the Mancos Shale as mapped by Willis et al. (1996) in the Agate Quadrangle. Rocks in the measured section have been grouped into 13 facies (Table 1) to facilitate stratigraphic interpretation. To expedite discussion, facies within the measured section have been grouped into units (Table 2) that correspond to facies successions.

Methods

The Westwater section was measured with a Jacob staff and Brunton compass. The section was measured up the steepest hill slopes to minimize the effects of colluvial cover. Even so, most of the lower part of the section (19 to 63.5m, Figure 4; units 4 though 20, Table 2) was hand-trenched with a pick and shovel to create the freshest possible exposures. Trenches ranged from 30cm to nearly 1m deep and were backfilled at the end of the field session. The traverse for the measured section (Figure 4) was surveyed with hand-held global positioning satellite (GPS) equipment, accurate to a ±3m radius around survey points. The traverse line was supplemented with GPS-based mapping of laterally continuous sandstone horizons (Figure 4) tied to depths on the measured section.

Field Description

Lithology was described continuously and logged at a scale of 1:40, or 1 inch = 1m (Appendix A). Observations, aided by 10X and 20X hand lenses, were made at a scale sufficient to record thin (< 2mm thick) altered volcanic ash (white to yellow-orange bentonite) beds. For field description, the proportion of clay versus silt was determined by mechanical means, either by mastication, trenching resistance, or by a simple plasticity (thread) test similar to that used in soil mechanics. All samples were tested for reaction with dilute (5%) HCl and recorded qualitatively using a scale of 0 to 100% for reactivity. Where reliably observable, degree of bioturbation also was qualitatively determined using a scale of 0 to 100%. However, the quality of the exposure, even in the trenches, did not permit many such observations, so bioturbation across those intervals was recorded as "not observable." In addition to description, digital photos of the outcrop were taken every meter and bag samples were collected at every meter from 14 to 74m. Bag samples were discontinued above 74m after realizing that extensive weathering of the shale precluded reliable geochemical analyses (discussed below).

Outcrop Gamma Ray

Scintillometer measurements (total counts per second, cps) were made at 1m intervals, supplemented by smaller intervals to capture lithologic changes not within the regular sampling interval. The procedure for scintillometer data collection consisted of placing the receiver directly in contact with a fresh outcrop surface at a sampling location and recording five readings in a field book. Data analysis for each sample location consisted of discarding the high and low readings and averaging the middle three readings to yield one data point at any given depth on the measured section. However, the radius of investigation of the scintillometer receiver is generally about 0.3 m, so any given reading represents an average of the surrounding lithology response. The resulting gamma ray-depth data (Appendix B) were imported into GeoPlus Petra™ and converted to an LAS file (also in Appendix B).

The gamma ray data were collected over two separate field sessions: the first in October 2005; the second in March 2006. In the second session, gamma ray data were re-measured to overlap with those of the October field session. The second dataset showed a >20 counts per second (cps) difference with the first set: the values in interbedded thin sandstone/shale sections were dominantly 40 and 50 cps, more typical of "clean sand." The origin of the discrepancy could be due to not digging deep enough, although the colluvial cover was thin to nil, and/or a change in the composition of the shale. The scintillometer was re-checked in the field and yielded consistent results. For the purposes of this study and the correlation of the outcrop gamma ray to surrounding well logs, the scintillometer curve from 76 to 93m is considered questionable and is not shown on the logs, although the raw data are included in Appendix B.

Laboratory Analyses

Between 14 and 74m in the Westwater section, bag samples were collected at 1m intervals, supplemented by smaller intervals as determined in the field. At least 200 grams of rock were collected for each sample and bagged onsite, recording the location on the measured section, and the depth of the sample below ground surface. Initially slated for complete organic geochemical analysis, a test set of samples revealed significant oxidation and, hence, unreliable measurements. Thus, no further laboratory analyses were conducted on the outcrop samples. Instead, cuttings from the correlative interval in a nearby well (Larsen State-1) were acquired, as discussed below. The depth of weathering in the Mancos Shale terrain of eastern Utah and westernmost Colorado is on the order of 6m (20 feet; Dr. Richard Grauch, USGS, oral communication). The large depth of weathering makes outcrop geochemical analyses questionable.

Lithofacies

Thirteen lithofacies (Table 1) were observed in the lowermost Mancos Shale: two carbonate, five mudrock (including bentonite), and six sandstone facies. Facies observed in the underlying Dakota Sandstone are not reported here, because they are beyond the scope of the study.

Facies designations were based on a combination of grain size, lithology (clastic vs. carbonate), color (Rock-Color Chart Committee, 1984), degree of burrowing, sedimentary structures, macrofossil content, and bed-weathering style, or fissility (especially for mudrocks). Most of these observations, except color and bed-weathering style, reflect original depositional processes.

Rock color is a function of diagenesis (including weathering), plus a component of initial deposition, as discussed below in the section on organic facies. Bed-weathering style in mudrocks, such as fissility, is likely a function of surficial weathering (Macquaker and Adams, 2003). While it may or may not relate to original depositional process, fissility is a repeatable observation in the field, hence its popular use by field geologists. Each lithofacies also has a characteristic range of outcrop gamma ray values, and the mudrocks show a range of geochemical parameters, discussed separately.

Long an under-appreciated portion of the clastic record, the science of working with mudrocks has advanced since the publication of "Sedimentology of Shale" (Potter et al., 1980). Macquaker and Adams (2003) suggest that classifying mudrocks using relative proportions of clay, silt, and sand is more meaningful than using field-based terms like mudstone and shale, which have variable definitions. However, reproducible field determination of mudrock components without the aid of thin sections or sieve analysis is very difficult. This study employs consistent field terms for mudrock facies, as described below.

Carbonate Lithofacies

Carbonate facies (Table 1) are rare within the Westwater study interval. A distinctive facies of thin-bedded structureless to laminated micritic limestone (Figure 5A) occurs at the base of the section at 20.5m in unit 5 (Table 2) and consists of a discontinuous, 10cm-thick horizon. The origin of this facies was not studied. The other carbonate facies consists of cone-in-cone limestone that is present as isolated concretions, encased in dark-gray shale (Figure 5B) and concentrated in mappable horizons at several positions within the measured section: units 19, 22, 33 and 35. Internally, concretions commonly show septarian structure. The more continuous and mappable concretionary horizons are present at either the bases or the tops of more sandstone-rich facies successions. In some cases, the centers of the concretions contain calcareous macrofossils. The gamma ray response of both carbonate facies is typically low, in the range of 62 cps.

Mudrock Lithofacies

The Westwater study interval contains several mudrock facies (Table 1), including bentonite, three types of shale, and two types of siltstone. Distinguishing features include the qualitative proportion of clay versus silt, rock color, and weathering characteristics. Bentonite (Figure 5C) is composed of highly plastic clay that is present in beds ranging from 2mm to 2cm thick. Originating as volcanic ash, bentonite beds commonly are clustered at certain intervals in the Westwater measured section, units 7, 12, 16, and 18, and are common within unit 34 (Table 2). Bentonite shows a range of very high gamma ray responses, 101-143 (average 121) cps, which exceeds those of other mudrock facies.

Three types of shale are differentiated in the field: calcareous and non-calcareous dark to medium gray shale and silty shale. Calcareous shale reacts vigorously in 5% HCl and is present only at the base of the section, between 18.2 and 20.5m in units 4 and 5 (Table 2). Noncalcareous dark-gray shale (Figure 5D) is common within the measured section, both as discrete intervals (units 6, 8, 12, 17, 19, 23, 25, 27, 29, 31, 34, 36) and interbedded with thin-bedded sandstone facies (such as units 28, 30, 32, 35, and 37). Silty shale has observable silt grains within it, based

on 20X hand-lens observations. Extremely poor exposures, even in trenches, make depositional interpretation difficult. Lack of macroscopic burrowing suggests low-oxygen conditions during deposition. Common abundance of fish scales confirms a marine environment. Differentiating deposition by suspension versus traction/turbidity processes is difficult without thin section analysis. Gamma ray responses of shale facies range from 74 to 128 cps (average 94).

The two types of siltstone facies typically are more yellow than the gray, shale facies, partly reflecting a larger grain size and lower proportion of clay minerals. They also display a blocky weathering pattern, commonly with observable macroscopic burrowing. As with shale facies, depositional processes are difficult to prove without thin section analysis. Significant intervals of siltstone facies (Table 2, Figure 3) are present at specific positions within the measured section: they are usually associated with coarsening upward trends culminating in sandstone facies. The increase in silt and very-fine sand sizes relative to the shale facies suggests a significant component of traction/turbidity transport. The more common presence of macroscopic burrowing suggests more oxygenated conditions during and/or shortly after deposition. Siltstone facies typically show a gamma ray response ranging from 72-91 cps (average 78), which is lower than that for shale.

Sandstone Lithofacies

Differences in grain size and sedimentary structures yield five sandstone facies (Table 1) across the lower Mancos study interval in the Westwater section. In general, the type of sedimentary structure corresponds to a particular grain-size range. Unidirectional and combined-flow ripple-laminated sandstone facies are mostly very-fine sand size, whereas swaley and hummocky cross-stratified facies are in the fine-sand size range. Degree of burrowing, however, does not correspond to sand grain-size: the bioturbated sandstone facies consists of fine sand, whereas the very fine, rippled and wavy laminated sandstone facies is sparsely burrowed, mostly on bedding surfaces. These differences reflect differing sediment delivery mechanisms residence times on the seafloor after deposition, and stratigraphic position. The gamma ray response of all sandstone facies ranges from 51 to 80 cps and averages 67 cps, which is similar to the response of carbonate facies.

The most dominant of the five sandstone facies is rippled and wavy laminated sandstone (Figure 6A, B) that is present at distinct positions in the measured section (Table 2). This facies occurs in thin beds, ranging from single ripple formsets about 2cm thick to amalgamated beds up to 20cm thick. The thinnest beds are commonly present in the uppermost part of the measured section between 76 and 93m (units 28, 30, 32, 35, 37). In these intervals, thin beds are arranged in quasi-rhythmic vertical clusters of 0.5 to 1m thick, separated by > 1m of dark gray fissile shale (Figure 6F). Sedimentary structures, bedding style, sparse low-diversity burrowing, rare small body fossils (ammonoids and pelecypods), common tool marks on bed bases and rhythmic clustering of beds strongly suggest storm-influenced turbidity currents as the sediment delivery process. These types of deposits are becoming more commonly recognized in the Cretaceous Interior Seaway (e.g. Edwards et al., 2005). At lower stratigraphic positions in the measured section, such as between 64 and 74m (units 20, 22, 26), amalgamated bedsets (< 20cm thick) of rippled and wavy-laminated facies form discontinuous lenses across the outcrop face, suggesting that they fill low-relief scours.

Swaley and hummocky sandstone facies (Figure 6C) are only observed at one position in the measured section that is laterally equivalent to 42.4 to 42.6m (unit 14, Table 2 and the 43-m scour surface mapped in Figure 4) on the line of transect. These facies occur as lenses <5m wide that fill scours <1m deep. The horizon of scouring is mappable within the local outcrop, and is most commonly represented by an amalgamated bedset of rippled to wavy-laminated facies that ranges from 10 to 20cm thick.

Macrofossil-rich sandstone is also a unique facies in the Westwater section. It constitutes a 1m-thick amalgamated bed (unit 10) that is mapped as the "Coon Spring Sandstone bed" by Willis et al. (1996). It consists of a nearly thoroughly bioturbated fine sandstone, with rare evidence of traction scour (Figure 6D) and ripple lamination at the base of the bed. The amalgamated bioturbated sandstone unit commonly weathers into distinct concretions up to 1m in diameter. The concretions are highly calcareous, likely due to the large amount of calcite-rich fossil shells within, such as the mid-Turonian index ammonite *Collignoniceras woollgari* (Molenaar and Cobban, 1991; Willis et al, 1996). The relatively sharp base and unique, high degree of macrofossil bioturbation in this unit suggest a marine bioherm origin on a relatively firm substrate. Subtle sedimentary structures suggest a traction/turbidity flow origin for the sand fraction.

Silty very-fine to fine sandstone (between 33.0 and 36.5 m, unit 13, Table 2) is another unique facies that directly overlies the 1-m thick Coon Spring Sandstone bed. Bedding in this interval is completely obscured by weathering. Under hand lens magnification (10X), the sandstone is poorly sorted, subangular and highly glauconitic. Poor sorting and grain angularity suggest little winnowing by turbulent traction flow, yet are compatible with mixed loads that would accompany more laminar turbidity flows.

The last sandstone facies, granule sandstone, consists of thin (< 1cm) discontinuous lenses of poorly sorted sand to granule grain sizes, including shark teeth and broken fossil shells. These facies are present at 68.9m (unit 22) and at 82.5m (unit 33).

Biostratigraphic and Sequence Stratigraphic Interpretation

Published accounts of biostratigraphic data for the lower Mancos Shale in the Westwater area are rare to non-existent, based on an examination of the literature and confirmed in discussions with Mark Kirschbaum (USGS, Denver, Colorado). This study reports an occurrence of an important index-ammonite, *Prionocyclus hyatti*, in the Westwater section and a palynological analysis of cuttings in the Larsen State-1 well (discussed below).

Ammonite biostratigraphy

Two ammonites, *Collignoniceras woollgari* and *Prionocyclus hyatti* (Figure 6E), provide temporal placement of the measured section within the ammonite zonation for the Western Interior Cretaceous seaway (e.g. Molenaar and Cobban, 1991). *C. woollgari* is the index fossil for the lower-middle Turonian Stage (zone 19 of Molenaar and Cobban, 1991) and is present in unit 10 of the Westwater section. It is also reported in the Coon Spring Sandstone Bed along the eastern San Rafael Swell at Woodside Dome and I-70 (Molenaar and Cobban, 1991). *P. hyatti* is the index fossil for the upper-middle Turonian Stage (zone 21 of Molenaar and Cobban, 1991) and occurs within unit 28 of the Westwater section. *P. hyatti* has been reported from marine

tongues of the Ferron Sandstone Member near Farnham Dome on the northeastern flank of the Rafael Swell by Molenaar and Cobban (1991, their cross section A-A'), and it directly underlies their "Juana Lopez Member," which in turn contains the index ammonite *Prionocyclus macombi*. A major flooding surface separates the zone of *P. hyatti* from the overlying Juana Lopez Member of Cobban and Molenaar (1991). This flooding zone (Figure 2) is also highly organic-rich (Gardner 1995, p. 256) and reflects a major transgression of the Western Interior Seaway.

Sequence Stratigraphy

The following discussion develops a sequence stratigraphic interpretation based on observations in the Westwater measured section tied to the existing literature. The discussion is referenced to the lithologic units (Table 2) in the measured section, and it integrates the ammonite biostratigraphy with existing stratigraphic interpretations. Reference also is made to regionally correlated tops in the database and shown on Figure 3.

The base of the Mancos Shale in the Westwater section is placed at the color change from yellow-gray silty shale (unit 3) to overlying gray shale (unit 4), at 18.2m (Figure 3).The contact, designated MTUNC (mid-Turonian unconformity), represents a hiatus in which three ammonite zones representing the lower Turonian Stage are missing (Figure 2; Cobban and Molenaar, 1991). Calcareous gray shale of unit 4 directly overlies the unconformity. A discontinuous 10cm-thick bed of micritic limestone (unit 5) interbedded with calcareous shale forms the top of the calcareous zone in the measured section. The top of the calcareous shale intervals (units 4 and 5) is approximated by BENT_27 (Figure 5A). The upward change to non-calcareous shale may reflect major changes in paleo-seawater chemistry, modulated by outcrop weathering affects. In terms of regional stratigraphic position and correlation, units 4 and 5 may reflect an increase in carbonate typical of the late part of the Greenhorn Cyclothem (e.g. Franczyk et al., 1992). This study suggests (Figure 3) that the calcareous units reflect at least one major condensed interval, associated with regional downlap onto the MTUNC unconformity (discussed below).

Within the Westwater section, four distinct sandstone-rich intervals are evidence of significant increases in sand supplied to the marine environment from coeval deltas to the west: units 9-11, 13-15, 20-22, and in alternating intervals with shale in units 26 through 37, culminating in unit 35 near the top of the measured section (Table 2, Figure 3). Within a sequence stratigraphic context, the bases of each of these sand-rich units represents a seaward-step in progradation, which is the signature of a sequence boundary and overlying lowstand systems tract. This study postulates, however, that the deposits studied in the Westwater section were never subjected to subaerial exposure and represent the marine equivalents of deltaic lowstands.

The oldest of these sand-rich intervals corresponds to the regionally widespread Coon Spring Sandstone Bed (units 9-11) recognized previously by Willis et al. (1996) and Molenaar and Cobban (1991) from the eastern San Rafael Swell and points eastward. The base of unit 10, however, is gradational over < 0.3m (1 ft) with underlying unit 9, suggesting that the sequence boundary is non-erosive. In addition, a thin wavy bedded-rippled sandstone bed in underlying unit 9 indicates an initial increase in sand influx that culminates in units 10 and 11. Unit 11 (exposed only by trenching) is an upward fining interval postulated as a marine turbidity current deposit due to abundant glauconite and fish scales and a composition of very poorly sorted silt and subangular very-fine to fine sand grains. A bentonite-rich interval, unit 12, represented by

BENT_38, is interpreted as a high-order condensed interval separating the Coon Spring Sandstone Bed from the next overlying sand-rich interval consisting of units 13-15.

Units 13-15 show a coarsening then fining upward increase from burrowed glauconitic siltstone (unit 13) to rippled and wavy-laminated to lenticular swaley sandstone (unit 14), overlain by about 1m of burrowed siltstone and sandstone in unit 15 (Figure 3). A locally mappable scour surface at 42.4m in the Westwater section underlies unit 14. The lenticular sandstone facies that fill shallow scours along the surface are wave-influenced, indicating a decrease in the average depth of storm wave base. The scour surface is interpreted as a high-order sequence boundary, CW_SB_2 (Figure 3). Units 13-15 are overlain by unit 16, which is a thick bentonitic shale section that represents a major condensed section (BENT_46). Unit 16 is overlain by > 17m (50 ft) of shale represented by units 17, 18 and 19, the latter two of which are separated by a regionally mappable bentonite horizon, BENT_57. This thick interval of shale (unit 16) may, in turn, contain several high-order sequences because it contains sand-rich intervals locally to the north, as interpreted in the regional correlation framework discussed below. The top of unit 15 represents the top of the Tununk Shale of Willis et al. (1996).

The third sand-rich interval in the measured section consists of units 20-22 and represents the lithostratigraphic base of the Ferron Sandstone of Willis et al. (1996). Unit 20 consists of discontinuous thin benches of rippled and wavy-laminated sandstone facies interbedded with siltstone. Discontinuous granule-sandstone lags are common within and above this unit. Unit 20 represents a significant increase in sand supply, likely due to increased seaward progradation of coeval deltas to the west. The base of unit 20, at 63.7m in the Westwater section, represents the "Ferron sequence boundary" of Willis et al. (1996) and is mapped as FE_SB_1 in this study. The top of the sand-rich interval, which culminates in unit 22 at 68.9 m, is characterized by discontinuous granule lags, cone-in-cone limestone concretions, and wave-influenced sandstone facies (combined-flow rippled sandstone), and possibly represents the last phases of relative sea-level rise (transgressive systems tract) in a submarine setting.

A thick shale interval (units 23-25) overlies unit 22, the top of which is mapped as the FJLM marker in this study. The dark-gray to black shale zone of unit 25 is interpreted as a condensed section, and it correlates to condensed section at the base of the Juana Lopez Member of Molenaar and Cobban (1991) and the top of Gardner's (1995) Hyatti sequence. Molenaar and Cobban also interpret this interval as a major regional flooding zone. This interpretation is supported by regional correlation and organic geochemical results from the analysis of cuttings in the Larsen State-1 well, each discussed below.

The youngest sand-rich interval in the Westwater section overlies unit 25 and consists of clusters of thin, rippled to wavy laminated sandstone interbedded with fissile black shale (units 26, 28, 30, 32, 35, and 37) alternating with fissile black shale (units 27, 29, 31, 33-34, and 36). The alternations reflect a high-frequency cyclicity of sand versus mud-dominated sediment-input to the Western Interior Seaway. Two discrete sandy successions are present within the gross interval between 72.7 and 93m (units 26 to 37). The lower one from 72.7 to 79.8m (units 27 to 32) is capped by a thin zone (unit 33) of granule-sandstone lags and limestone concretions. The top of unit 33 is represented by the FJ1 marker at 82.5m in the section (Figure 3). The overlying shale (unit 34) consists of bentonitic, fissile, dark gray shale (Figure 5D). Macroscopically, it is identical to the dark-gray shale interbedded with the sandstone in the underlying sandy units. The

sand-rich interval from 87 to 93m is also characterized by clusters of thin beds of rippled, wavy laminated sandstone beds alternating with fissile dark-gray shale (e.g. Figure 6F). Within this interval, rare small inoceramid and ammonoid casts and molds are found on the tops of the thin sandstone beds, indicating a marine environment. Trace fossils (ichnofauna) are of very low diversity and consist largely of isolated *Planolites*. The two sand-rich successions are interpreted as parts of two separate sequences (Figure 3). The uppermost sequence culminates above the top of the measured section.

Summary

In summary, the stratigraphic succession present in the Westwater measured section consists of at least five sequences, described by the following pairs of tops: MTUNC to CW_SB_1 (sequence 1); CW_SB_1 to CW_SB_2 (sequence 2); CW_SB_2 to FE_SB_1 (sequence 3); FE_SB_1 to approximately FJ1 (sequence 4); and FJ1 to the top of the section (partially measured sequence 5). Each sequence contains a condensed interval of shale that provides the framework for regional correlation. As indicated by the geochemical analyses, discussed below, the shale intervals also are variable in terms of organic richness. Isochore maps of selected portions of these sequences show temporal facies changes that help predict the distributions of potential sandstone reservoirs juxtaposed with shale reservoir/source rocks.

Larsen State-1 Well Cuttings

The Carter Oil, Larsen State-1 well (API 4301915317) is located in section 2, T20S-R24E in the Seiber Nose field (Chidsey et al., 2004) and is 6.5 km (about 4 miles) west-southwest of the Westwater measured section (Figure 1). Drilled in 1955, the well spudded in the lower-middle Mancos and reached total depth (1439 ft) in the Morrison Formation (Willis et al., 1996). A 1955-vintage gamma ray log was run from ground surface to total depth (Figure 7). The unspecified units of the old gamma ray log were converted qualitatively to API units by visual comparison to adjacent wells with more modern gamma ray logs.

The Larsen State-1 well is located on the eastern flank of an asymmetric north-northwest plunging anticline (Seiber Nose) that is cut by the Little Dolores River basement fault on the east flank (Willis et al., 1996). The well penetrates a flexure in the Dakota Sandstone in which strata dip approximately 11° to the north through the wellbore path (Willis et al., 1996). The dip "stretches" the well-log measured depth by 19% (sine 11° or about 19 feet per hundred). Comparing the Larson well log to that of the nearby Broadhead Patsantaras-C (API 4301930916, section 3, T20S, R24E) which was drilled through flatter strata about 2 km to the east on the crest of the anticline, suggests that structural dip in the Larsen well is on the order of 7° to 14° (Figure 8), which is compatible with the structure map of Willis et al. (1996). Alternately the borehole path of the Larsen well is deviated through the interval between 675 and 900 ft MD, which creates a similar log stretch. Understanding the log stretch is important for understanding correlations, discussed below.

Cuttings studied in the Larsen State-1 well span the interval from 473 to 1105 ft MD. Collected at approximately 10-ft intervals, the cuttings were obtained from the collection at the USGS Core Research Center in Lakewood, Colorado. Cuttings were described with a 10X to 20X binocular microscope, recording color (Rock-Color Chart Committee, 1984), dominant grain size, minor

grain size, reaction in dilute (5%) HCl, accessory minerals such as pyrite and glauconite, and fossils such as *Inoceramus* prisms and fish scales for 73 samples.

The descriptive sample log (Figure 7) shows four discrete siltstone and sandstone-rich intervals above the Dakota Sandstone (represented by the MTUNC top), each separated by shale. From oldest to youngest they are at 1059 to 1065, 1015 to 948, 940 to 900 and 491 to 562 ft MD. Glauconite is a common accessory mineral in all sandstone-rich intervals, and fish scales are also common, confirming a marine origin. Intervening intervals are dominated by dark to medium gray shale, commonly calcareous, and with abundant fish scales and less commonly with cubic pyrite. The fine sand in the interval between 1000 and 980 ft MD is notable for consisting of poorly sorted, subangular very-fine to fine sand-sized grains, similar to the silty very-fine to fine sandstone facies (Table 1) in the Westwater section in unit 11 (33 to 36.7 m, Table 2, Figure 3). The correlation of the Larsen State-1 well to adjacent wells and the Westwater measured section is discussed below.

Analyses of Cuttings Samples

The following analyses were carried out on cuttings samples from the Larsen State-1 well:

Rock-Eval / TOC (73 samples)
Vitrinite reflectance / visual kerogen (7 samples)
Carbon and oxygen isotopic analysis of carbonate (14 samples)
X-ray diffraction of whole rock and clay fraction (12 samples)
Palynological analysis (12 samples), funded separately by the Utah Geological Survey

A series of figures (Figures 9 through 22) accompanies the following discussion and presents the data results for each appropriate section. Figures showing data distributed vertically through the lower Mancos section have the same format: the gamma-ray log for the Larsen State-1 well on the left, a data track in the middle, and the cuttings description log (from Figure 7) on the right. Relevant tops are shown on the logs, using the mnemonics described in Figure 2. In addition, three horizontal color bars are present on each log. The orange bar represent a sandstone (the Coon Spring Sandstone) interval above CW_SB_1; the yellow bar represents another sandstone interval developed above CW_SB_2, and the red bar represents an organic-rich shale directly above the FJLM top, discussed below.

Rock-Eval / TOC

Total organic carbon (TOC) contents ranged from a minimum of 0.44% to a maximum of 4.32%, averaging 1.23% TOC over the sampled interval (Figure 9, Table 3). Within the lower Mancos interval, there is significant variability in TOC content. In the lower sequences (1 through 3), organic carbon content is relatively low, generally less than 1.0%. Two samples from the uppermost Dakota Formation, immediately underlying sequence 1, have TOC values of 1.67% and 4.32% and contain coal fragments. Particularly low values in sequences 2 and 3 correspond to a sand-rich interval between 970 and 1010 feet.

The sequence richest in organic carbon is sequence 4. There is a distinct upward increase in TOC from sequence 3 to sequence 4 (across the FE_SB_1 surface). Maximum TOC values in the entire section are recorded at the maximum flooding surface within sequence 4, with values in

excess of 2% recorded over an interval of nearly 50 feet (841 to 890). TOC values gradually decrease upward to 0.70% TOC at the F1 surface, corresponding to a sandy interval at approximately 550 feet depth in the Larsen State-1 well.

Hydrogen index (HI) values, in combination with oxygen index (OI) values, provide an indication of the 'oil-proneness' or 'gas-proneness' of organic matter and the origin of organic matter in relatively immature samples. In the Larsen State-1 well, HI values in general closely track TOC values (Figure 10). The interval of sequence 4 with the highest TOC values also has the highest HI values. As with the TOC profile there is a distinct increase in HI values from approximately 100 to up to 200 across the sequence 3 to 4 boundary, then a striking increase in HI at the sequence 4 maximum flooding surface. Over the 820 to 890 foot depth range, HI values range from 343 to 457, indicating a concentration of oil-prone organic matter in this interval.

A cross-plot of hydrogen index versus oxygen index values is an effective way of displaying the type of kerogen present and the oil-proneness or gas-proneness of the organic matter. In the Larsen State-1 Mancos section, much of the data cluster at relatively low HI and OI values (Figure 11), suggesting that the organic matter was deposited in a relatively oxidizing environment. However one set of points tracks the Type II kerogen trend, indicating the presence of good-quality, oil-prone organic matter. With one exception, all of these high HI points occur between depths of 820 and 890 feet, largely within sequence 4.

Most of the data show a systematic increase in HI values with increasing TOC values (Figure 12). This overall trend suggests that lower TOC intervals in the section were associated with higher degrees of oxidation in the depositional environment, which would have had the effect of reducing HI. Two points should be noted: 1) The high TOC samples in the uppermost Dakota Formation have low HI values; these two samples are coaly, an interpretation supported by visual observation of coal fragments in the cuttings samples; and 2) sequence 5 samples plot on a trend with somewhat lower values and lower slope than the other Mancos samples. This suggests that water chemistry in the Cretaceous Seaway was somewhat different, possibly more oxidizing, than during deposition of the underlying four sequences.

Vitrinite Reflectance / Visual Kerogen Analysis

Seven high-quality vitrinite reflectance (VR) measurements were obtained on cuttings samples from the Larsen State-1 well in the Mancos interval (Figure 13 and Table 4). These show an increase in VR from 0.68% Ro near the top of the lower Mancos interval (522 feet) to 0.89% Ro in the uppermost Dakota. These values place the lower Mancos within the upper part of the oil window, as conventionally interpreted based on a top of oil window at 0.6% Ro. These values are slightly higher than the equivalent Tmax values from Rock-Eval analysis (Table 4), which range from about 433° to 438°C over this interval. The Thermal Alteration Index of 2+ from analysis of palynomorphs places the section in the upper part of the oil window, which is consistent with the vitrinite data.

Visual kerogen / palynofacies analysis (Table 4) indicates a change in the organic matter assemblage between sequences 3 and 4, approximately corresponding to the increase in TOC at that boundary. Two samples below the FE_SB_1 surface contain ≤80% amorphous marine

kerogen, with the remainder coaly fragments; the five samples from sequences 4 and 5 contain ≥95% amorphous marine kerogen.

Carbon / Oxygen Isotopes

Carbon and oxygen isotope values were determined on the carbonate fraction in fourteen samples from the lower Mancos section (Table 5).

Oxygen isotopic compositions typically range between -5‰ and -10‰ PDB (Figure14), with the exception of two samples in sequence 3 at 971 and 982.5 feet, which have distinctly more negative oxygen (-15.2 and -15.7‰). The fact that adjacent samples in the lower Mancos section have similar isotopic compositions suggests that there is a probably a real stratigraphic structure to oxygen isotopic compositions in this section; however, the current sampling density is not sufficient to make that structure clear.

Carbon isotopic compositions of carbonate are tightly clustered around 0.00‰ PDB in most samples, ranging from -0.50‰ to +0.50‰ (Figure 15). Two exceptions are samples as the top of the lower Mancos sequence which are slightly more negative (sample 536: -2.76‰; and sample 608: -1.07‰). Samples from 971 and 982.5 feet are considerably more negative, -7.14‰ and -8.77‰, respectively. The latter two samples are the same two samples with relatively negative $\delta^{18}O$ compositions.

The combination of negative carbon and oxygen isotopic compositions that characterizes the two samples from sequence 3 (Figure 16) is typical of carbonate that forms under the influence of meteoric water (Anderson and Arthur, 1983). Taylor et al. (2000) describe isolated concretions and laterally extensive carbonate-cemented horizons in the Book Cliffs with similarly negative compositions. They interpret the concretions as having precipitated during major sea-level lowstands. During these lowstands, meteoric water penetrated the sands at an updip position, dissolving pre-existing carbonate and transported it to a downdip position; where meteoric water encountered more saline, marine-influence pore waters, it became supersaturated with respect to dolomite, resulting in carbonate precipitation. The laterally extensive carbonate zones are interpreted as nucleating below organic-rich maximum flooding surfaces. The carbon isotopic composition of pore water was modified to relatively negative values by the organic matter; however subsequent meteoric water influence is indicated by the relatively negative oxygen isotopic composition.

The two samples characterized by light oxygen and carbon isotopic compositions occur in relatively sandy sediments underlying the sequence boundary separating sequences 3 and 4. We hypothesize that updip of the Larsen well, sediments in sequence 3 were exposed during the lowstand that generated the FE_SB_1 sequence boundary. Meteoric water penetrated downdip along permeable sand-rich beds.

Mineralogy / Clay Mineralogy

Whole rock and clay (≤ 4 µm) x-ray diffraction analysis was carried out on twelve samples. Both air-dried and glycolated mounts were prepared for clay analysis to determine the expandability of the clays.

The concentration of minerals identified on the whole rock x-ray diffractograms was classified as major, minor or trace (Table 6). Minerals generally present included quartz, albite, K-feldspar, calcite, dolomite, kaolinite, glauconite and pyrite. Quartz was abundant in every sample. Relative concentrations of the other minerals are displayed in Figures 17 through 22.

The calcite and dolomite contents (Figures 17 and 18) of the lower Mancos exhibit systematic stratigraphic variation. The content of both calcite and dolomite are variable but relatively low in the lower part of the section, in sequences 1 through 3. The calcite content (Figure 17) increases above the maximum flooding surface in sequence 4 and remains high through the top of the lower Mancos section. The dolomite content (Figure 18) is variable but relatively low up to the sequence boundary separating sequence 4 from sequence 5 and is relatively high from that point to the top of the lower Mancos section. These variations could either be related to the production of biogenic carbonate in the seaway and/or to the contribution of preexisting carbonate from the erosion of older carbonate rocks in the source terrane for these sediments.

The clay minerals glauconite and kaolinite are present in whole rock x-ray diffractograms. Glauconite is present throughout the section and relatively constant in its concentration. Glauconite concentration is largely controlled by water chemistry in the Cretaceous Seaway. Kaolinite concentration (Figure 19) is more variable, in general more abundant in sequences 4 and 5 than in sequences 1, 2 and 3; this variation probably reflects changes in the contributions from different source terranes and possibly climatic effects on weathering rates.

Orthoclase (Figure 20) is relatively abundant in sequences 1 and 5 and less abundant in sequences 2, 3 and 4. Plagioclase (Figure 21) is most abundant in the upper part of sequence 1, in sequences 2 and 3 and near the top of sequence 5. As with kaolinite, this variability is probably a function of varying source terrane and possibly to climatically controlled weathering rates.

Pyrite concentration (Figure 22) is low throughout the lower part of the lower Mancos section. It increases at the maximum flooding surface in sequence 4 and is relatively abundant through the shaliest part of the section, then decreases upward as sand content increases. This relationship suggests that the deepest water environment and most reducing condition occurred during deposition of sequence 4 and the lower part of sequence 5.

Chlorite and mixed-layer illite/smectite were identified in the clay separates of most samples. The illite/smectite has a composition of approximately 30-40% illite.

Palynological Analyses

Appendix C contains the complete results of a palynological study of 12 composited cuttings samples by Dr. Gerald Waanders, Consulting Palynologist, funded separately by the Utah Geological Survey. Dr. Waanders' results are summarized below from his report. Comparison with the correlation framework of this study is discussed in the next section.

Sample Group from 473-804 ft MD

Age: **Coniacian**
Environment: **Nearshore Open Marine**
T.A.I.: **0.4-0.5% Estimated R_0**

This interval is represented by a diverse assemblage of dinoflagellate cysts. Frequent to common occurrences of *Hystrichodinium pulchrum, Palaeohystrichophora infusorioides, Odontochitina costata* and *Surculosphaeridium longifurcatum* suggest a Coniacian age. The high diversities of dinoflagellate species indicate an open marine paleoenvironment for the interval. The kerogens, however, are mixed with fairly high concentrations of land derived, woody materials along with moderate diversities of spores and pollen suggesting nearshore conditions.

The late Cretaceous aged palynomorphs in these samples are light brown in color and estimated to be at a maturation level of 0.4-0.5 R_0 or at the threshold of peak oil generation. The recycled palynomorphs (Late Devonian to Mississippian) in the interval may be of a slightly higher maturation level. The organic recoveries for the samples in this interval were all very good and worthy of checking for source rock potential. The kerogens were mixed and indicate potential for both oil and gas generation.

Sample Group from 804-880 ft MD

Age: **Coniacian**
Environment: **Restricted Marine or Lacustrine**
T.A.I.: **0.4-0.4% Estimated R_0**

When compared to the interval described above, this unit shows a distinct drop in species diversities, a shift to higher relative concentrations of amorphous kerogens and probably a somewhat higher total organic recovery in the samples. Higher organic recoveries coupled with increased concentrations of amorphous kerogens suggest quieter water (possibly deeper) with reducing conditions. The reduction in microplankton diversity, however, indicates a restricted marine or possibly basinal lacustrine paleoenvironment. Thermal alteration values are unchanged from above. The overall kerogen content is mostly amorphous or oil generating.

Sample Group from 900-1087 ft MD

Age: **Coniacian**
Environment: **Nearshore Open Marine**
T.A.I.: **0.4-0.5 Estimated R_0**

The paleoenvironment for this interval is the same as noted higher in the well at 473-804' where open marine conditions are suggested by higher dinoflagellate diversities and a nearshore conditions is indicated by increased amounts of terrestrial kerogens and higher numbers of spores and pollen.

The late Cretaceous aged palynomorphs in these samples are light brown in color and estimated to be at a maturation level of 0.4-0.5 R_0 or at the threshold of peak oil generation. The recycled palynomorphs in the interval may be of a slightly higher maturation level. The organic recoveries for the samples in this interval were good to very good and worthy of checking for source rock potential. The kerogens were mixed and indicate potential for both oil and gas generation.

Sample Group from 1100-1105 ft MD

Age: **Turonian?**
Environment: **Deltaic/ Estuarine**
T.A.I.: **0.4-0.5 Estimated R_0**

There was a gap in samples from 1087-1100' and this deepest interval is represented by only one 5' sample. It contains the first occurrences of *Appendicisporites matesovae* and *Trilobosporites marylandensis* and they would normally suggest an age at least as old as Turonian. However, the age of the sample is problematic because it also contains several recycled Late Devonian to Mississippian aged spores and we are left wondering whether or not these older Cretaceous taxa might be recycled as well. Increased spore/pollen diversities and decreased microplankton diversities suggest a paleoenvironment that is somewhat shallower than the interval above. The thermal maturation, kerogen quality and total organic recovery for this sample are all similar to the interval above.

Summary

The organic geochemical analysis indicates that two main intervals have source-rock potential: the best and thickest is present between 820 to 890 ft MD in sequence 4 and the other is more limited in thickness, from 787 to 789 ft MD above the FJL marker in or above sequence 5. The organic rich section in sequence 4 has the highest TOC, hydrogen index values, and tracks the Type II trend, indicating good-quality oil-prone organic matter. Palynological analyses further show this interval to represent restricted, possibly deeper, anoxic water conditions. The higher concentration of pyrite in this interval further supports a reducing environment.

Vitrinite reflectance, TAI, and Tmax values show a systematic increase from the upper to lower portion of the interval studied. These data place the lower Mancos section at the Larsen well in the upper part of the oil window.

Oxygen and carbon isotopic data suggest that updip of the Larsen well, sediments in sequence 3 were exposed during the lowstand that generated the above the FE_SB_1 sequence boundary. During this time, meteoric water penetrated downdip along permeable sand-rich beds, creating isotopically light carbon and oxygen values.

Qualitative XRD analyses of mineralogy show variations in carbonate type and abundance that either reflect the production of biogenic carbonate in the seaway and/or reflect the contribution of carbonate from older sources during erosion. Higher kaolinite abundances and proportions of plagioclase versus orthoclase in sequences 4 and 5 may reflect changes in provenance and/or weathering rates. Illite/smectite has a composition of approximately 30-40% illite.

Correlation

The regional correlation framework is based on 216 wells and four measured sections that cover the lowermost Mancos Shale and uppermost Dakota Sandstone, mostly clustered in the southern and eastern Uinta basin and along the Book Cliffs outcrop belt (Figure 1). The primary correlation logs were natural gamma ray supplemented by resistivity logs. Most logs were raster images that were qualitatively normalized in GeoPlus Petra™ by adjusting the margins of the gamma-ray depth track to enhance the definition of gamma ray logs across many vintages and scales.

A series of 13 tops (Table 2, Figures 3, 7, and 8) were correlated over a 650-foot interval of the lower Mancos Shale throughout the study area. The correlation strategy relied on identifying condensed sections, which are commonly characterized by bentonite clusters such as those described in the Westwater measured section (Figure 3). Condensed sections also have long, basin-scale correlation lengths in marine environments. In distal marine settings, correlating condensed intervals is more reliable than correlating sequence boundaries, and importantly for this study, condensed sections tend to concentrate organic matter, which is critical for organic geochemical characterization (e.g. Loutit et al., 1988; Creaney and Passey, 1993). The only tops in the correlation framework that are not associated with condensed sections are the three sequence boundaries (CW_SB_1, CW_SB_2 and FE_SB_1) and the basal unconformity (MTUNC). With the exception of the basal unconformity (discussed below) the sequence boundary picks were interpreted after the bentonite-rich condensed intervals had been correlated and iteratively loop-tied and mapped. The resulting correlation framework is similar to and expands on those interpreted by Molenaar and Cobban (1991), Kirschbaum (2003), and Edwards et al. (2005).

Correlation of Westwater Measured Section to Larsen State-1 and other Subsurface Wells

Correlation of the Westwater measured section to the Larsen State-1 and adjacent wells (Figure 23) is based on: 1) character tie of the outcrop to the subsurface gamma ray logs; 2) the stratigraphic positions of bentonite groups; 3) distinctive sandstone facies (lithologies) at specific stratigraphic positions; and 4) vertical gamma-ray patterns representing vertical facies successions. High gamma-ray bentonite intervals that are present at 27m (BENT_27), 38m (BENT_38), 46m (BENT_46), and 57m (BENT_57) on the Westwater measured section correlate to bentonitic intervals in the gamma-ray logs of five wells within 20 miles of the Westwater outcrop (Figure 23). The FJ1 top that coincides with a bentonite-rich interval in the Westwater section at 84m projects into the Larsen State-1 well at a high gamma-ray interval at 832 ft MD. The FJL condensed-section top in the Larsen State-1 well projects above the top of the Westwater measured section (Figure 23). Correlation of sequence boundaries interpreted in the Westwater section is based on stratigraphic position relative to the bentonite clusters (condensed sections) and a generally consistent gamma-ray signature (Figure 23). Regional correlation of sequence boundaries, however, is more interpretive than that for condensed sections.

The palynological analysis (presented above and in Appendix C) of cuttings composites for interval from 473 to 804 ft MD in the Larsen State-1 well suggests that this interval, corresponding to the FENB to approximately the FJL marker, represents an open marine environment of Coniacian age, which is consistent with the interpretation of this study. The interval from 804 to 880 ft MD in the Larsen well shows a distinct change in depositional environment, characterized by quieter, possibly deeper, water with reducing conditions. This interval corresponds to the FJL to FJLM isochore interval, which contains the highest TOC and HI values within the studied interval (Figures 9, 10 and 23). The base of this interval also corresponds to a major marine condensed zone, discussed below. The ammonite *P. hyatti* is present at the base of the interval, confirming a late middle Turonian age, which is in conflict with the Coniacian age reported by the palynological study. The interval from 900 to 1087 ft MD corresponds to several deltaic-sourced sequences (1 through 3 and the HST of sequence 4, approximately from the FJLM to the MTUNC tops) with an open marine depositional

environment also influenced by nearshore terrestrial influence. This interpretation is also consistent with the facies assemblages interpreted in the Westwater measured section. The possible existence of turbidite-derived sandstone would account for the influx of nearshore flora to the open marine environment. The sample from 1100 to 1105 ft MD is within the uppermost part of the Dakota Sandstone, which underlies the regional unconformity, MTUNC, identified by Molenaar and Cobban (1991) and also correlated in this study. The age of this section is thought to be older than Turonian and is a topic of the study by McPherson et al. (2006, in preparation).

Database Tops

The characteristics of the 13 tops in the database are discussed below in four groups defined by stratigraphic significance and log responses. Appendix D contains a digital list of tops for each well in the study. Wells are listed by API number, latitude and longitude, and section, township and range location.

Hiatus at the Base of the Lower Mancos (MTUNC)

Correlating the hiatus (MTUNC) at the base of the lower Mancos interval (Figure 2) was addressed in three ways in order to converge on a consistent interpretation. First, Molenaar and Cobban (1991) described a strategy for correlating the unconformity surface that relied on a change in continuity and persistence of log patterns above and below the surface. Above the unconformity, log patterns are “layer-cake” (highly consistent, laterally repeatable patterns) over >30 miles, whereas those below the unconformity are highly discontinuous laterally (change over <1 mi). A second way to pick the unconformity surface relies on a color change upward from yellow-brown to gray shale, a characteristic observed in cuttings for the Larsen State-1 well (Figure 7), in the Westwater measured section, as discussed above, and in description of cuttings from mud logs for other wells (Mary McPherson, personal communication; McPherson et al., 2006). The color change always coincides with the change in lateral correlatability of log patterns. Finally, tops picked for the unconformity (MTUNC) were compared with those of McPherson et al. (2006, in preparation) to facilitate compatibility between their Cedar Mountain-Dakota study and this lower Mancos study. The resulting unconformity-surface picks (e.g. Figures 3, 7, 8, 23) in the two studies are within 10 feet of each other.

Condensed Sections

Tops representing condensed sections include, from oldest to youngest: BENT_27, BENT_38, BENT_46, and BENT_57, FJLM, FJ1, FJL, F3, F2, F1, and FENB (Figures 7, 23). High gamma ray responses associated with bentonite clusters represent times of high preservation of volcanic ash-fall events, a typical characteristic of condensed sections (e.g. Loutit et al., 1988). The bentonitic intervals defined in the Westwater section (top-name prefix = BENT) and the FJ1, F3 and F2 tops show regionally correlatable high gamma-ray spikes <2 ft (about 0.6m) thick on well logs, which is at the resolution of a gamma ray log. The correlative intervals in outcrop show a concentration of thin (<1cm) bentonite beds within about 2m of vertical section. The bentonite clusters provide a reproducible time-stratigraphic framework from which to analyze other facies successions and make stratigraphic interpretations.

The FJLM and FJL tops (Figures 7, 23) are picked at the bases of high gamma-ray intervals that are up to 8 ft thick, as opposed to the thin spikes characterizing the bentonite clusters. These

intervals are regionally persistent, and in the in the Larsen State-1 well have TOC content > 2% and hydrogen indices >400. These characteristics are also typical of condensed intervals (Loutit et al., 1988; Creaney and Passey, 1993).

The F1 and FENB tops are picked at high gamma-ray responses that bound a glauconitic sand-rich interval at the top of the lower Mancos interval in this study (Figures 7, 23). The F1 top is within a high gamma-ray zone below the sand-rich interval defined by cuttings in the Larsen State-1 well. While this study interprets the zone to represent a condensed interval, it could also be merged with a sequence boundary represented by the base of the sandy interval. This interpretation awaits further study. The FENB top is further defined by the base of a persistently high gamma ray and high resistivity interval recognized by Molenaar and Cobban (1991). The high resistivity response is postulated to reflect an increase in calcareous lithology (Molenaar and Cobban, 1991), possibly representing the incursion of Niobrara calcareous facies into the study area. This response is present throughout the study area, but shows internal changes above the FENB top, suggesting lateral facies changes.

Sequence boundaries

Three sequence boundaries interpreted in the Westwater measured section include CW_SB_1, CW_SB_2 and FE_SB_1, as discussed above. On well logs they correspond to upward changes in vertical log patterns within the temporal framework provided by the condensed intervals. The CW_SB_1 and CW_SB_2 sequence boundaries are generally picked at the bases of silty/sand-rich intervals, expressed as slightly lower gamma-ray values. The FE_SB_1 is picked at an upward change from moderately low to high gamma-ray (Figures 7, 8, 23) and/or at a thin "sand" (lower gamma ray) that occurs at this contact in some well logs. The sequence-boundary picks are more interpretive than those for condensed intervals.

Summary

This study interprets eleven condensed intervals that form the basic correlation framework. Two of these, FJLM and FJL, are important for source-rock characterization. Three sequence boundaries within the temporal framework of the condensed intervals are associated with potential reservoir sandstone units that are probably the fully marine equivalents of deltaic lowstands. A hiatus at the base of the lower Mancos study-interval has been correlated basin wide in collaboration with McPherson et al. (2006, in preparation).

Isochore Maps

The following discussion focuses on isochore maps of selected time-stratigraphic and facies intervals that bear on the distribution of potential reservoir sandstone successions and shale source-rock intervals. Isochore maps are generally equal to isopach maps (true thickness), except in areas where strata dip more than 5°, such as represented by the Larsen State-1 well (Figure 8). Exceedingly few wells in the study area, however, penetrate strata that dip >5°. Wells in which faults cut out (normal fault) or repeat (thrust or reverse faults) a mapped stratigraphic interval were not used for isochore mapping in that particular interval.

Contour maps were generated in GeoPlus Petra™ using a grid-cell size of 5 by 5 km (about 3 by 3 miles) in order to represent the widely spaced well control. The disadvantage of the large cell

size is that the contouring algorithm does not honor closely spaced data that falls within the cell. Hence, the maps reflect regional trends as opposed to local variability. The algorithm used was least squares with grid flexing; no other attempt was made to edit the maps. This decision maximizes reproducibility of maps as opposed to emphasizing geologic interpretation.

Mapping several sand-rich and organic-rich shale zones on raster logs within the identified sequences entailed defining them as "pay zones" on the gamma ray log within GeoPlus Petra™. The colored bars displayed on stratigraphic cross sections (e.g. Figure 23) show the vertical boundaries of each of the zones mapped and discussed below. This interpretation is necessarily qualitative because of using raster images. In a digital well-log workflow, the gamma ray logs would be normalized, and API cutoffs would be specified to more quantitatively define these zones. Hence, the trends discussed below reflect relative values.

Dakota Silt

The BENT_38 to MTUNC isochore (Figure 24A) represents all of sequence 1 and the basal part (LST/TST) of sequence 2 as defined in this study (Figure 3). The reason for mapping such a thick interval is its common usage by oil and gas operators as the "Dakota Silt" (e.g. Molenaar and Cobban, 1991), an interval that is widely correlatable across the southern and eastern Uinta basin. As interpreted in this study, the interval pinches out to the northeast by downlap onto the underlying MTUNC unconformity (Figure 25) as also shown by Molenaar and Cobban (1991). North of Rangely and Dinosaur, Colorado, this unit is absent in outcrop due to stratigraphic termination by downlap (see zero contour-line on Figure 24 and point labeled "M"). The Dakota Silt, which lies above the MTUNC unconformity is unrelated stratigraphically to the underlying Dakota Sandstone, and is, instead, genetically related to progradation of lower-middle Turonian deltas to the southwest, as indicated by the thick isopach values (>150 ft) at the southwestern corner of the study area (Figure 24A).

Within the Dakota Silt isochore interval, the base of sequence 2 (LST/TST) is represented by the Coon Spring Sandstone Bed of Molenaar and Cobban (1991). A net sand map (Figure 24B) of this interval shows a thick >30 ft in the southwestern part of the study area that coincides with the thick part of the Dakota Silt isopach (Figure 24A). The thick part of the Coon Spring Sandstone Bed spreads out radially to the northeast, gradually changing facies to shale at its limit in the easternmost Uinta basin. The Coon Spring Sandstone Bed also is absent in the outcrop belt north of Rangely, Colorado (Figure 24B, point labeled "M"). The fan-shaped geometry of the net sand distribution and the distinct, poorly sorted lithology of the upper part of the Coon Spring Sandstone Bed, discussed above, strongly suggest a turbidite origin that is fed from a channelized source, likely associated with a coeval delta-front to the southwest.

Organic-rich interval FJ1 to FJLM

The FJ1 to FJLM isochore interval (Figure 26A) corresponds to an organic-rich interval defined by geochemical analysis of the cuttings in the Larsen State-1 well, in which TOC values are >2% and hydrogen indices are >400. Palynological analysis shows that this interval is very restricted and anoxic. Lithofacies in this interval consist of alternating dark gray shale and clustered thin beds of wavy-laminated, rippled sandstone facies, interpreted to be turbidites. Ichofauna is sparse, reflecting the anoxia; rare, small ammonoids and inoceramids suggest a stressed, yet marine environment. This interval also largely represents the HST of sequence 4, culminating in

the nearly merged sequence boundary and condensed interval of sequence 5 as defined in this study (Figure 3). The highly organic-rich high gamma-ray portion at the base of the interval immediately overlying marker FJLM (mapped in Figure 26B) contains the ammonite *P. hyatti* and correlates to the organic rich flooding zone at the top of the Hyatti sequence of Gardner (1995) and the base of the Juana Lopez Member of Molenaar and Cobban (1991). This is a major regional condensed interval that has good source-rock qualities.

The isochore map of the gross interval shows a distinct thick trend in the northwestern part of the study area that thins to the southwest, south and east (Figures 26A, 27). The pattern suggests a dominant sediment source to the northwest, which trends 90° from the dominantly southwest source suggested for the underlying Dakota Silt isochore (Figure 24). The isochore of the organic rich condensed interval at the base of the interval (Figure 26B) thickens to the southwest, reaching a maximum of about 8 ft in the southeastern part of the study interval. The organic-rich shale interval is thickest where the gross interval thins, also suggesting that the shale represents the condensed section, or downlap surface, for the gross FJ1-FJLM interval. While the isochore map represents the gross distribution of shale within the condensed section, it does not imply that the organic richness will be the same at all locations. Rather, more data are needed to assess the regional organic-content distribution of the condensed section.

Organic-rich shale at base of the F3 to FJL Interval

Another organic-rich high-gamma ray interval identified by cuttings analysis of the Larsen State-1 well is present at the base of the F3-FJL interval above the FJL top (Figures 7, 23, 27). The isochore map of the gross F3-FJL interval (Figure 28A), shows a thick representing a sediment source to the northwest, and it shows a second thick to the southwest, suggesting sediment input from that direction, also. The isochore map of the organic-rich shale interval, above the FJL marker (Figures 27, 28A), like that of the FJ1-FJLM interval, is thick where the entire interval is thin, as would be expected for a condensed section. The isochore map of the organic-rich shale interval does not imply that the organic richness will be the same at all locations.

Thin Sandstone at base of F2 to F3 Interval

A thin sandstone interval at the base of the F2-F3 isochore (Figures 27, 29) was evaluated due to its regional persistence and its likely correlation to “Frontier” outcrops north of Rangely as described by Molenaar and Cobban (1991). The gross interval, F2-F3, shows a thick to the northwest, like older successions, that implies a northwestern sediment source. The distribution of the thin sandstone interval, however, trends southwest to northeast, and is thick where the gross interval is thin. This type of compensating pattern for sandstone distribution is unusual if the depositional environment represents the shoreface/upper delta front. Inspection of the outcrops around the Skull Creek anticline (marked “M” on Figure 29) strongly suggest that the thin sandstone beds have turbidite origins. The entire interval in F2-F3 shows log characteristics that could represent slope and/or basin floor turbidite deposition. This hypothesis bears further study that is beyond the scope of this report.

Summary

The isochore maps show the distribution of several important source-rock and potential interbedded reservoir intervals across the study area. The reservoir sandstone intervals (Coon Springs Sandstone Bed, between the CW_SB_1 and BENT_38 markers, and a thin sandstone at

the base of the F2-F3 interval are postulated to have turbidite depositional origins, based on facies relationships and map distribution patterns. Two major condensed sections, one at the base of the uniquely organic rich FJ1-FJLM interval and the other at the base of the F3-FJL interval are distributed across the southern and southeastern Uinta basin. Dominant sediment sources from coeval deltas were to the southwest and northwest, as inferred from isochore thicknesses. The two sources appear to dominate at different times. A major switch to the northwest source during deposition of the Ferron-Frontier (interval between FE_SB_1 and F2 markers) may have caused an embayment along the western margin of the Cretaceous Seaway that led to more anoxic conditions favorable to more accumulation of organic-rich condensed intervals.

Burial History and Basin Modeling

A burial history (Figure 30) for the sedimentary section in the Westwater Canyon area (including the Larsen State-1 well) was developed based on stratigraphic relations observed in the area (this report) and stratigraphic thicknesses and ages from Nuccio and Roberts (2003). In this model, the Mancos Formation was deposited between 97 and 80 Ma, underwent rapid subsidence to 25 Ma, followed by a period of uplift and erosion lasting to the present. The Mancos reached a maximum burial depth of 8010 feet at the top of the formation and 9860 feet at the base of the formation. The erosional event beginning at 25 Ma removed 8000 feet of section, including 4200 feet of Wasatch and Green River Formations, 1850 feet of Mesaverde Group and 1900 feet of Mancos Formation. As a result, the present-day base of the Mancos is at a depth of 1840 feet.

The removal of 8000 feet of section is consistent with erosion models proposed by Nuccio and Roberts (2003). They proposed uplift and erosion of 8050 feet of section in a pseudo-well near the town of Green River beginning at 37 Ma, and removal of 4000 feet of section in the Texaco #2 Seep Ridge well, Uintah County (approximately 50 miles north of the Westwater area), beginning at 10 Ma. Such models for extensive uplift and erosion are supported by results of apatite fission track analysis in a regional study of the west-central Colorado Plateau (Dumitru et al., 1994). Furthermore, it is not possible to match the measured vitrinite reflectance data from the Larsen State-1 well with less than this amount of uplift and erosion, unless geothermal gradients are increased to unreasonably high values.

If a geothermal gradient of 1.98°F/100 feet (36.1°C/km) is assumed, a calculated maturation profile places the present-day top of the Mancos Formation (at the surface) at a thermal maturity of 0.70% Ro and the present-day base of the Mancos Formation (at a depth of 1860 feet) at a thermal maturity of 0.87% Ro (Figure 31). The geothermal gradient assumed here is very similar to those used by Nuccio and Roberts (2003) for the town of Green River pseudo-well and the Texaco #2 Seep Ridge well. The calculated thermal maturities are close to measured Ro values in the Larsen State-1 well, which are 0.68% Ro at the top of the Mancos section and 0.89% Ro at the base of the Mancos section.

Models for oil and gas generation and expulsion were created for the Mancos Formation in the Westwater Canyon area, assuming a starting organic carbon content of 2.5% TOC, Type II marine kerogen and a starting hydrogen index of 450. These values are consistent with the present-day TOC, HI and thermal maturity values in the richest interval (sequence 4) from the Larsen State-1 well; however they do not represent the entire Mancos, much of which contained 0.75 to 1.5% TOC of much less oil-prone organic matter. The model assumes kinetics for Type

II hydrocarbon generation based on experimental studies at the Lawrence-Livermore National Laboratory.

The modeling shows oil generation beginning in the Mancos at 50 Ma and continuing until 22 Ma (Figure 32), at which time uplift of the section effectively shut down oil generation. At the time when oil generation ceases, approximately 32% of the organic matter had been converted to oil at the base of the formation and 4.6% had been converted at the top of the formation. Oil expulsion began at 38 Ma at the base of the Manco and, at that stratigraphic level, approximately 11% of the organic matter had been converted to expelled oil. Oil expulsion never began at the top of the Mancos, because insufficient oil had been generated to reach a saturation threshold of 20%.

Gas generation began and ended at approximately the same time as oil generation, 50 Ma and 22 Ma, respectively (Figure 33). The amount of gas generated was equivalent to approximately 5.8% of the total organic carbon at the base of the Mancos Formation and 0.9% of the total organic carbon at the top of the Mancos. Expulsion of gas began at 38 Ma and ended at 22 Ma. The total gas expelled at base-Mancos level was equivalent to approximately 2% of the total organic carbon content of the shale.

Summary and Conclusions

The goal of this study was to characterize the lateral and vertical distributions of shale facies within a sequence stratigraphic framework and to integrate the depositional facies with geochemical analysis as a basis for assessing the lower Mancos Shale in the south-central Uinta basin as a shale-gas resource play. A related goal was to evaluate the potential for tight-gas sandstone reservoirs that may be interbedded with lower Mancos mudrocks.

Deliverables for this study include: 1) a digital correlation database consisting of 13 tops representing a sequence stratigraphic framework for 216 wells; 2) description of a 93m- thick measured section near Westwater, Utah that contains 79m (259 ft) of lower Mancos Shale and 14m of underlying Dakota Sandstone; 3) an outcrop gamma-ray log and associated LAS file for the measured section; 4) cuttings description combined with palynological and geochemical analyses for 73 samples over a 632-ft (192m) interval in the Carter Larsen State-1 well near Westwater, Utah; and 5) this final report.

Eleven condensed intervals form the basic correlation framework for a 650-ft thick interval of the lower Mancos Shale in the southern and southeastern Uinta basin study area. Two of these, represented by the FJLM and FJL tops, are important for source-rock characterization. Three sequence boundaries within the lower Mancos Shale are associated with potential reservoir sandstone units that are probably the fully marine equivalents of deltaic lowstands. The three sequence boundaries are interpreted from the 93-m thick Westwater measured section and correlated through the subsurface. At least five sequences, described by the following pairs of tops: MTUNC to CW_SB_1 (sequence 1); CW_SB_1 to CW_SB_2 (sequence 2); CW_SB_2 to FE_SB_1 (sequence 3); FE_SB_1 to approximately FJ1 (sequence 4); and FJ1 to the top of the section (partially measured sequence 5) are interpreted from the outcrop portion of the study. A hiatus at the base of the lower Mancos study-interval has been identified in outcrop and correlated basin wide in collaboration with McPherson et al. (2006, in preparation).

Isochore maps show the distribution of several important source-rock and potential interbedded reservoir intervals across the study area. The reservoir sandstone intervals (Coon Springs Sandstone Bed, between the CW_SB_1 and BENT_38 markers, and a thin sandstone at the base of the F2-F3 interval are postulated to have turbidite depositional origins, based on facies relationships and map distribution patterns. Two major condensed sections, one at the base of the uniquely organic rich FJ1-FJLM interval and the other at the base of the F3-FJL interval are distributed across the southern and southeastern Uinta basin. Dominant sediment sources from coeval deltas were to the southwest and northwest, as inferred from isochore thicknesses. The two sources appear to dominate at different times. A major switch to the northwest source during deposition of the Ferron-Frontier (FE_SB_1 to F2 markers) may have created an embayment along the western margin of the Cretaceous Seaway that led to more anoxic conditions favorable to more accumulation of organic-rich condensed intervals.

Organic geochemical analysis of cuttings in the Larsen State-1 well indicates that two main intervals have source-rock potential: the highest quality and thickest is present between 820 to 890 ft MD in sequence 4, while the other is more limited in thickness, from 787 to 789 ft MD above the FJL marker in or above sequence 5. The organic rich section in sequence 4 has the highest TOC, hydrogen index values, and tracks the Type II kerogen trend, indicating good-quality oil-prone organic matter. Palynological analyses further show this interval to represent restricted, possibly deeper, anoxic water conditions. The higher concentration of pyrite in this interval also supports and interpretation of a reducing environment. Vitrinite reflectance, TAI, and Tmax values from Larsen State-1 cuttings show a systematic increase from the upper to lower portion of the interval studied. These data place the lower Mancos section at the Larsen well in the upper part of the oil window.

Oxygen and carbon isotopic analyses of 14 samples from the Larsen well suggest that updip of the Larsen well, sediments in sequence 3 were exposed to meteoric waters during the lowstand that generated the FE_SB_1 sequence boundary. During this time, meteoric water penetrated downdip along permeable sand-rich beds, forming carbonate with isotopically light carbon and oxygen values.

Qualitative XRD analyses of mineralogy show variations in carbonate type and abundance that either reflects the production of biogenic carbonate in the seaway and/or the contribution of carbonate from older sources during erosion. Higher kaolinite abundances and proportions of plagioclase versus orthoclase in sequences 4 and 5 may reflect changes in provenance and/or weathering rates. Illite/smectite has a composition of approximately 30-40% illite.

Basin modeling analysis requires that a substantial thickness of section overlying the Mancos Shale in the Westwater Canyon - Larsen State-1 area must have been eroded, in order to match vitrinite reflectance data from the Larsen State-1 well. A reasonable fit to the vitrinite reflectance data was achieved by assuming 8000 feet of missing section, eroded between 25 Ma and present-day, and a geothermal gradient of 36°C/km (1.98°F/100 feet). Given these parameters, the Mancos section in the Westwater Canyon area is in the oil window and has generated significant amounts of oil and some gas at the base-Mancos level.

In conclusion, two organic-rich source-rock quality shale intervals are distributed widely across the study area, as shown by correlation and isochore mapping. In addition, several widespread

thin-bedded sandstone intervals, interpreted as turbidite deposits, occur throughout the 650-ft thick stratigraphic study interval across the study area. These beds are in close juxtaposition to the organic-rich shales and could be charged under the right burial/maturity conditions. Burial history and maturity modeling show that the Westwater area, in the southernmost part of the study area, contains organic-rich oil-prone source intervals that are in the uppermost oil window. Hence, with deeper burial conditions to the north, in the subsurface of the Uinta basin, higher maturity levels would be expected, yielding the conditions favorable for dominantly gas generation within the lower Mancos Shale interval.

References Cited

Anderson, T.F., and M.A. Arthur, 1983, Chapter 1: Stable isotopes of oxygen and carbon and their application to sedimentologic and paleoenvironmental problems, *in* Stable Isotopes in Sedimentary Geology (M.A. Arthur, T.F. Anderson, I.R. Kaplan, J. Veizer and L.S. Land, authors): SEPM Short Course No. 10, notes, p. 1-1 – 1-151.

Chidsey, T.C., Jr., S. Wakefield, B.G. Hill, and M. Hebertson, 2004, Oil and gas fields map of Utah: Utah Geological Survey Map 203 DM (CD-ROM), 1:500,000.

Creaney, S. and Q.R. Passey, 1993, Recurring patterns of total organic carbon and source rock quality within a sequence stratigraphic framework: American Association of Petroleum Geologists Bulletin, v. 77, p. 386-401.

Dumitru, T.A., Duddy, I.R., and P.F. Green, 1994, Mesozoic-Cenozoic burial, uplift, and erosion history of the west-central Colorado Plateau: Geology, v. 22, p. 499-502.

Edwards, C.M., D.M. Hodgson, S.S. Flint, and J.A. Howell, 2005, Contrasting styles of shelf sediment transport and deposition in a ramp margin setting related to relative sea-level change and basin floor topography, Turonian (Cretaceous) western interior of central Utah, USA: Sedimentary Geology, v. 179, p. 117-152.

Franczyk, K.J, T.D. Fouch, R.C. Johnson, C.M. Molenaar, and W.A. Cobban, 1992, Cretaceous and Tertiary paleogeographic reconstructions for the Uinta-Piceance Basin study area, Colorado: U.S. Geological Survey Bulletin 1787-Q, 37 p.

Gardner, M.H., 1995, Tectonic and eustatic controls on the stratal architecture of mid-Cretaceous stratigraphic sequences, central western interior foreland basin of North America, *in* S.L. Dorobek and G.M. Ross, eds., Stratigraphic evolution of foreland basins: SEPM (Society for Sedimentary Geology) Special Publication 52, p. 243-281.

Greene, G.N., 1992, Digital geologic map of Colorado in ARC/INFO format: http://pubs.usgs.gov/of/1992/ofr-92-0507/colorado.htm, digital version of O. Tweto, 1979, Geologic map of Colorado: scale 1:500,000.

Hintze, H.F., G.C. Willis, D.Y.M. Laes, D.A. Sprinkel, and K.D. Brown, 2000, Digital Geologic map of Utah: Utah Geological Survey Map 179 DM (CD-ROM), 1:500,000.

Jarvie, D.M., Claxton, B.L., Henk, F.B., and Breyer, T.T., 2001, Oil and shale gas from the Barnett Shale, Ft. Worth Basin, Texas: Annual Meeting Expanded Abstracts, American Association of Petroleum Geologists, v. 2001, p. 100.

Kirschbaum, M., 2003, Geologic assessment of undiscovered oil and gas resources of the Mancos/Mowry total petroleum system, Uinta-Piceance province, Utah and Colorado, Chapter 6: U.S. Geological Survey Digital Data Series DDS-69-B, version 1.0 (CD-ROM), 45 p.

Loutit, T.S., J. Hardenbol, P.R. Vail, and G.R. Baum, 1988, Condensed sections: The key to age determination and correlation of continental margin sequences, *in* Wilgus,

C.K. et al, eds., Sea-level changes: An integrated approach: SEPM Special Publication 42, p. 183-260.

Macquaker, J.H.S. and A.E. Adams, 2003, Maximizing information from fine-grained sedimentary rocks: An inclusive nomenclature for mudstones: Journal of Sedimentary Research, v. 73, p. 735-744.

McPherson, M.L., Currie, B.S., and Pierson, J.S., 2006 (in preparation), Reservoir characterization of the Cretaceous Cedar Mountain and Dakota formations, southern Uinta basin: Year-One Report: Utah Geological Survey, open-file report, in prep.

Molenaar, C.M. and W.A. Cobban, 1991, Middle Cretaceous stratigraphy on the south and east sides of the Uinta Basin, northeastern Utah and northwestern Colorado: U.S. Geological Survey Bulletin 1787-P, 34 p.

Nuccio, V.R., and L.N.R. Roberts, 2003, Chapter 4 - Thermal maturity and oil and gas generation history of petroleum systems in the Uinta – Piceance province, Utah and Colorado, *in* Petroleum Systems and Geologic Assessment of Oil and Gas in the Uinta – Piceance Province, Utah and Colorado: U.S. Geological Survey Digital Data Series, DDS-69-B, 39 p.

Potter P. E, Maynard, J.B., and Pryor, W.A., 1980, Sedimentology of shale: New York, Springer-Verlag, 306 p.

Rock-Color Chart Committee, 1984, Rock-Color Chart: Geological Society of America: Boulder, Colorado, unpaginated.

Sprinkel, D.A., 1999, Digital geologic resources atlas of Utah: Utah Geological Survey Bulletin 129DF (CD-ROM).

Taylor, K.G., R.L. Gawthorpe, C.D. Curtis, J.D. Marshall,.and D.N. Awwiller, 2000, Carbonate cementation in a sequence-stratigraphic framework: Upper Cretaceous sandstones, Book Cliffs, Utah-Colorado: Journal of Sedimentary Research, v. 70, p. 360-372.

Willis, G.C., H.H. Doelling, and M.L. Ross, 1996, Geologic map of the Agate quadrangle, Grand County, Utah: Utah Geological Survey Map 168, 1:24,000.

Table 1. Lithofacies in Westwater measured section.

Color Code	Facies Name	Grain Size, Composition	Rock Color	Bedding, Faunal Characteristics	Weathering Characteristics	Interpretation
	Micritic Limestone	100% calcite	White	Massive beds (<10 cm) to <1 mm laminations	resistant ledges	marine precipitates (?)
	Cone-in-Cone Limestone	100% calcite	Dark Gray (N3)	Massive cone-in-cone structure, abundant ammonoids, pelecypods	resistant concretions < 1m diameter	diagenetically altered nodules
	Bentonite	Clay	White, Yellow-orange	< 1 mm laminations, no burrows	crumbly streaks	altered volcanic ashfall deposits
	Dark Gray Shale	Clay, rare pyrite	Black, dark to medium gray (N3,N4)	< 1 mm, no burrows, abundant fish scales	fissile, platy	marine suspension deposits
	Calcareous Gray Shale	Clay, calcite	Black, dark to medium gray (N3, N4)	< 1 mm laminations, no burrows	fissile	marine suspension deposits
	Gray Silty Shale	Clay, minor silt	Dark to medium gray (N4, N5)	< 1 mm laminations, fish scales, no burrows	blocky to fissile	marine suspension and turbidity? deposits
	Clayey Siltstone	Silt, lesser clay	Yellow-gray (5Y 7/2)	< 2 mm lamination, no burrows	blocky, slightly fissile	marine suspension & turbidity? deposits
	Burrowed Clayey-Sandy Siltstone	Silt, lesser clay, vfL sand, glauconitic	Yellow-gray (5Y 7/2)	100% sand-filled burrows	blocky, massive	marine suspension & turbidity? deposits,
	Silty Vfn-Fn Sandstone	Vfn-Fn sand, lessersilt	Yellow-gray (5Y 7/2), Lt. olive gray (5Y 5/2)	< 5 cm laminations, sand-filled burrows	slope-forming, blocky, massive	marine turbidity & traction deposits
	Rippled & Wavy Laminated Sandstone	vfU to fU Sand	Mod. Yellow-brown (10 YR 5/4)	dominantly unidirectional ripples, wavy laminations, sparse burrows	thin ledges	marine turbidity & storm deposits
	Macrofossil-rich Sandstone	fL and fU sand	Mod. Yellow-brown (10 YR 5/4)	100% burrowed, pelecypod-ammonoid shells/molds	discontinuous ledge	marine traction deposits & bioherm on firmground
	Swaley-Laminated Sandstone	fL and fU sand	Mod. Yellow-brown (10 YR 5/4)	swaley to slightly HCS sets in lenticular scours	isolated ledges	marine traction (storm) deposits filling scoured firmground
	Granule Sandstone	granules & Crs to fU sand	Mod. Yellow-brown (10YR 5/4), Lt. Olive-Gray (5Y 5/2)	thin (< 10 cm), lenses: shark teeth, abdt fossil pieces, ss & chert granules	non-resistant, in slope	marine lags deposited on firmground

Unit	From (m)	To (m)	thickness (m)	thickness (feet)	Facies	Top in database	Comments
37	93.0	91.5	1.5	4.9	Rippled & Wavy Lam Ss, Dk Gry Shale		
36	91.5	91.0	0.5	1.6	Dk Gry Shale		
35	91.5	87.0	4.5	14.8	Rippled & Wavy Lam Ss, Dk Gry Shale, CIC Ls concretions at base		
34	87.0	82.5	4.5	14.8	Dk Gry Shale, Bentonite, Rare Rippled & Wavy Lam Ss		
33	82.5	82.0	0.5	1.6	Lag at top, CIC concretionary Horizon, Dk Gray Sh	FJ1 @ appx 82.5m	possible sequence boundary interval, seaward shift in sand supply
32	82.0	79.8	2.2	7.2	Rippled & Wavy Lam Ss, Dk Gry Sh, Rare CIC concretions		
31	79.8	78.6	1.2	3.9	Dk Gray Sh		
30	78.6	78.2	0.4	1.3	Rippled & Wavy Lam Ss, Dk Gray Sh		
29	78.2	77.0	1.2	3.9	Dk Gray Shale, Rare Bentonite		
28	77.0	75.8	1.2	3.9	Rippled & Wavy Lam Ss, Dk Gray Sh, rare Bentonite		*Prionocyclus hyatti* @ 76 m
27	75.8	74.0	1.8	5.9	Dk Gray Sh, Rare Bentonite		
26	74.0	72.7	1.3	4.3	Gray Sh, Lenses of Rippled & Wavy Laminated Ss, Rare Bentonite		
25	72.7	71.7	1.0	3.3	Dk Gray to Black Sh	FJLM	Condensed interval, Organic-rich (see Geochemistry Discussion)
24	71.7	71.0	0.7	2.3	Clayey Siltstone		
23	71.0	68.9	2.1	6.9	Dk Gray Sh		
22	68.9	68.6	0.3	1.0	Lag at top, CIC concretionary Horizon, Swaley Lam Ss, Rippled & Wavy Lam Ss in Lenses		
21	68.6	63.7	4.9	16.1	Burrowed Clayey-Sandy Siltstone, 2 Bentonites		
20	63.7	63.2	0.5	1.6	Rippled & Wavy Lam Ss, burrowed	FE_SB_1 @ 63.7	Ferron Sequence boundary of Willis et al., 1996
19	63.2	62.7	0.5	1.6	CIC Concretionary Horizon, Dk Gray Sh		
18	62.7	56.7	6.0	19.7	Dk Gray Sh, Bentonite cluster	Bentonite_57	
17	56.7	46.5	10.2	33.5	Dk Gray Sh		
16	46.5	43.2	3.3	10.8	Dk Gray Sh, Bentonite cluster	Bentonite_46	possible condensed interval
15	43.2	42.6	0.6	2.0	Burrowed Clayey-Sandy Siltstone		
14	42.6	42.4	0.2	0.7	Swaley-Laminated Ss Lenses on Scour Surface		
13	42.4	38.7	3.7	12.1	Burrowed Clayey-Sandy Siltstone		
12	38.7	36.7	2.0	6.6	Dk Gray Sh, Bentonite cluster	Bentonite_38	Top of "Dakota Silt"
11	36.7	33.0	3.7	12.1	Silty VF-Fn Ss		Glauconitic poorly sorted Ss

Table 2. Stratigraphic units, Westwater measured section

Unit	From (m)	To (m)	thickness (m)	thickness (feet)	Facies	Top in database	Comments
10	33.0	31.8	1.2	3.9	Macrofossil-rich Ss	CW_SB_1	Coon Spring Sandstone bed of Willis et al., 1996, with *Collignoniceras woollgari*
9	31.8	29.8	2.0	6.6	Rippled & Wavy-bedded Ss		
8	29.8	27.4	2.4	7.9	Dk Gray Sh		
7	27.4	25.9	1.5	4.9	Dk Gray Sh, Bentonite cluster	Bentonite_27	
6	25.9	20.5	5.4	17.7	Dk Gray Sh		
5	20.5	20.4	0.1	0.3	Micritic Ls		Change from Calcareous to Non calcareous in outcrop
4	20.4	18.2	2.2	7.2	Calcareous Gray Sh		
3	18.2	16.6	1.6	5.2	Clayey Siltstone	MT_UNC @ 18.2	Lower-middle Turonian unconformityof Molenaar & Cobban (1991)
2	16.6	14.0	2.6	8.5	Silty VF-Fn Ss		
1	14.0	0.0	14.0	45.9	Dakota Ss	Dakota	Top of "Dakota SS" map unit of Willis et al., 1996

Table 2. Stratigraphic units, Westwater measured section

Table 3
Colorado School of Mines, #1 Larsen State

HGS No.	Well Name	Top Depth (ft.)	Bottom Depth (ft.)	Median Depth (ft.)	Sample Type	Leco TOC	S1	S2	S3	Tmax (°C)	Calc. %Ro	HI	OI	S2/S3	S1/TOC	PI	Notes Checks	Notes Pyrogram
06-3448-134553	#1 Larsen State	473	483	478	cuttings	0.72	0.17	0.51	0.30	432	0.62	71	42	2	24	0.25	c, lc	n
06-3448-134554	#1 Larsen State	483	491	487	cuttings	0.75	0.12	0.36	0.19	434 *	0.65	48	25	2	16	0.25		n
06-3448-134555	#1 Larsen State	491	500	495.5	cuttings	0.84	0.13	0.45	0.20	435 *	0.67	54	24	2	15	0.22		n
06-3448-134556	#1 Larsen State	500	510	505	cuttings	0.87	0.13	0.52	0.20	436	0.69	60	23	3	15	0.20		n
06-3448-134557	#1 Larsen State	510	522	516	cuttings	1.13	0.17	1.03	0.32	436	0.69	91	28	3	15	0.14	lc	n
06-3448-134558	#1 Larsen State	522	530	526	cuttings	1.07	0.17	1.18	0.24	436	0.69	110	22	5	16	0.13		n
06-3448-134559	#1 Larsen State	530	542	536	cuttings	0.71	0.12	0.47	0.18	439 *	0.74	66	25	3	17	0.20		n
06-3448-134560	#1 Larsen State	542	552	547	cuttings	0.65	0.10	0.31	0.17	437 *	0.71	48	26	2	15	0.24		n
06-3448-134561	#1 Larsen State	552	562	557	cuttings	0.70	0.13	0.45	0.19	435 *	0.67	64	27	2	19	0.22		n
06-3448-134562	#1 Larsen State	562	575	568.5	cuttings	0.84	0.14	0.61	0.24	437	0.71	73	29	3	17	0.19		n
06-3448-134563	#1 Larsen State	575	584	579.5	cuttings	0.94	0.19	0.81	0.21	437	0.71	86	22	4	20	0.19	lc	n
06-3448-134564	#1 Larsen State	595	604	599.5	cuttings	0.93	0.20	0.84	0.21	437	0.71	90	23	4	22	0.19		n
06-3448-134565	#1 Larsen State	604	612	608	cuttings	0.91	0.19	0.74	0.21	437	0.71	81	23	4	21	0.20		n
06-3448-134566	#1 Larsen State	612	623	617.5	cuttings	0.90	0.17	0.64	0.22	436	0.69	71	24	3	19	0.21		n
06-3448-134567	#1 Larsen State	623	634	628.5	cuttings	1.05	0.20	0.97	0.26	437	0.71	92	25	4	19	0.17		n
06-3448-134568	#1 Larsen State	634	642	638	cuttings	1.18	0.19	0.85	0.27	438	0.72	72	23	3	16	0.18		n
06-3448-134569	#1 Larsen State	642	652	647	cuttings	1.12	0.22	0.89	0.32	435	0.67	79	29	3	20	0.20	lc	n
06-3448-134570	#1 Larsen State	652	660	656	cuttings	0.99	0.18	0.69	0.25	437	0.71	70	25	3	18	0.21		n
06-3448-134571	#1 Larsen State	660	665	662.5	cuttings	1.03	0.18	0.60	0.34	438	0.72	58	33	2	17	0.23		n
06-3448-134572	#1 Larsen State	665	670	667.5	cuttings	1.36	0.22	1.21	0.39	438	0.72	89	29	3	16	0.15		n
06-3448-134573	#1 Larsen State	670	676	673	cuttings	1.44	0.28	1.24	0.35	436	0.69	86	24	4	19	0.18	lc	n
06-3448-134574	#1 Larsen State	676	682	679	cuttings	1.36	0.29	1.52	0.33	436	0.69	112	24	5	21	0.16	c	n
06-3448-134575	#1 Larsen State	682	690	686	cuttings	1.26	0.18	0.51	0.46	437	0.71	40	37	1	14	0.26		n
06-3448-134576	#1 Larsen State	690	699	694.5	cuttings	1.28	0.31	1.80	0.26	437	0.71	141	20	7	24	0.15		n
06-3448-134577	#1 Larsen State	711	725	718	cuttings	1.66	0.30	1.34	0.56	436	0.69	81	34	2	18	0.18		n
06-3448-134578	#1 Larsen State	725	733	729	cuttings	1.57	0.31	2.58	0.34	437	0.71	164	22	8	20	0.11		n
06-3448-134579	#1 Larsen State	733	741	737	cuttings	1.42	0.32	2.34	0.33	438	0.72	165	23	7	23	0.12	lc	n
06-3448-134580	#1 Larsen State	741	750	745.5	cuttings	1.53	0.36	2.75	0.38	438	0.72	180	25	7	24	0.12		n
06-3448-134581	#1 Larsen State	750	757	753.5	cuttings	1.65	0.36	2.81	0.41	435	0.67	170	25	7	22	0.11		n
06-3448-134582	#1 Larsen State	757	767	762	cuttings	1.43	0.31	2.10	0.37	437	0.71	147	26	6	22	0.13		n
06-3448-134583	#1 Larsen State	767	775	771	cuttings	2.49	0.55	7.14	0.46	437	0.71	287	18	16	22	0.07		n
06-3448-134584	#1 Larsen State	775	783	779	cuttings	1.39	0.30	1.62	0.40	437	0.71	117	29	4	22	0.16		n
06-3448-134585	#1 Larsen State	783	790	786.5	cuttings	1.70	0.31	1.35	0.51	438	0.72	79	30	3	18	0.19		n
06-3448-134586	#1 Larsen State	790	797	793.5	cuttings	1.88	0.40	2.92	0.50	437	0.71	155	27	6	21	0.12	lc	n
06-3448-134587	#1 Larsen State	797	804	800.5	cuttings	1.92	0.44	4.10	0.43	437	0.71	214	22	10	23	0.10		n
06-3448-134588	#1 Larsen State	804	812	808	cuttings	1.94	0.44	4.07	0.48	438	0.72	210	25	8	23	0.10		n
06-3448-134589	#1 Larsen State	812	820	816	cuttings	1.78	0.44	3.33	0.51	438	0.72	187	29	7	25	0.12		n
06-3448-134590	#1 Larsen State	820	829	824.5	cuttings	1.99	0.49	6.82	0.34	436	0.69	343	17	20	25	0.07	c	n
06-3448-134591	#1 Larsen State	829	841	835	cuttings	1.84	0.47	7.56	0.26	434	0.65	411	14	29	26	0.06	c	n
06-3448-134592	#1 Larsen State	841	852	846.5	cuttings	2.46	0.53	9.55	0.44	437	0.71	388	18	22	22	0.05	lc	n
06-3448-134593	#1 Larsen State	852	861	856.5	cuttings	2.16	0.62	8.72	0.30	436	0.69	404	14	29	29	0.07		n
06-3448-134594	#1 Larsen State	861	870	865.5	cuttings	2.21	0.52	7.93	0.51	435	0.67	359	23	16	24	0.06		n
06-3448-134595	#1 Larsen State	870	880	875	cuttings	2.52	0.72	11.52	0.27	435	0.67	457	11	43	29	0.06		n
06-3448-134596	#1 Larsen State	880	890	885	cuttings	2.45	0.58	10.44	0.31	434	0.65	426	13	34	24	0.05		n

Table 3
Colorado School of Mines, #1 Larsen State

HGS No.	Well Name	Top Depth (ft.)	Bottom Depth (ft.)	Median Depth (ft.)	Sample Type	Leco TOC	S1	S2	S3	Tmax (°C)	Calc. %Ro	HI	OI	S2/S3	S1/TOC	PI	Notes Checks	Notes Pyrogram
06-3448-134597	#1 Larsen State	890	900	895	cuttings	1.23	0.26	2.05	0.27	436	0.69	167	22	8	21	0.11	lc	n
06-3448-134598	#1 Larsen State	900	909	904.5	cuttings	1.27	0.31	2.60	0.27	436	0.69	205	21	10	24	0.11		n
06-3448-134599	#1 Larsen State	909	920	914.5	cuttings	1.49	0.34	2.42	0.34	436	0.69	162	23	7	23	0.12		n
06-3448-134600	#1 Larsen State	930	940	935	cuttings	0.79	0.16	0.47	0.28	433 *	0.63	59	35	2	20	0.25	lc	n
06-3448-134601	#1 Larsen State	940	948	944	cuttings	0.93	0.20	0.95	0.28	435	0.67	102	30	3	22	0.17		n
06-3448-134602	#1 Larsen State	948	954	951	cuttings	0.70	0.19	0.91	0.23	436	0.69	130	33	4	27	0.17		n
06-3448-134603	#1 Larsen State	954	959	956.5	cuttings	0.76	0.18	0.96	0.18	436	0.69	126	24	5	24	0.16		n
06-3448-134604	#1 Larsen State	959	963	961	cuttings	0.81	0.18	0.73	0.21	434	0.65	90	26	3	22	0.20		n
06-3448-134605	#1 Larsen State	963	968	965.5	cuttings	0.87	0.21	0.85	0.21	432	0.62	98	24	4	24	0.20		n
06-3448-134606	#1 Larsen State	968	974	971	cuttings	0.46	0.16	0.49	0.12	433 *	0.63	107	26	4	35	0.25	lc	n
06-3448-134607	#1 Larsen State	974	980	977	cuttings	0.44	0.18	0.50	0.11	434	0.65	114	25	5	41	0.26		n
06-3448-134608	#1 Larsen State	980	985	982.5	cuttings	0.46	0.14	0.43	0.11	432 *	0.62	93	24	4	30	0.25		n
06-3448-134609	#1 Larsen State	985	991	988	cuttings	0.50	0.15	0.39	0.08	434 *	0.65	78	16	5	30	0.28		n
06-3448-134610	#1 Larsen State	991	1000	995.5	cuttings	0.74	0.13	0.66	0.21	435	0.67	89	28	3	18	0.16		n
06-3448-134611	#1 Larsen State	1000	1007	1003.5	cuttings	0.80	0.17	0.63	0.19	435	0.67	79	24	3	21	0.21		n
06-3448-134612	#1 Larsen State	1007	1015	1011	cuttings	0.79	0.18	0.89	0.24	435	0.67	113	30	4	23	0.17		n
06-3448-134613	#1 Larsen State	1015	1024	1019.5	cuttings	0.90	0.19	1.22	0.17	436	0.69	136	19	7	21	0.13		n
06-3448-134614	#1 Larsen State	1024	1034	1029	cuttings	1.02	0.27	1.89	0.19	436	0.69	185	19	10	26	0.13	lc	n
06-3448-134615	#1 Larsen State	1034	1040	1037	cuttings	0.67	0.17	0.57	0.23	437	0.71	85	34	2	25	0.23		n
06-3448-134616	#1 Larsen State	1040	1046	1043	cuttings	0.75	0.18	0.74	0.24	437	0.71	99	32	3	24	0.20		n
06-3448-134617	#1 Larsen State	1046	1053	1049.5	cuttings	0.74	0.22	0.75	0.22	437	0.71	101	30	3	30	0.23		n
06-3448-134618	#1 Larsen State	1053	1059	1056	cuttings	0.73	0.18	0.64	0.24	437	0.71	88	33	3	25	0.22		n
06-3448-134619	#1 Larsen State	1059	1065	1062	cuttings	0.74	0.20	0.63	0.19	435	0.67	85	26	3	27	0.24	lc	
06-3448-134620	#1 Larsen State	1065	1073	1069	cuttings	0.74	0.19	0.74	0.19	437	0.71	100	26	4	26	0.20		n
06-3448-134621	#1 Larsen State	1073	1080	1076.5	cuttings	0.69	0.19	0.67	0.21	435	0.67	97	30	3	28	0.22		n
06-3448-134622	#1 Larsen State	1080	1087	1083.5	cuttings	0.70	0.19	0.63	0.18	435	0.67	90	26	3	27	0.23		n
06-3448-134623	#1 Larsen State	1087	1096	1091.5	cuttings	4.32	0.25	3.63	0.37	441	0.78	84	9	10	6	0.06	lc	n
06-3448-134624	#1 Larsen State	1096	1100	1098	cuttings	1.67	0.18	1.91	0.27	443	0.81	114	16	7	11	0.09		n
06-3448-134625	#1 Larsen State	1100	1105	1102.5	cuttings	0.75	0.13	0.52	0.15	438	0.72	69	20	3	17	0.20		n
						1.23												

Note: "-1" indicates not measured or meaningless ratio

* Tmax data not reliable due to poor S2 peak

TOC = weight percent organic carbon in rock
S1, S2 = mg hydrocarbons per gram of rock
S3 = mg carbon dioxide per gram of rock
Tmax = °C

HI = hydrogen index = S2 x 100 / TOC
OI = oxygen index = S3 x 100 / TOC
S1/TOC = normalized oil content = S1 x 100 / TOC
PI = production index = S1 / (S1+S2)
Calculcated%VRo = 0.0180 x Tmax - 7.16 (Jarvie et al., 2001)
Measured %Ro = measured vitrinite reflectance

Notes:
c = Rock-Eval analysis checked and confirmed
lc = Leco TOC analysis checked and confirmed

Pyrogram:
n=normal
ltS2sh = low temperature S2 shoulder
ltS2p = low temperature S2 peak
htS2p = high temperature S2 peak
f = flat S2 peak
na = printer malfunction pyrogram not available

Table 4
Thermal Alteration, Kerogen Type, and Palynofacies

Colorado School of Mines
#1 Larsen State

				Source Quality						% Source Material							Preservation			Recovery		Palynofacies						Ro Data		
HGS ID	Depth 1 (ft.)	Depth 2 (ft.)	Mean Depth (ft.)	TOC	S2	Hydrogen Index (HI)	Tmax (°C)	Color	TAI	Amorphinite Debris	Finely Dissem. OM	Herb. Plant Debris	Woody Plant Debris	Coaly Fragments	Algal Debris	Palynomorphs	GOOD	FAIR	POOR	Very poor	Barren	MARINE	NEARSHORE	CONTINENTAL	LACUSTRINE	UNKNOWN	% OM Fluorescing	Measured Ro (%)	No. of Readings	*Comments*
06-3448-134558	522	530	526	1.07	1.18	110	436	OB	2+	95				5		P			X			X					0	0.68	28	
06-3448-134565	604	612	608	0.91	0.74	81	437	OB	2+	95				5		R			X			X					0	0.73	29	
06-3448-134575	682	690	686	1.26	0.51	40	437	OB	2+	98				2		N			X			X					0	0.74	23	
06-3448-134578	725	733	729	1.57	2.58	164	437	OB	2+	98				2		N			X			X					0	0.80	29	
06-3448-134595	870	880	875	2.52	11.52	457	435	OB	2+	98				20		N			X			X					0	0.81	29	
06-3448-134604	959	963	961	0.81	0.73	90	434	OB	2+	20				80		R			X			X					0	0.83	26	
06-3448-134623	1087	1096	1091.5	4.32	3.63	64	441	LB	3	80				20		C			X			X					0	0.89	28	

*Tmax data not reliable due to poor S2 peak

Color Abbreviations:

GLY	Green-Light Yellow	B	Brown
Y	Yellow	DBDG	Dark Brown-Dark Gray
YO	Yellow-Orange	DGBL	Dark Gray-Black
OB	Orange-Brown	BLK	Black
LB	Light Brown		

TAI Scale:

1=Unaltered	4=Strong alteration
1+ or 1.5	4+ or 4.5
2=Slight alteration	5=Severe alteration
2+ or 2.5	
3=Moderate alteration	
3+ or 3.5	

Palynomorph Key

A = Abundar
C = Common
P = Present
R = Rare
N = None Seen

Table 5.
Carbon and oxygen isotopic analyis of carbonate from Larsen State-1 well

Well Name	Top Depth (ft.)	Bottom Depth (ft.)	Median Depth (ft.)	Sample Type	δ18O (SMOW)	δ18 O	δ13C
#1 Larsen State	530	542	536	cuttings	24.15	-6.513	-2.76
#1 Larsen State	552	562	557	cuttings	23.79	-6.854	-0.43
#1 Larsen State	604	612	608	cuttings	22.10	-8.502	-1.17
#1 Larsen State	642	652	647	cuttings	24.48	-6.192	0.25
#1 Larsen State	682	690	686	cuttings	23.73	-6.915	-0.13
#1 Larsen State	725	733	729	cuttings	23.72	-6.928	0.09
#1 Larsen State	767	775	771	cuttings	23.49	-7.146	0.09
#1 Larsen State	797	804	800.5	cuttings	23.91	-6.745	0.28
#1 Larsen State	852	861	856.5	cuttings	21.04	-9.522	-0.63
#1 Larsen State	880	890	885	cuttings	21.87	-8.723	-1.59
#1 Larsen State	968	974	971	cuttings	15.14	-15.249	-7.14
#1 Larsen State	980	985	982.5	cuttings	14.66	-15.714	-8.77
#1 Larsen State	1024	1034	1029	cuttings	25.24	-5.450	0.24
#1 Larsen State	1087	1096	1091.5	cuttings	23.48	-7.158	0.03
#1 Larsen State	1096	1100	1098	cuttings	23.32	-7.310	-0.02

Table 6.
Results of X-Ray Diffraction Analysis

3 = major, 2 = minor, 1 = trace, 0 = not detected

Well Name	Top Depth (ft.)	Bottom Depth (ft.)	Median Depth (ft.)	Sample Type	calcite	dolomite	glauconite	kaolinite	albite	ksp	pyrite
#1 Larsen State	530	542	536	cuttings	3	2	2	1	2	2	0
#1 Larsen State	552	562	557	cuttings	3	2	2	2	2	2	0
#1 Larsen State	604	612	608	cuttings	3	2	2	1	1	2	0.5
#1 Larsen State	642	652	647	cuttings	3	2	1	1	1	2	0.5
#1 Larsen State	725	733	729	cuttings	3	1	2	2	1	2	1
#1 Larsen State	767	775	771	cuttings	3	1	2	2	1	1	0.5
#1 Larsen State	852	861	856.5	cuttings	3	0	2	2	0	1	1
#1 Larsen State	880	890	885	cuttings	2	0	2	2	1	1	1
#1 Larsen State	968	974	971	cuttings	1	1	2	1	2	1	0
#1 Larsen State	980	985	982.5	cuttings	2	0	2	1	2	1	0
#1 Larsen State	1024	1034	1029	cuttings	1	2	2	1	2	2	0.5
#1 Larsen State	1087	1096	1091.5	cuttings	1	0	2	1	1	2	0

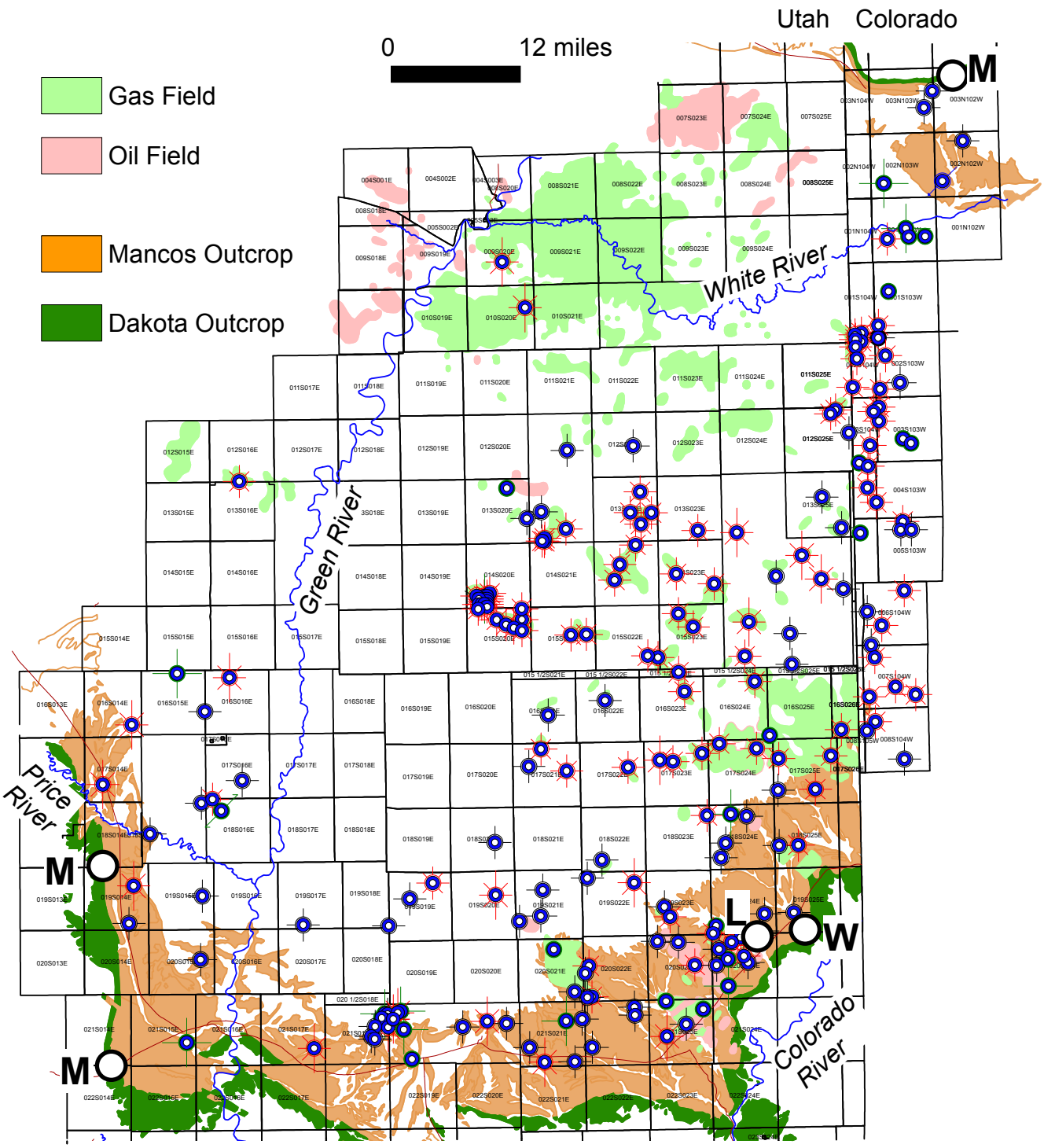

Figure 1. Study area showing Mancos-Dakota outcrop belts, wells used in study, the Larsen State-1 well (circle, labeled "L"), Westwater measured section (circle, labeled "W"), three measured sections by Moleaar and Cobban (1991; circles labeled "M"), and basic geography of southern and southeastern Uinta basin. Land grid is in townships. Compiled from Sprinkel, (1999), Hintze et al., (2000), Chidsey et al., (2004), Greene (1992).

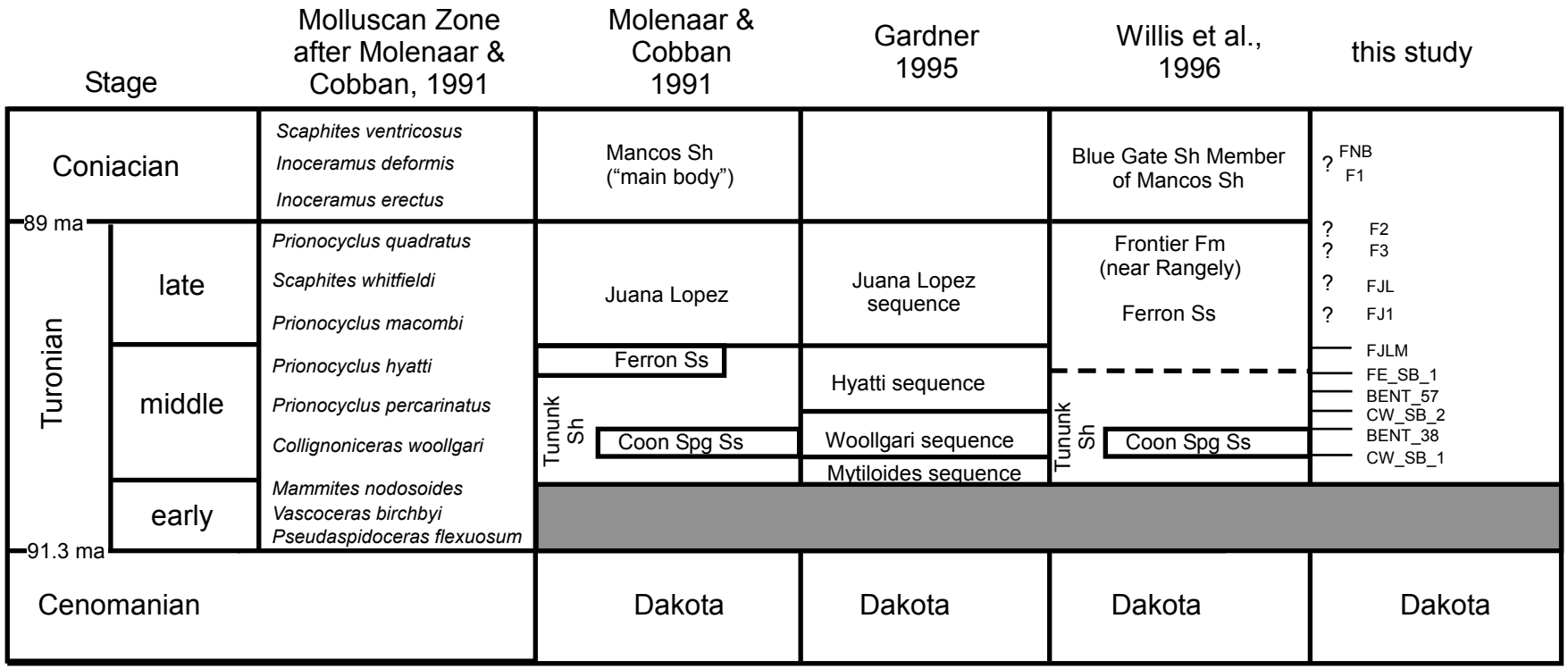

Figure 2. Correlation of stratigraphic units for lower Mancos interval of this study. Gray shading indicates a hiatus. Compiled from Molenaar and Cobban (1991) and other references noted at top of each column. Rational for column labeled "this study" is developed in text. Questions marks indicate uncertainty in assignment of molluscan zone, which is based on correlation. Mnemonics for tops in the study are as follows: BENT = bentonite; CW= Coon Springs-Woollgari; F, FE = Ferron; JL, J=Juana Lopez; M=Molenaar; NB=Niobrara; SB=sequence boundary. Numbers indicate position in Westwater measured section or general position in lower Mancos interval.

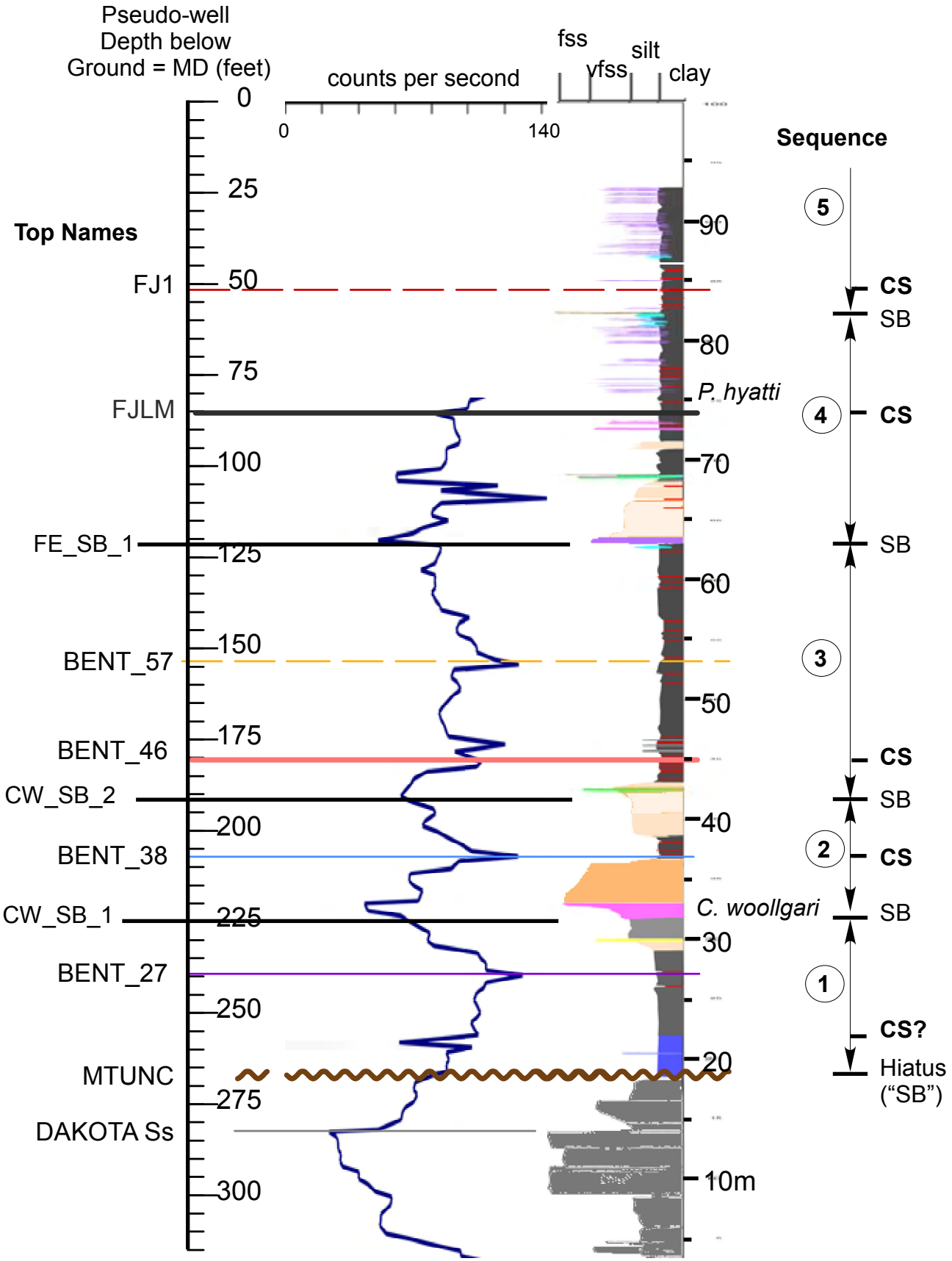

Figure 3. Westwater measured section (section 33, T 19S, R25E) with facies interpretations, outcrop gamma ray log and key tops in database, including five sequences with sequence boundaries (SB) and condensed sections (CS) interpreted for this study. Index ammonites *P. hyatti* and *C. woollgari* discussed in text. Facies colors as in Table 1. For field data sheets, see Appendix A.

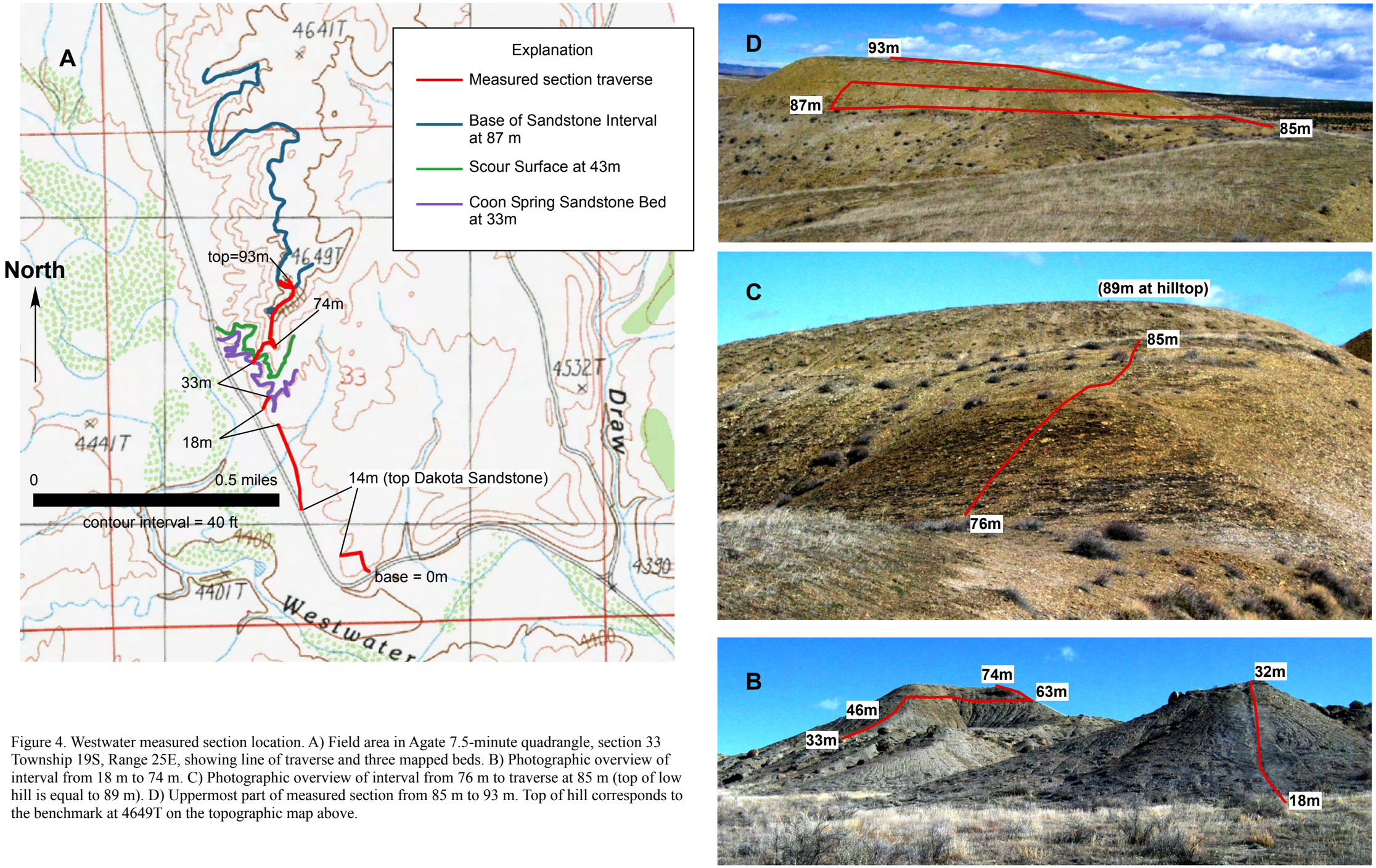

Figure 4. Westwater measured section location. A) Field area in Agate 7.5-minute quadrangle, section 33 Township 19S, Range 25E, showing line of traverse and three mapped beds. B) Photographic overview of interval from 18 m to 74 m. C) Photographic overview of interval from 76 m to traverse at 85 m (top of low hill is equal to 89 m). D) Uppermost part of measured section from 85 m to 93 m. Top of hill corresponds to the benchmark at 4649T on the topographic map above.

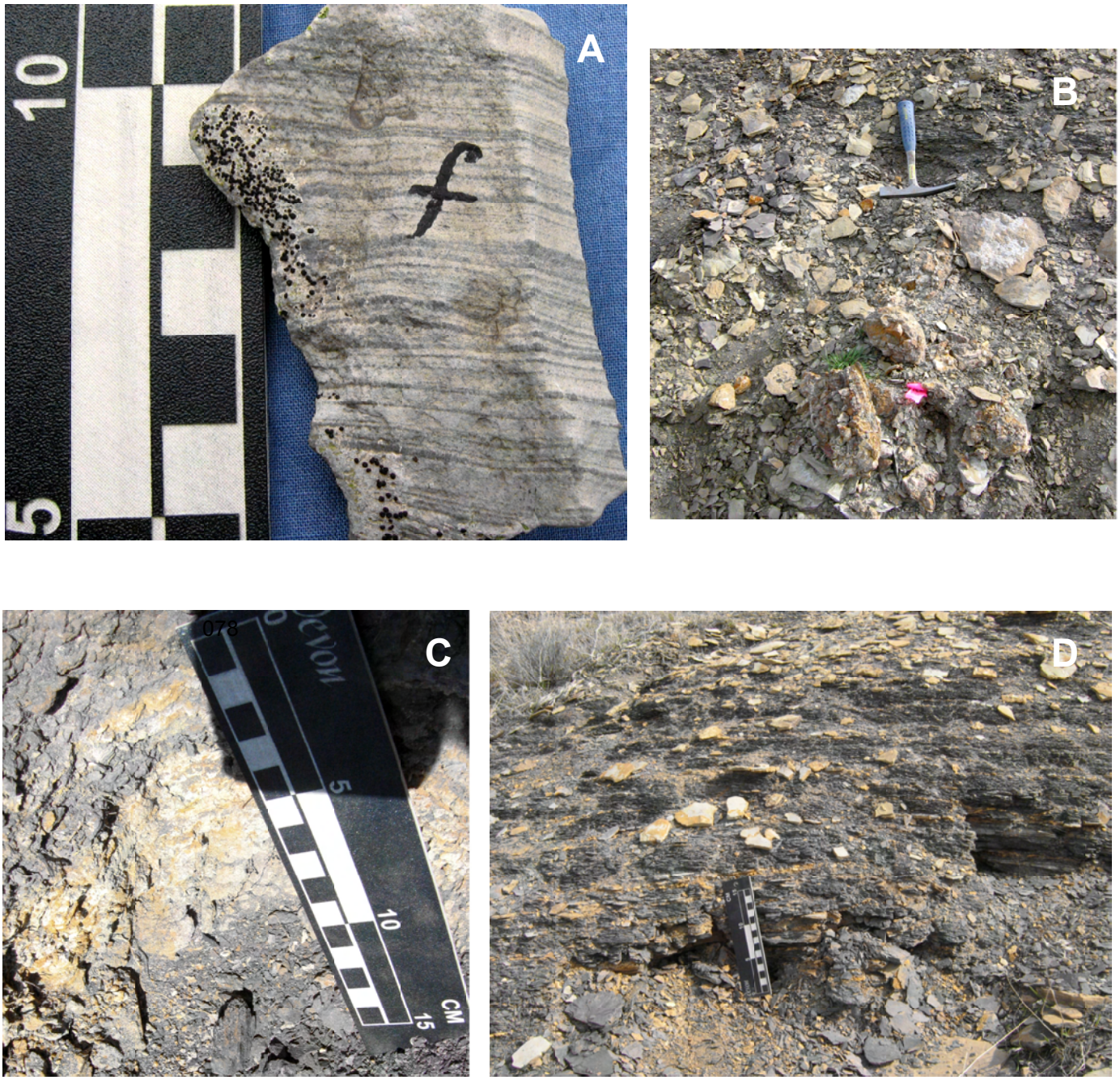

Figure 5. Carbonate, bentonite and shale facies of the Westwater measured section. Ruler in cm, pick is 24 cm. A) Laminated micritic limestone at 20.5 m. B) Cone-in-cone limestone concretion horizon (at pink flag) at 87 m. Pick rests on fissile dark-gray shale. C) Altered volcanic ash beds (bentonites) at 73. D) Fissile dark-gray shale at 84 m. Orange streaks are weathered horizons, possibly slightly bentonitic.

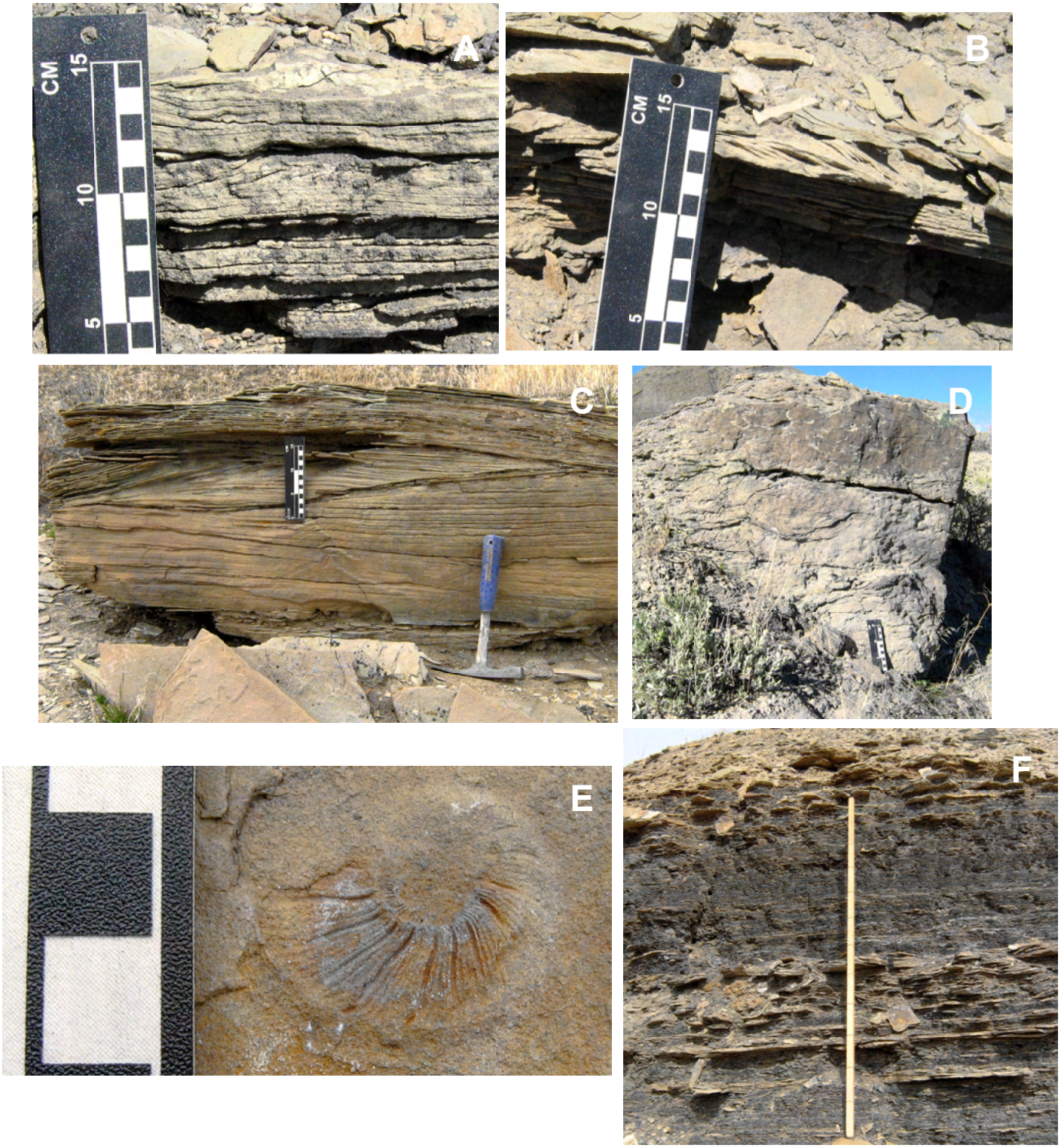

Figure 6. Sandstone facies of the Westwater measured section. Ruler in cm, pick is 24 cm long, stick is 1.5 m long. A) Rippled and wavy bedded very-fine sandstone succession at 68.6 m is laterally discontinuous. B) Combined-flow ripple lamination shows rounded crests, suggesting wave modification: rippled and wavy bedded facies at 74 m. C) Swaley to hummocky cross-stratified fine sandstone at 42.5 m consists of discontinuous lenses filling shallow scours along a mappable horizon in the outcrop belt at Westwater. D) Macrofossil-rich sandstone with faint internal scours forms distinctive mappable concretionary horizon termed the "Coon Spring Sandstone bed" with commonly abundant *Collignoniceras woollgari*. E) *Prionocyclus hyatt*i, juvenile form at 76 m, identified by Dr. William Cobban, USGS emeritus. F) Overview of rippled and wavy bedded sandstone separated by dark-gray shale at approximately 88 to 90 m.

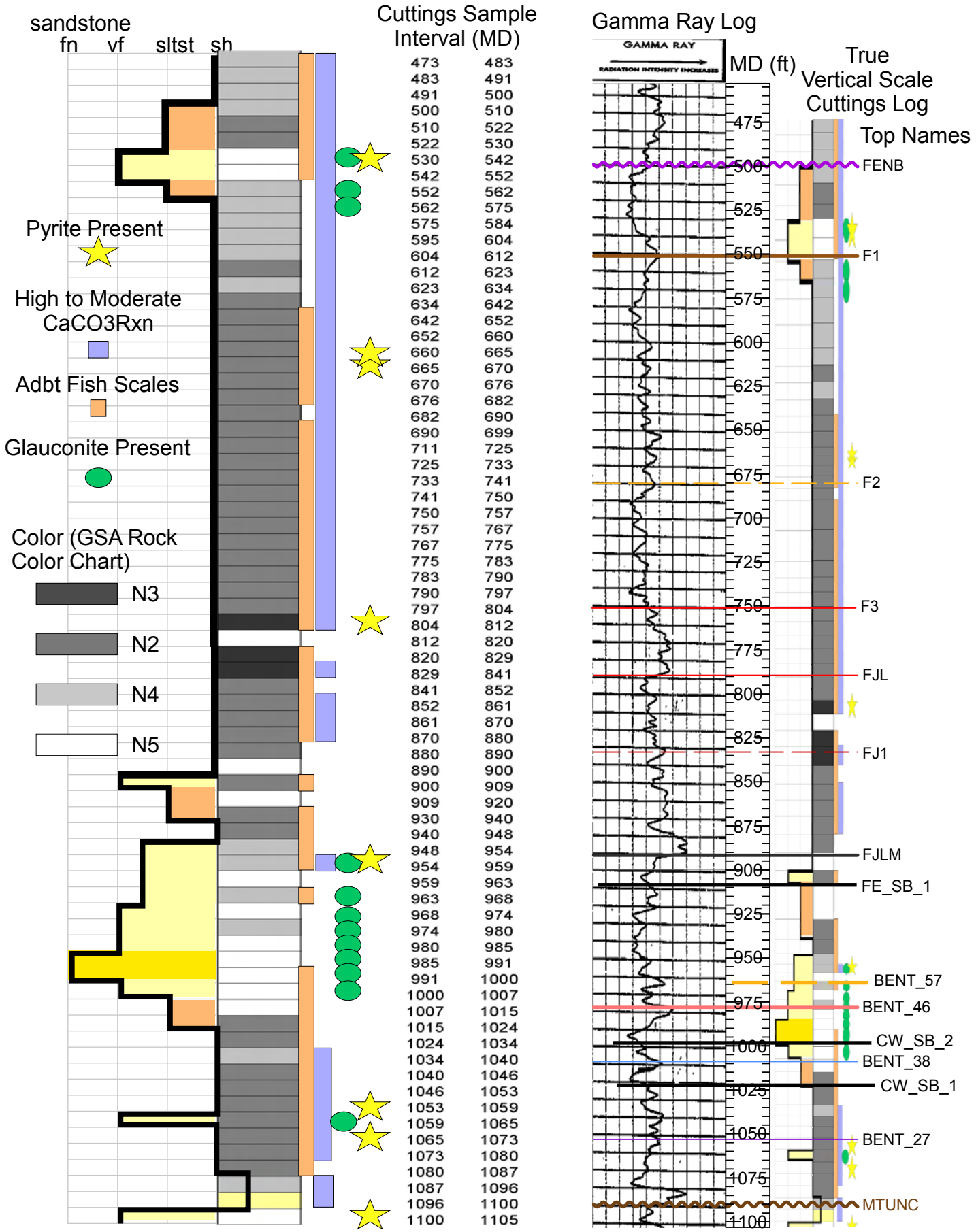

Figure 7. Carter Larsen State-1 (API 4301915317, section 2, T20S, R24E) cuttings description strip log (version on left is not to true vertical scale), gamma ray log, and tops.

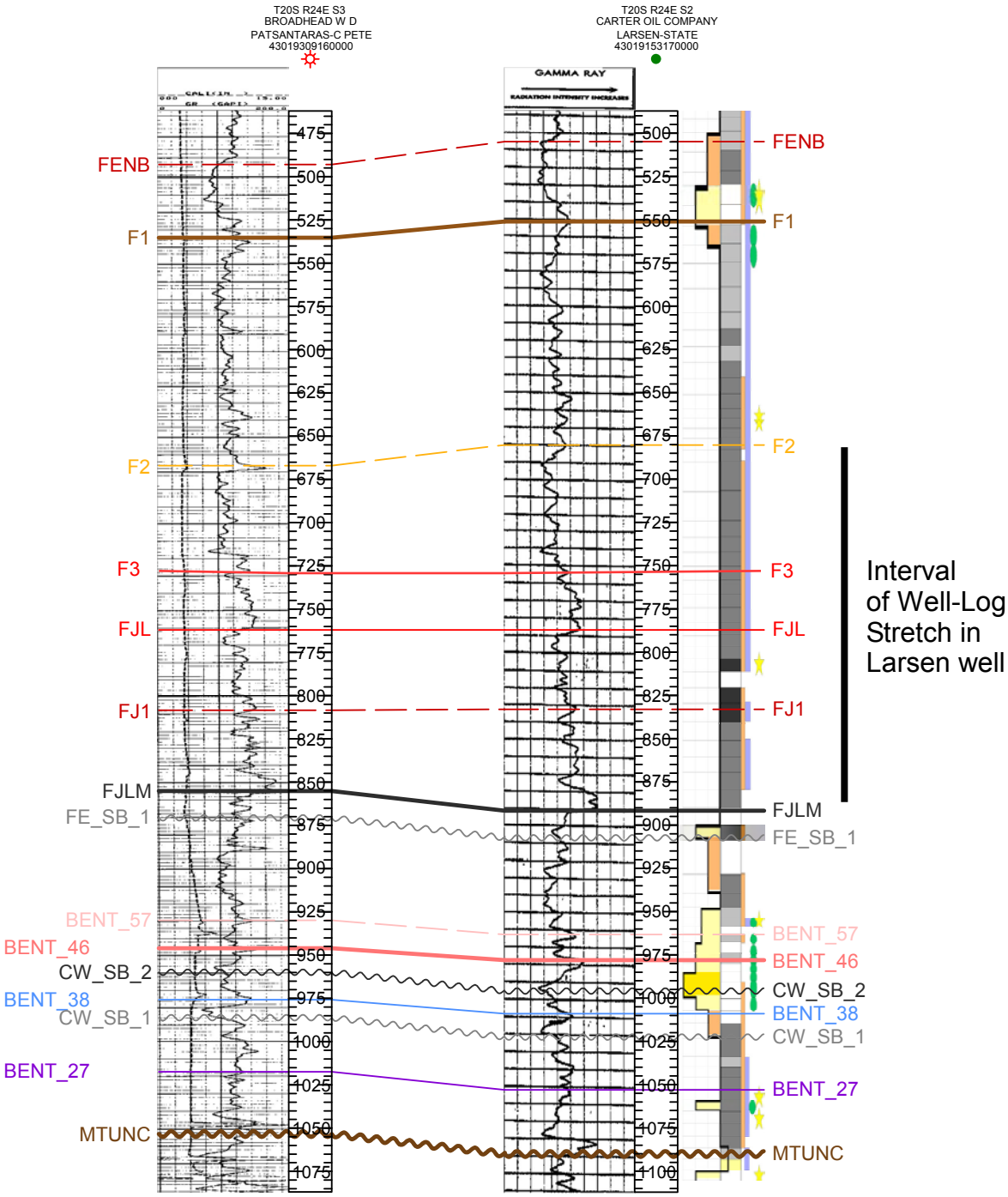

Isochore Interval	Broadhead	Larsen	% Difference (x)	arcsin x/100
F2 to FJL	94.9	106.9	13%	7*
FJL to FJ1	93.2	104.6	12%	6.8*
FJ1 to FJLM	46.6	58.7	25%	14.4*

Figure 8. Comparison of log stretch in Carter Larsen State-1 to the Broadhead Patsantaras-C (API 4301930916, section 3, T20S, R24E), which is 2 km to east and drilled through flat-lying strata. Comparison of isochore values for intervals between markers FJLM and F2 suggest steep dips or a deviated wellbore path in the Carter Larsen well (discussed in text).

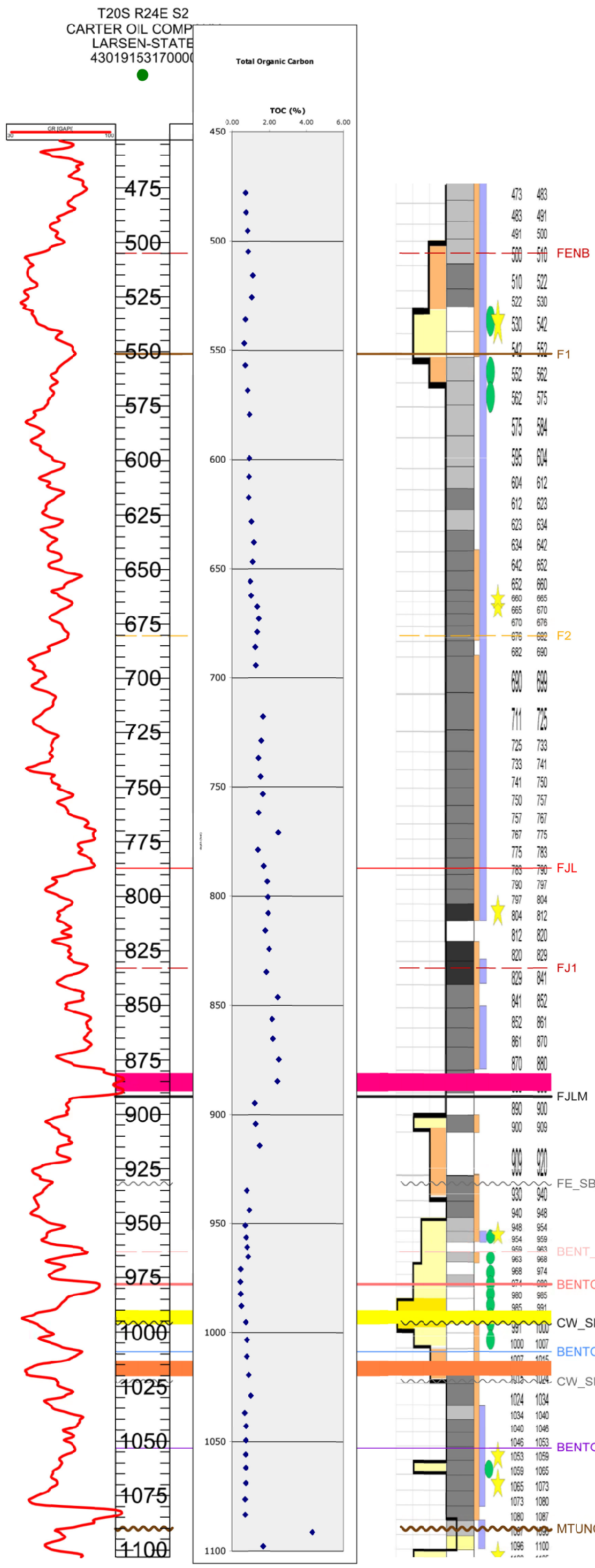

Figure 9. Larsen State-1: Total Organic Carbon data. Colored bars and tops discussed in text.

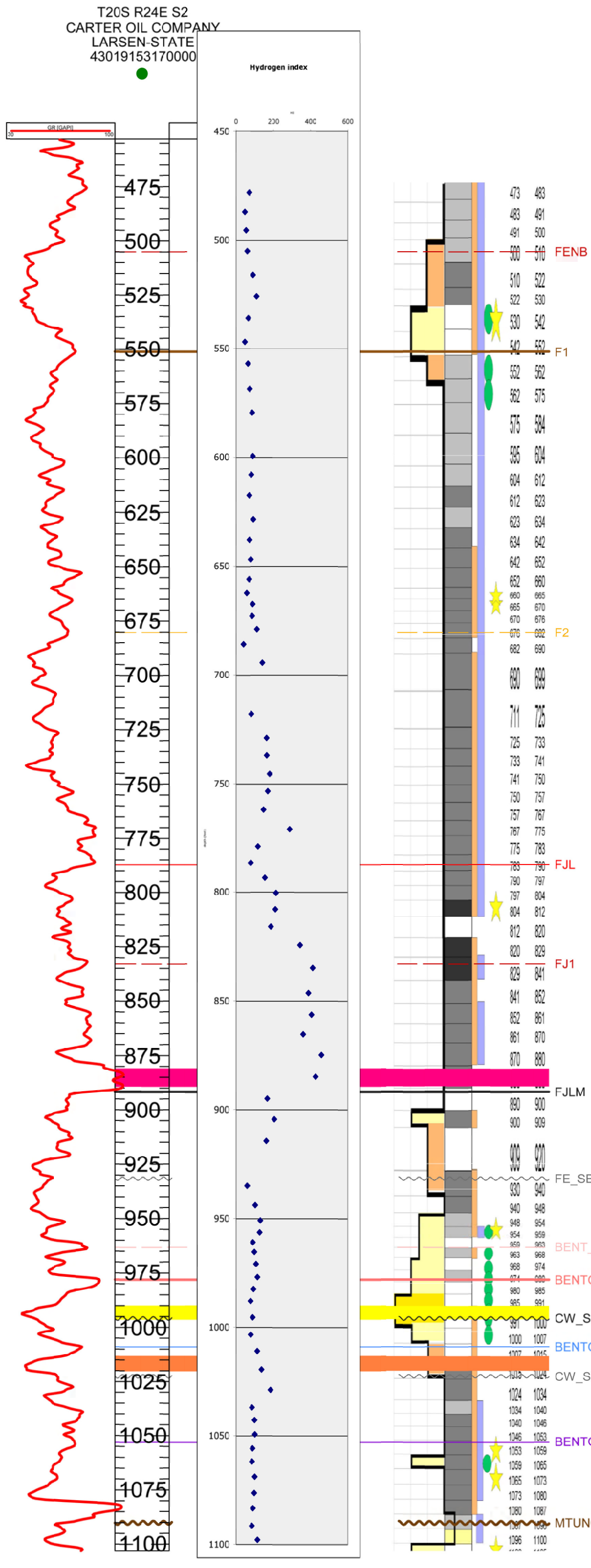

Figure 10. Larsen State-1: Hydrogen Index (from Rock-Eval analysis) data. Colored bars and tops discussed in text.

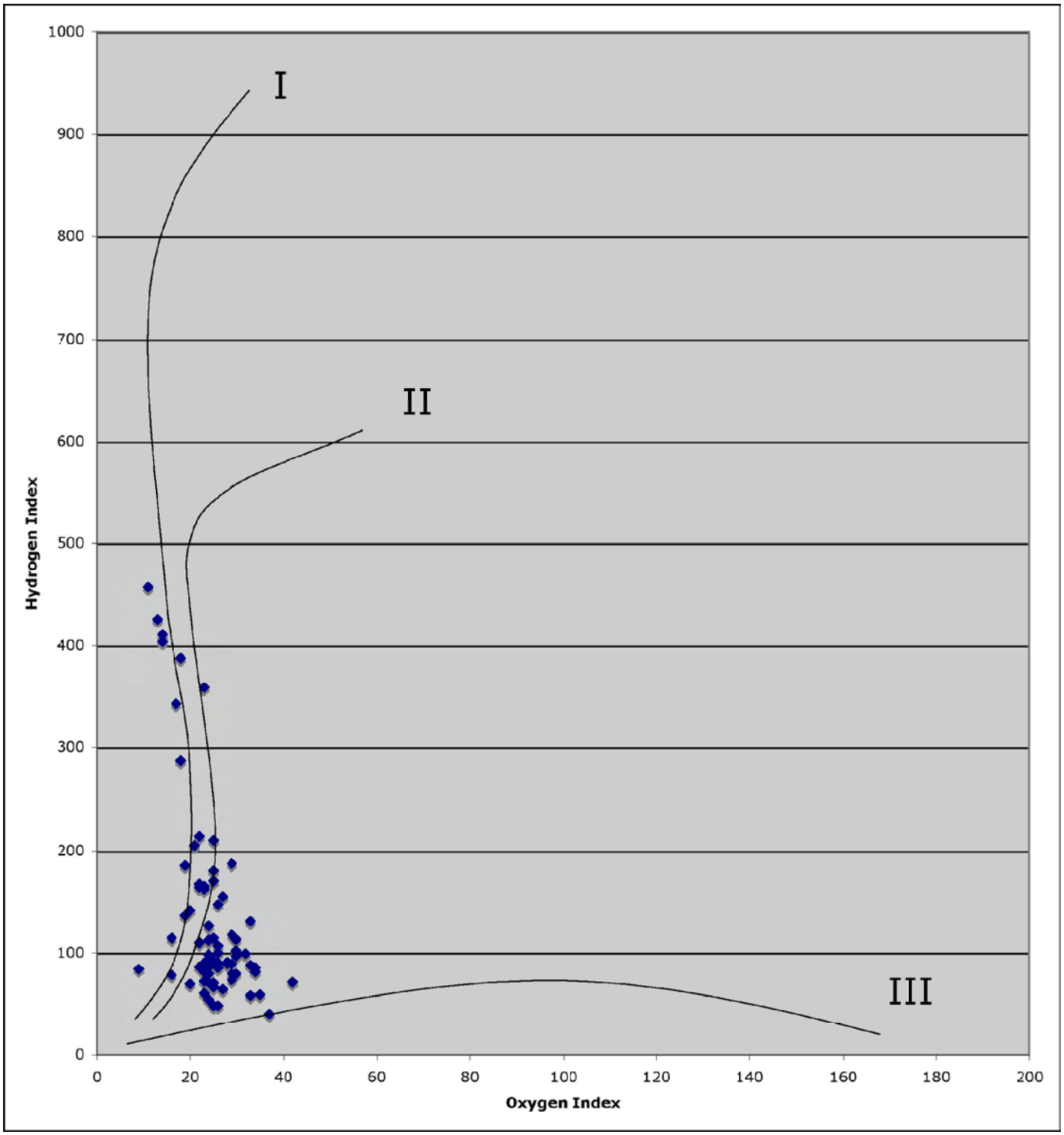

Figure 11. Larsen State-1: Cross-plot of hydrogen index and oxygen index (from Rock-Eval analysis) data.

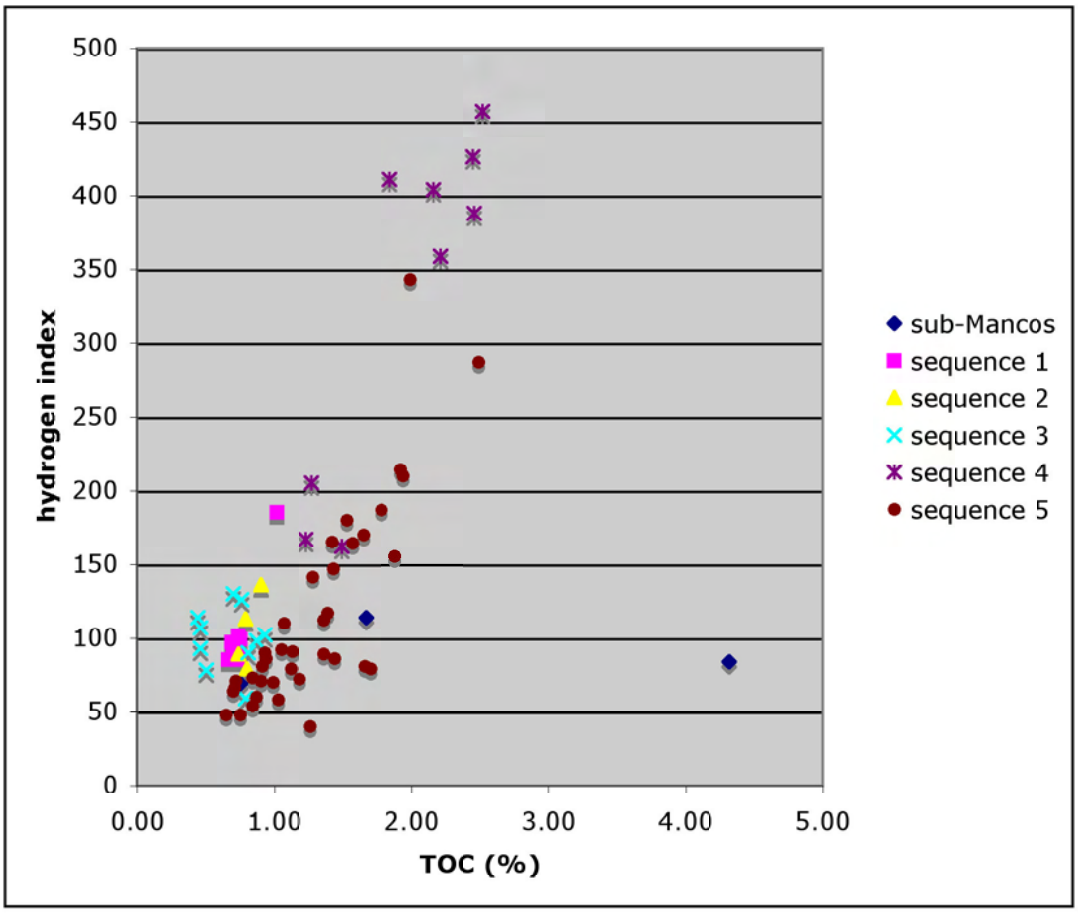

Figure 12. Larsen State-1: Cross-plot of Total Organic Carbon and hydrogen index data by sequence.

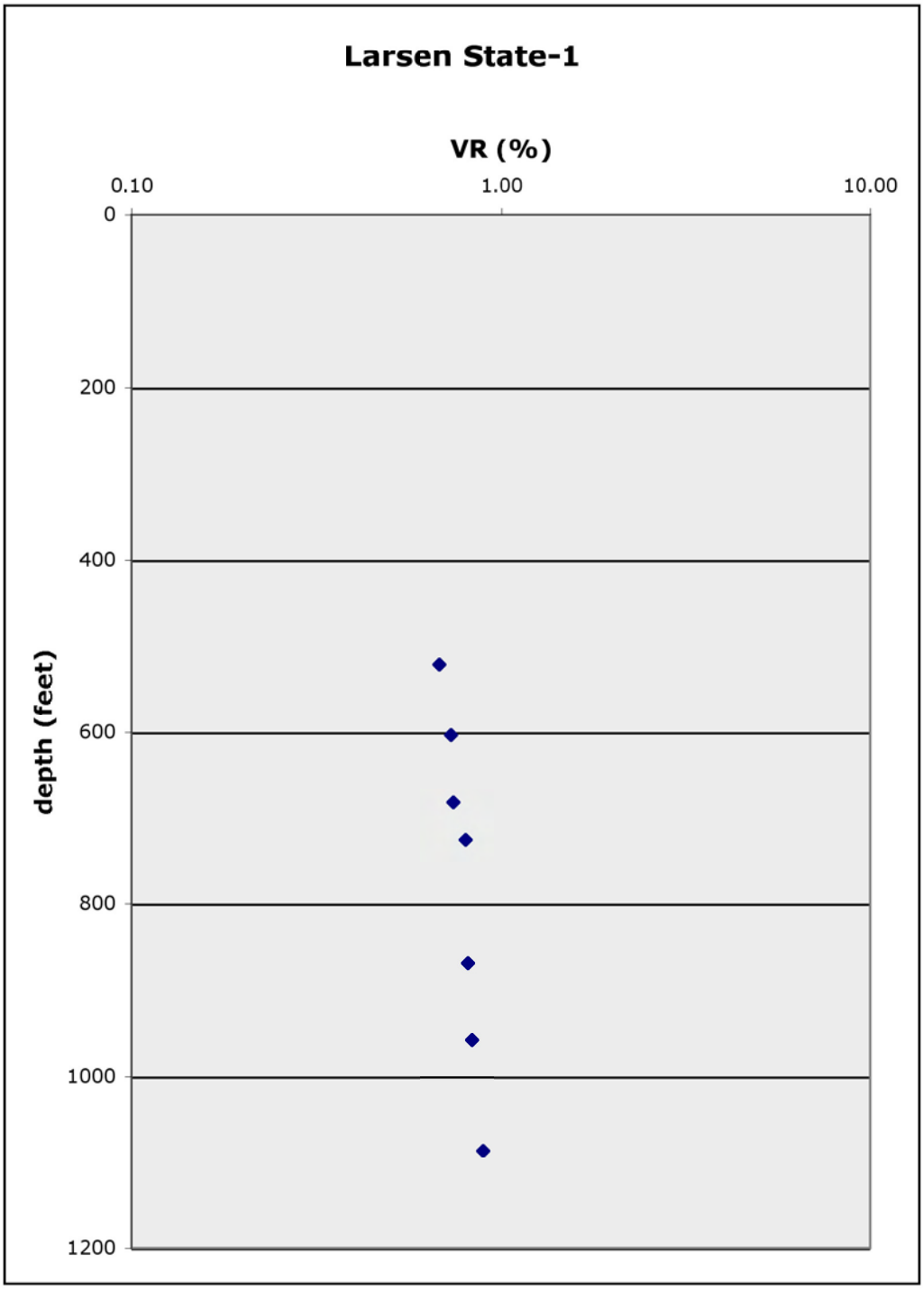

Figure 13. Larsen State-1: Vitrinite reflectance profile in Mancos Shale.

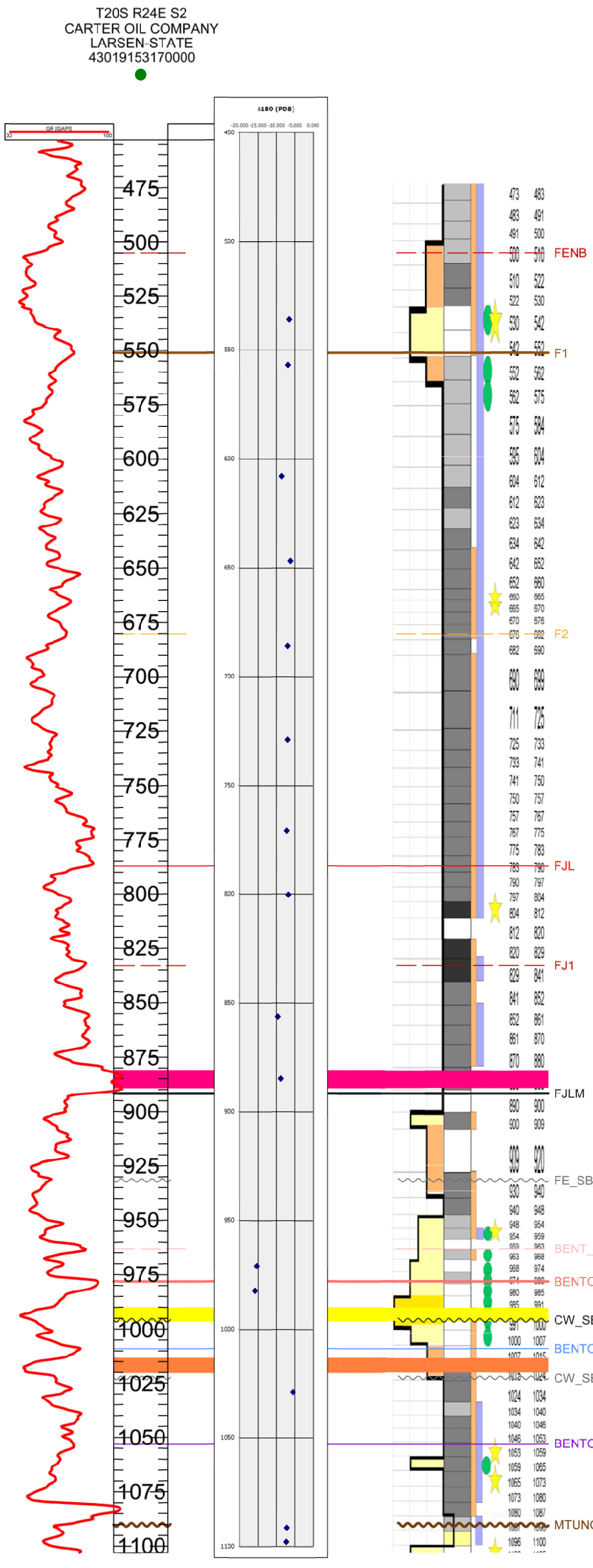

Figure 14. Larsen State-1: Oxygen isotopic composition of carbonate in Mancos Shale. Values are in per mil notation, with respect to PDB standard. Colored bars and tops discussed in text.

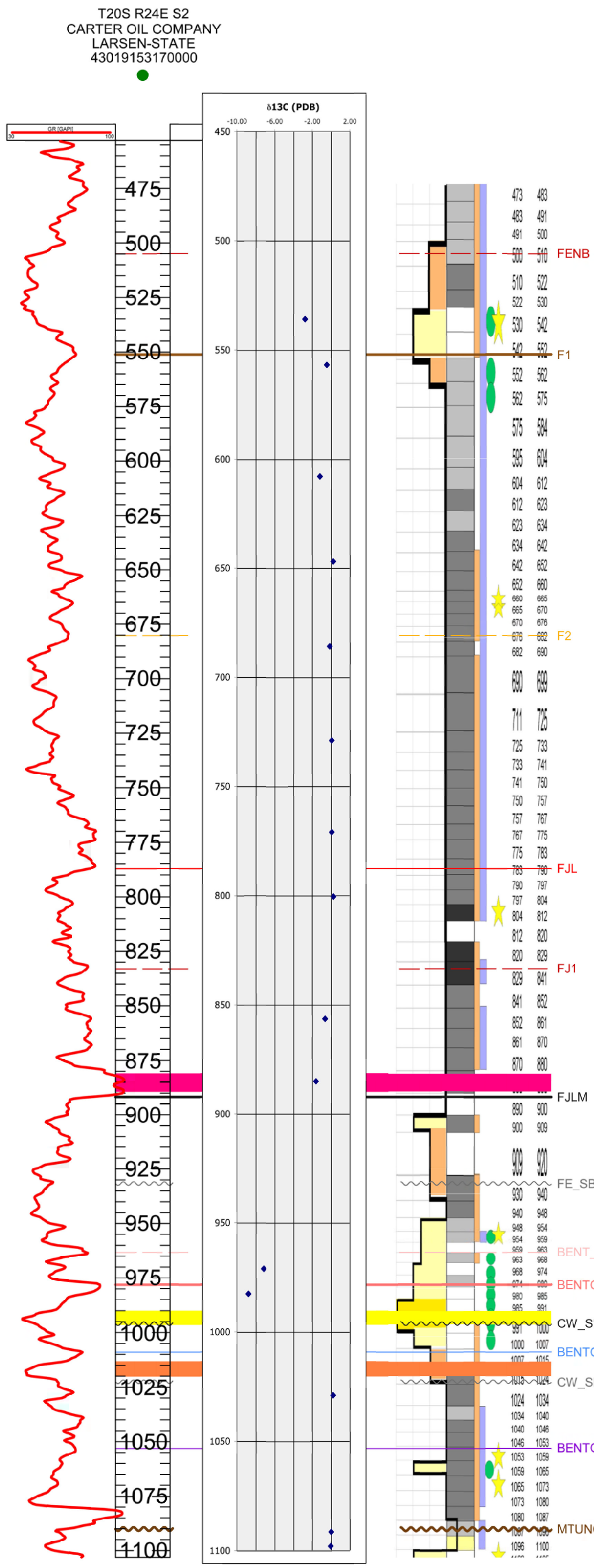

Figure 15. Larsen State-1: Carbon isotopic composition of carbonate in Mancos Shale. Values are in per mil notation, with respect to PDB standard. Colored bars and tops discussed in text.

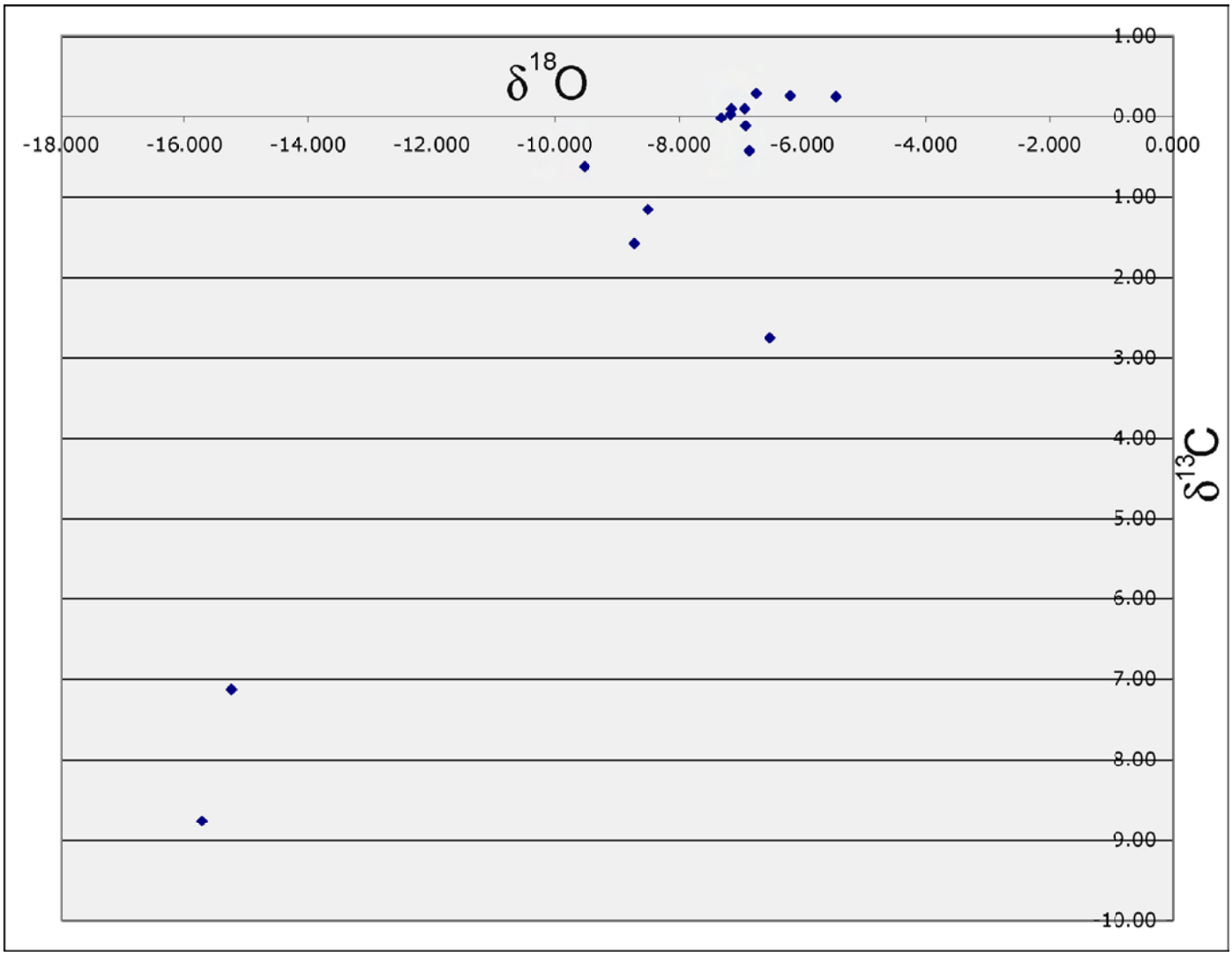

Figure 16. Larsen State-1: Cross-plot of carbon and oxygen isotopic compositions of carbonate from the Mancos Shale.

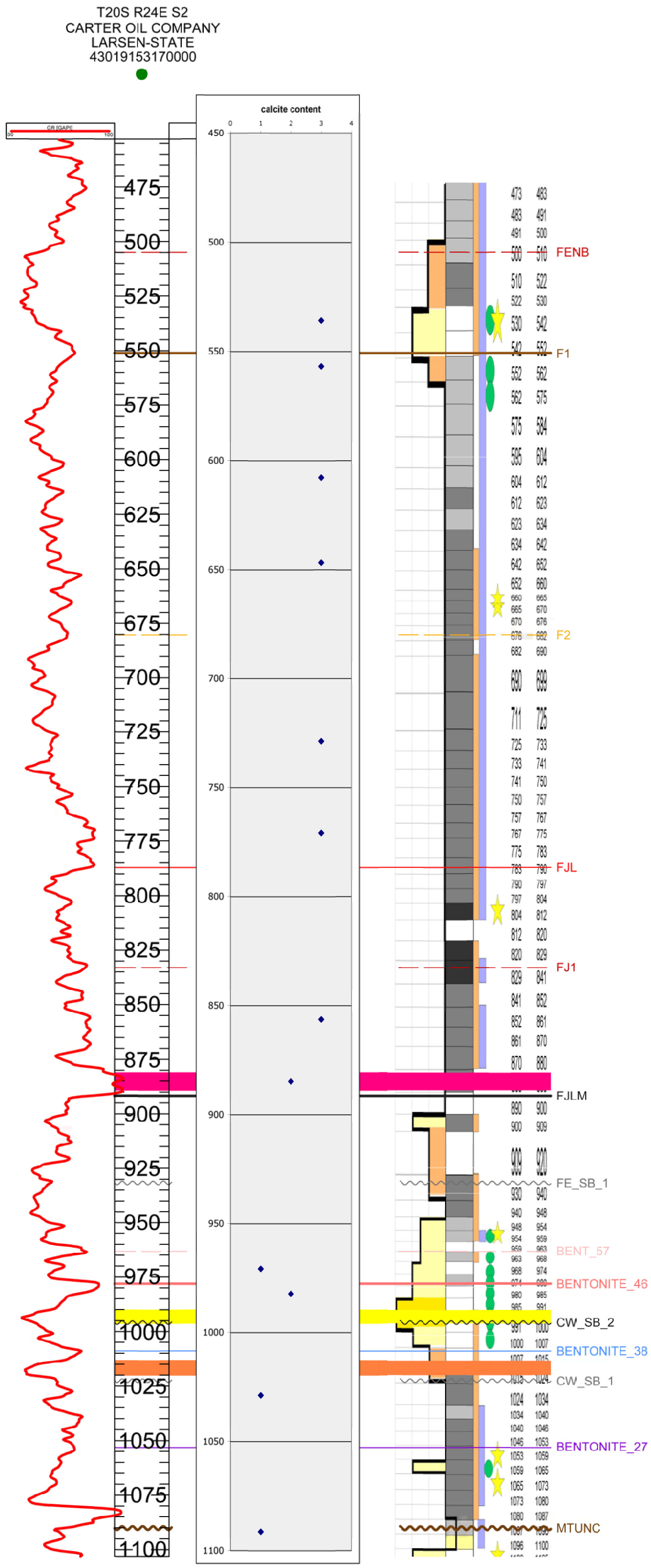

Figure 17. Larsen State-1: Calcite content of Lower Mancos Shale samples; qualitative determination from XRD analysis. Colored bars and tops discussed in text.

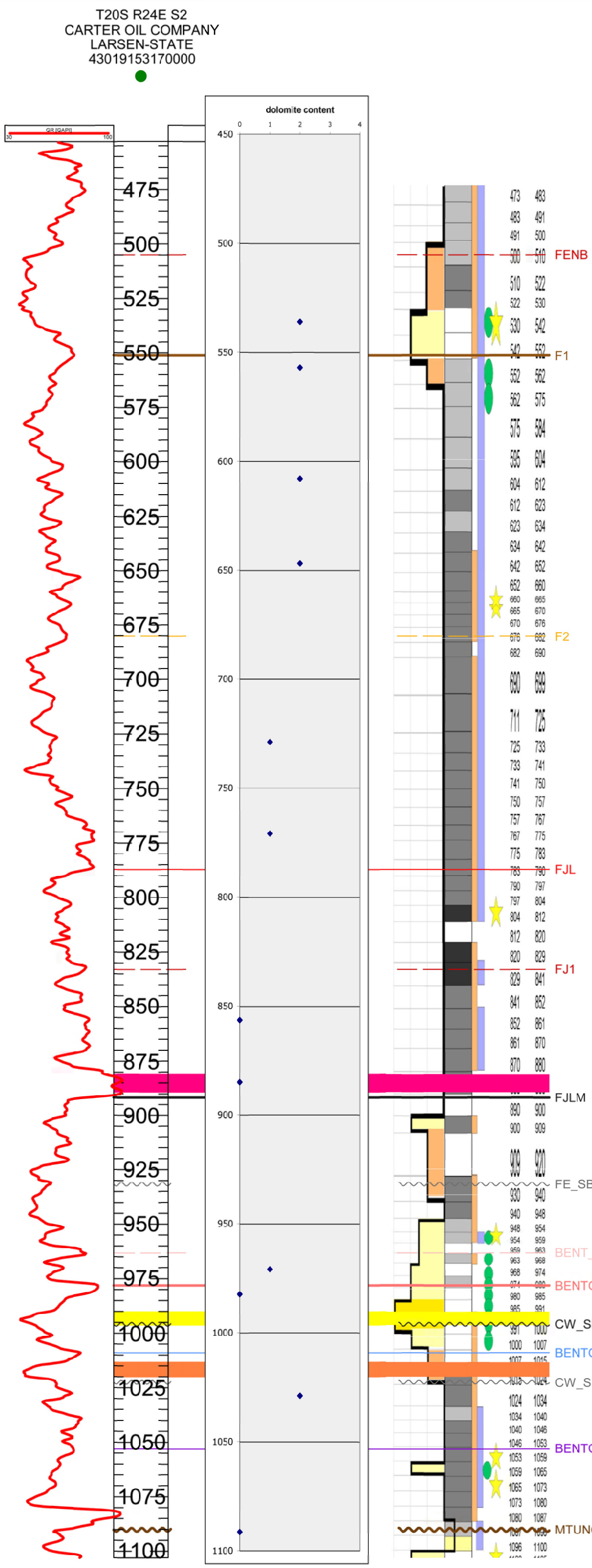

Figure 18. Larsen State-1: Dolomite content of Lower Mancos Shale samples; qualitative determination from XRD analysis. Colored bars and tops discussed in text.

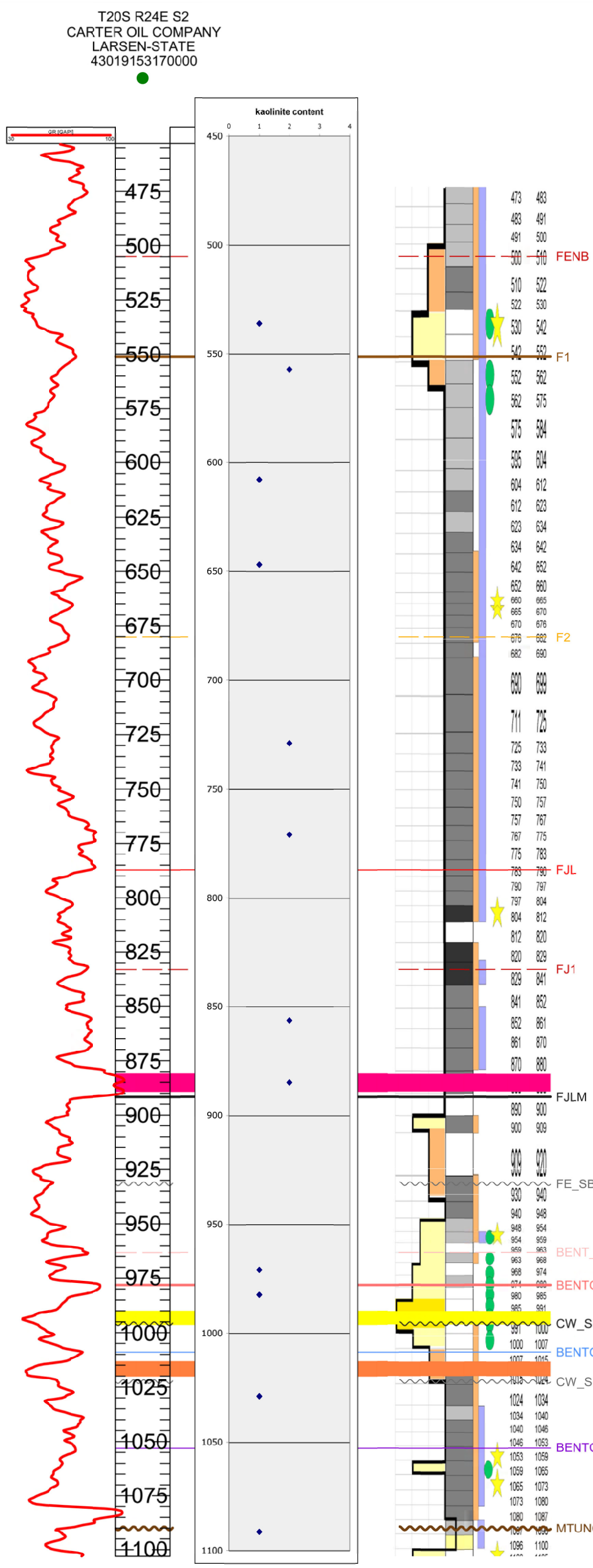

Figure 19. Larsen State-1: Kaolinite content of Lower Mancos Shale samples; qualitative determination from XRD analysis. Colored bars and tops discussed in text.

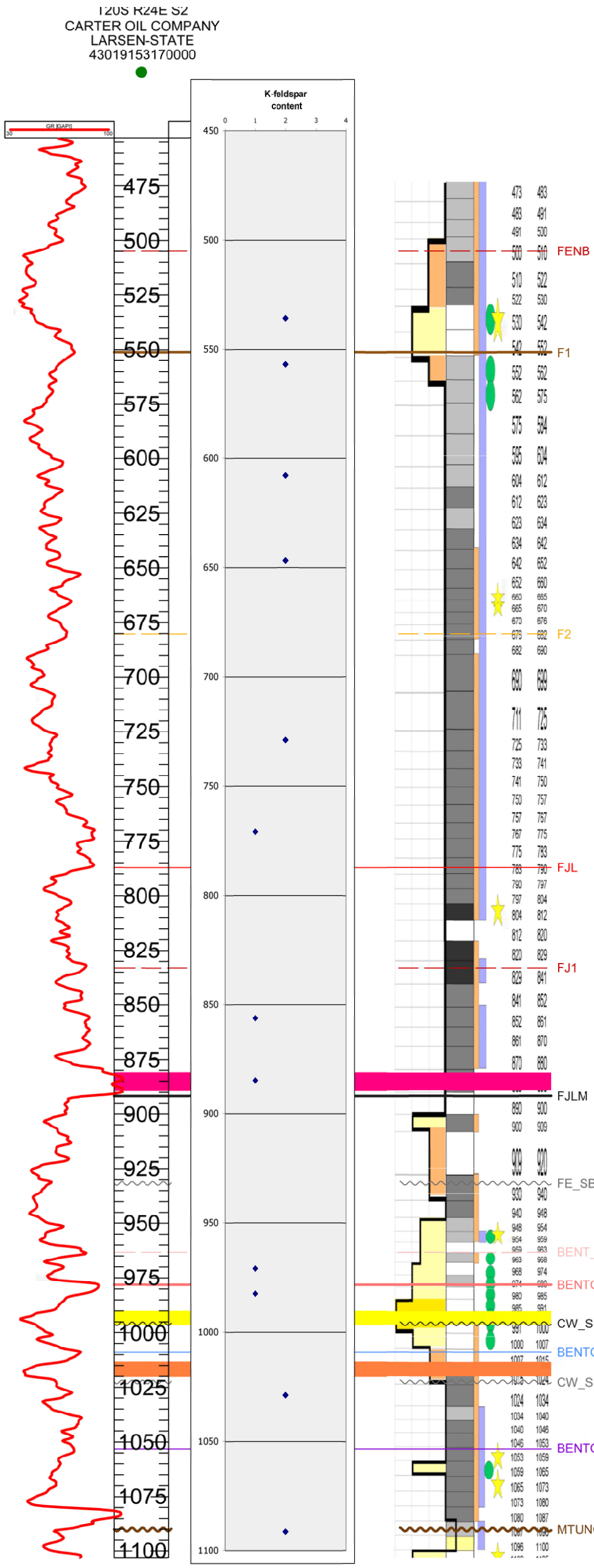

Figure 20. Larsen State-1: Orthoclase content of Lower Mancos Shale samples; qualitative determination from XRD analysis. Colored bars and tops discussed in text.

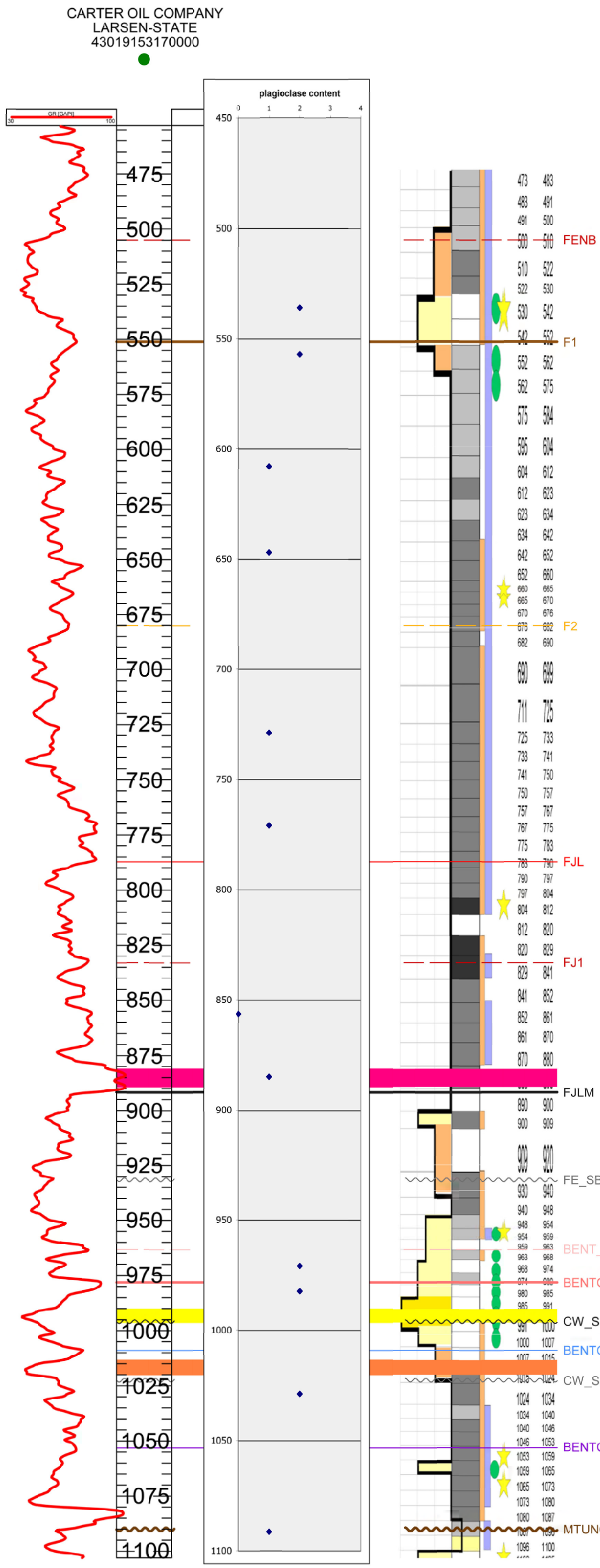

Figure 21. Larsen State-1: Plagioclase content of Lower Mancos Shale samples; qualitative determination from XRD analysis. Colored bars and tops discussed in text.

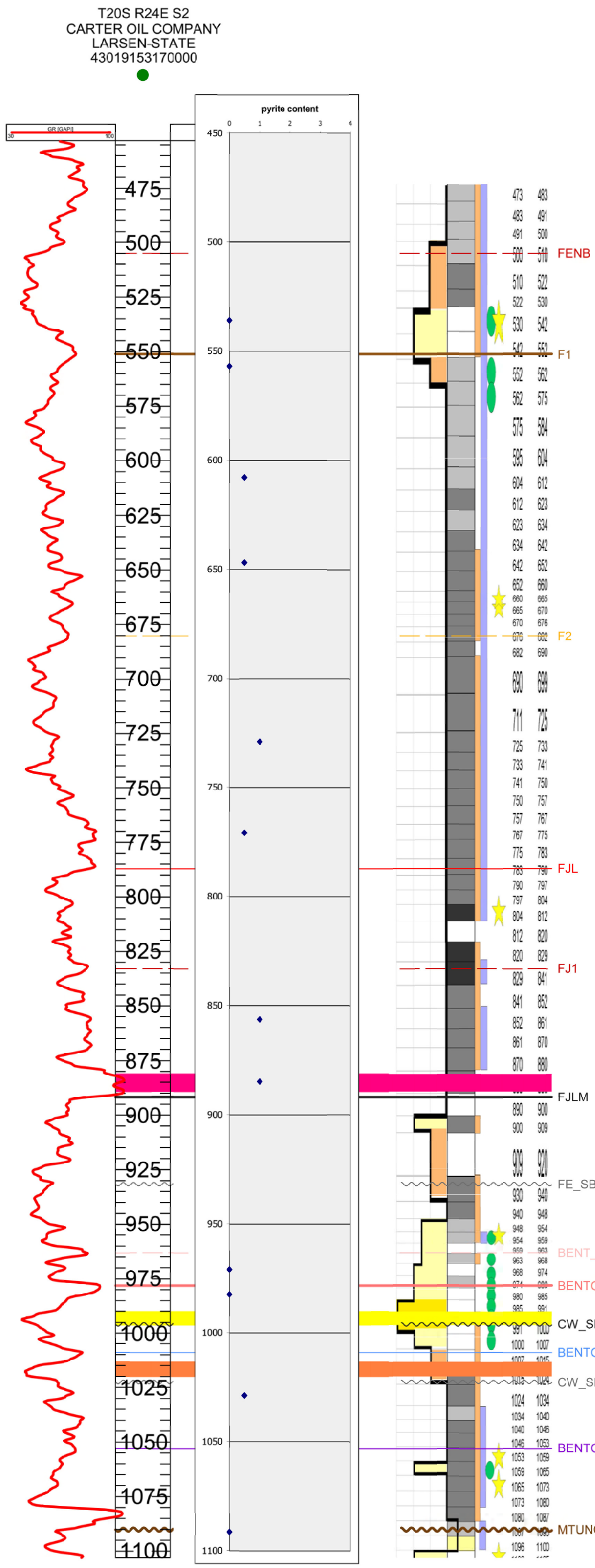

Figure 22. Larsen State-1: Pyrite content of Lower Mancos Shale samples; qualitative determination from XRD analysis. Colored bars and tops discussed in text.

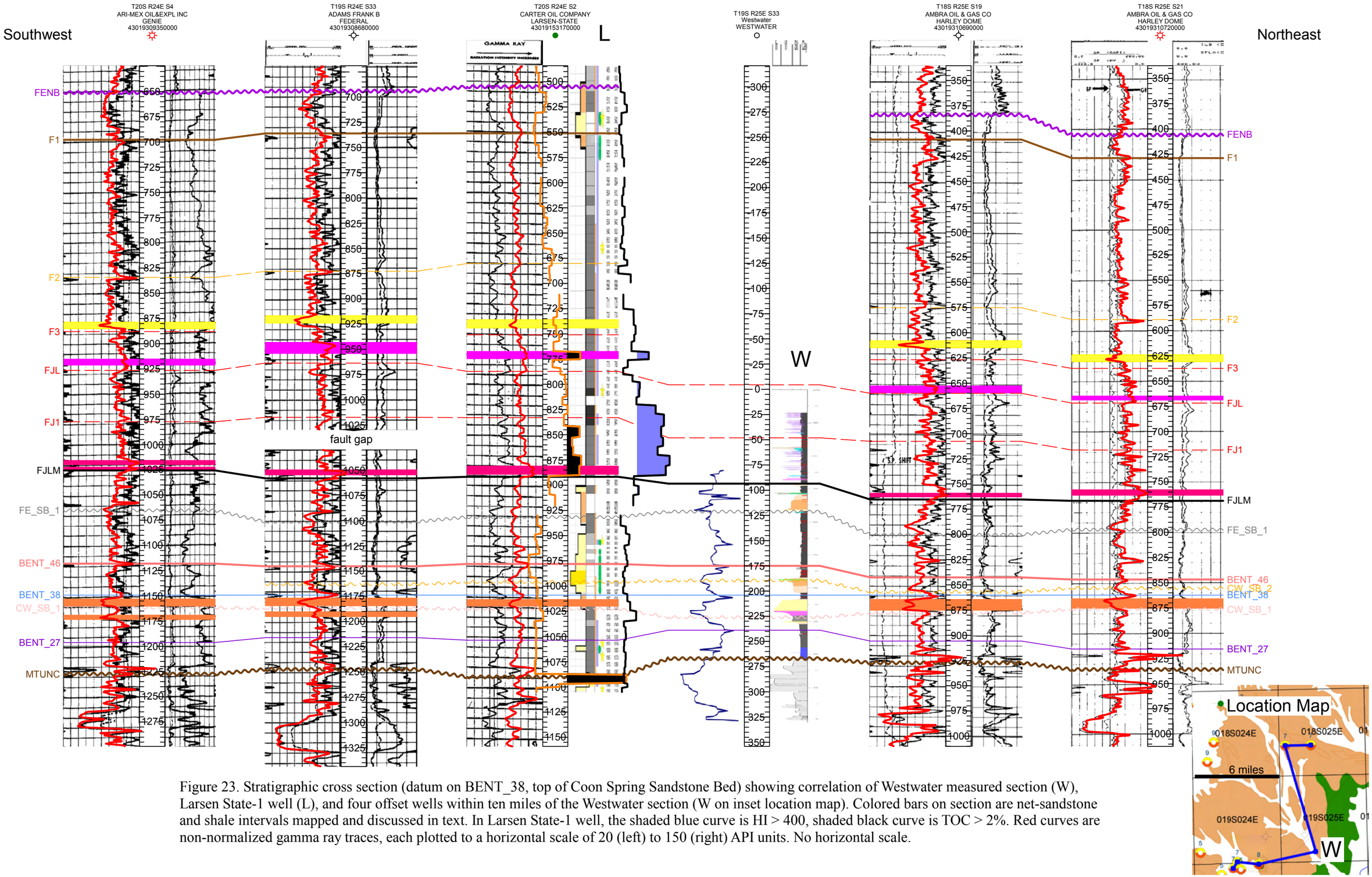

Figure 23. Stratigraphic cross section (datum on BENT_38, top of Coon Spring Sandstone Bed) showing correlation of Westwater measured section (W), Larsen State-1 well (L), and four offset wells within ten miles of the Westwater section (W on inset location map). Colored bars on section are net-sandstone and shale intervals mapped and discussed in text. In Larsen State-1 well, the shaded blue curve is HI > 400, shaded black curve is TOC > 2%. Red curves are non-normalized gamma ray traces, each plotted to a horizontal scale of 20 (left) to 150 (right) API units. No horizontal scale.

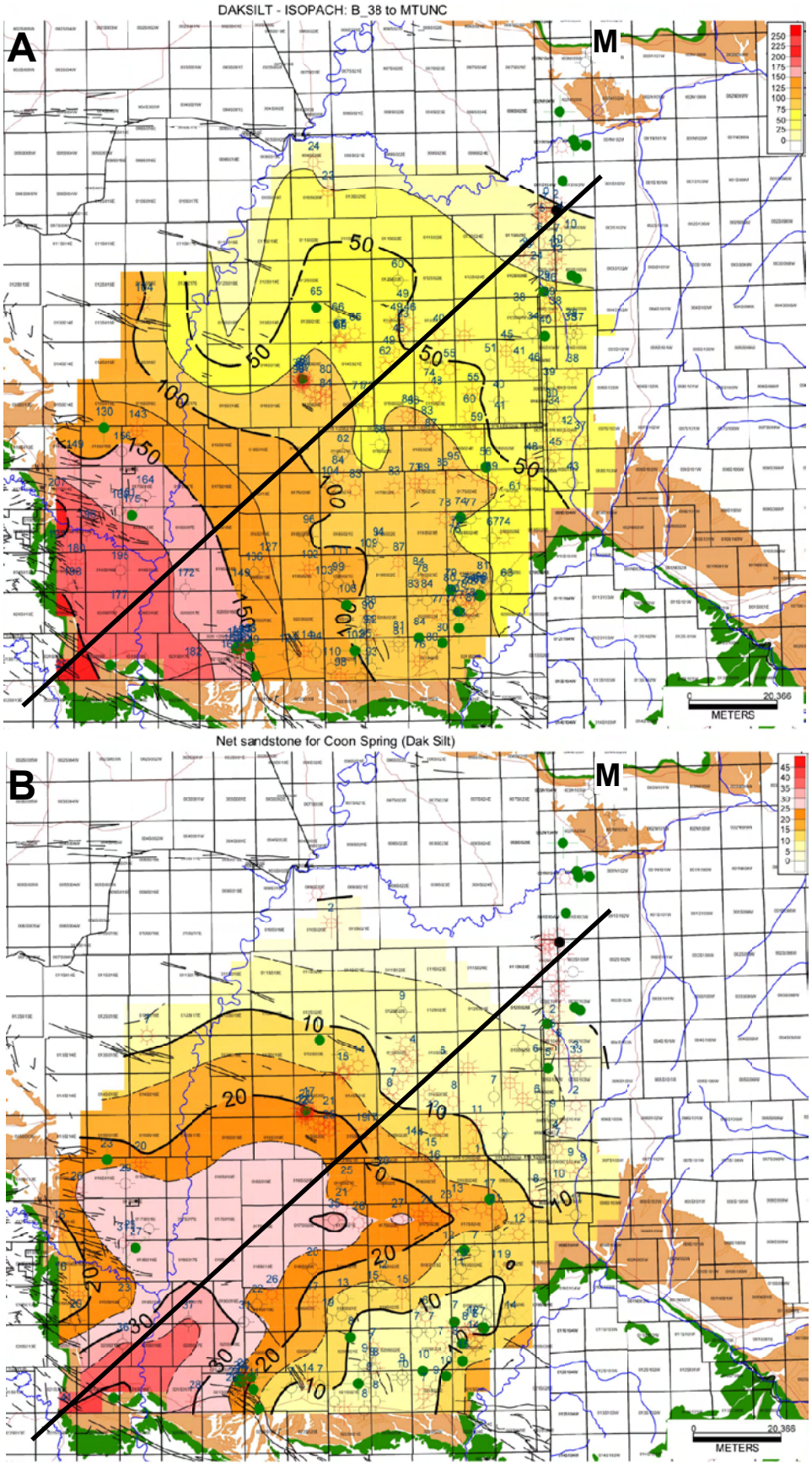

Figure 24. Isochore maps: green dots are oil wells, open circles are gas wells and/or dry holes. Letter "M" is location of measured section north of Rangely. Stratigraphic cross section location (Figure 25) shown as solid black line. A) "Dakota Silt: Bentonite_38 to MTUNC, sequences #1,2. B) Net sandstone at top of Dakota Silt, at base of sequence #1, is the Coon Spring Sandstone Bed.

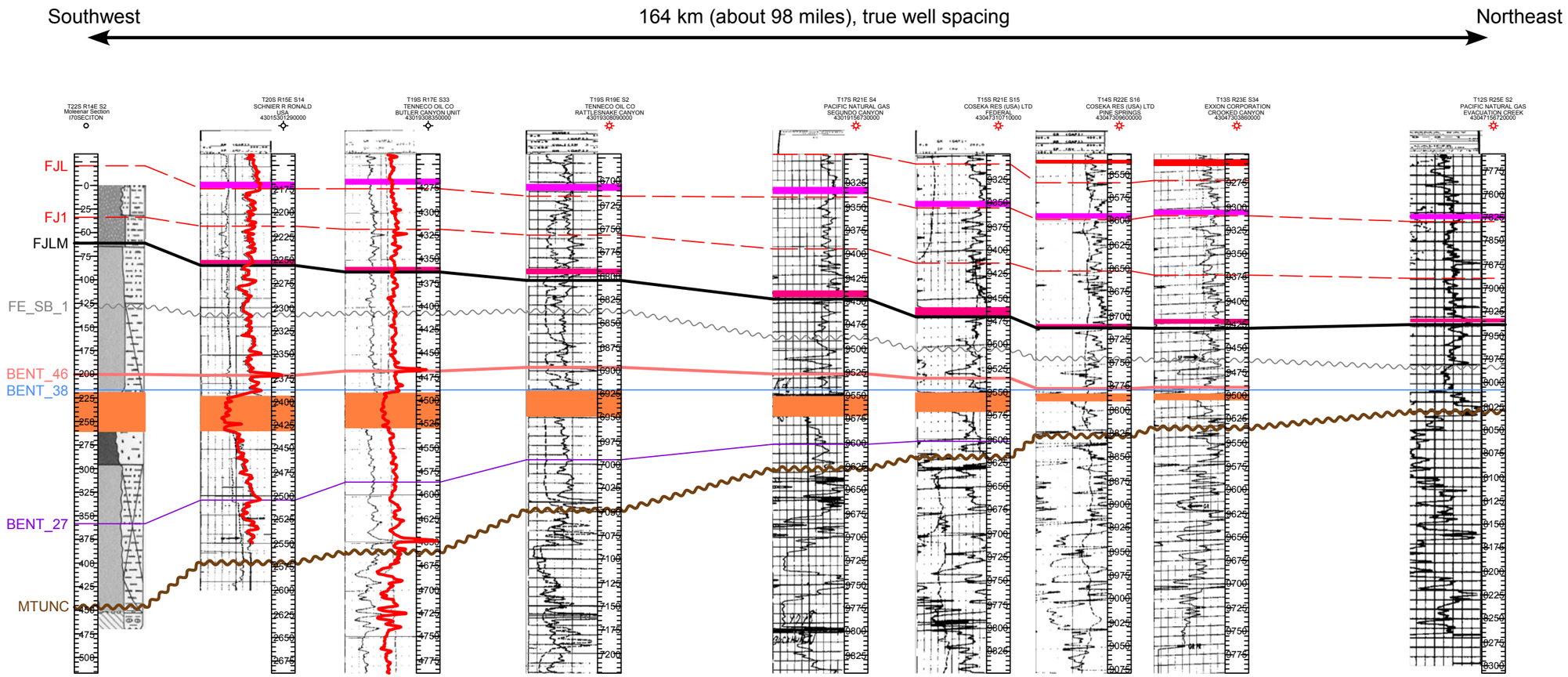

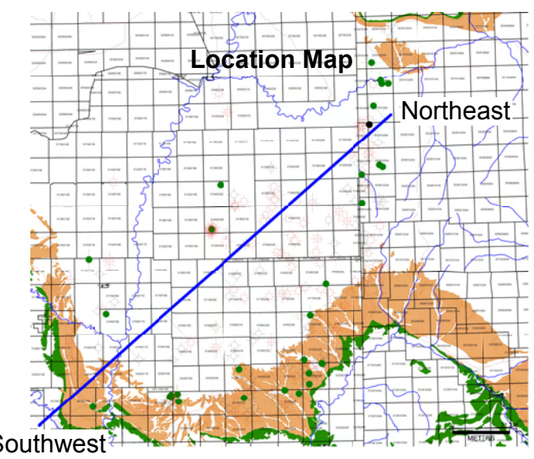

Figure 25. Southwest to northeast stratigraphic cross section of Dakota Silt interval (BENT_38 to MTUNC), showing downlap of bentonite markers below BENT_38 datum onto MTUNC and pinchout of Coon Springs Sandstone bed (orange bar below BENT_38 marker on each log) to a zero edge in the northeast on the Douglas Creek arch (inset map). The orange bars are the "net sandstone" interval mapped in Figure 24B. Other markers and color bars are discussed separately in text. Inset map shows location of cross section: land grid is townships (6 x 6 miles). Measured section from Moleaar and Cobban (1991). Gamma ray logs shown on left side of depth tracks.

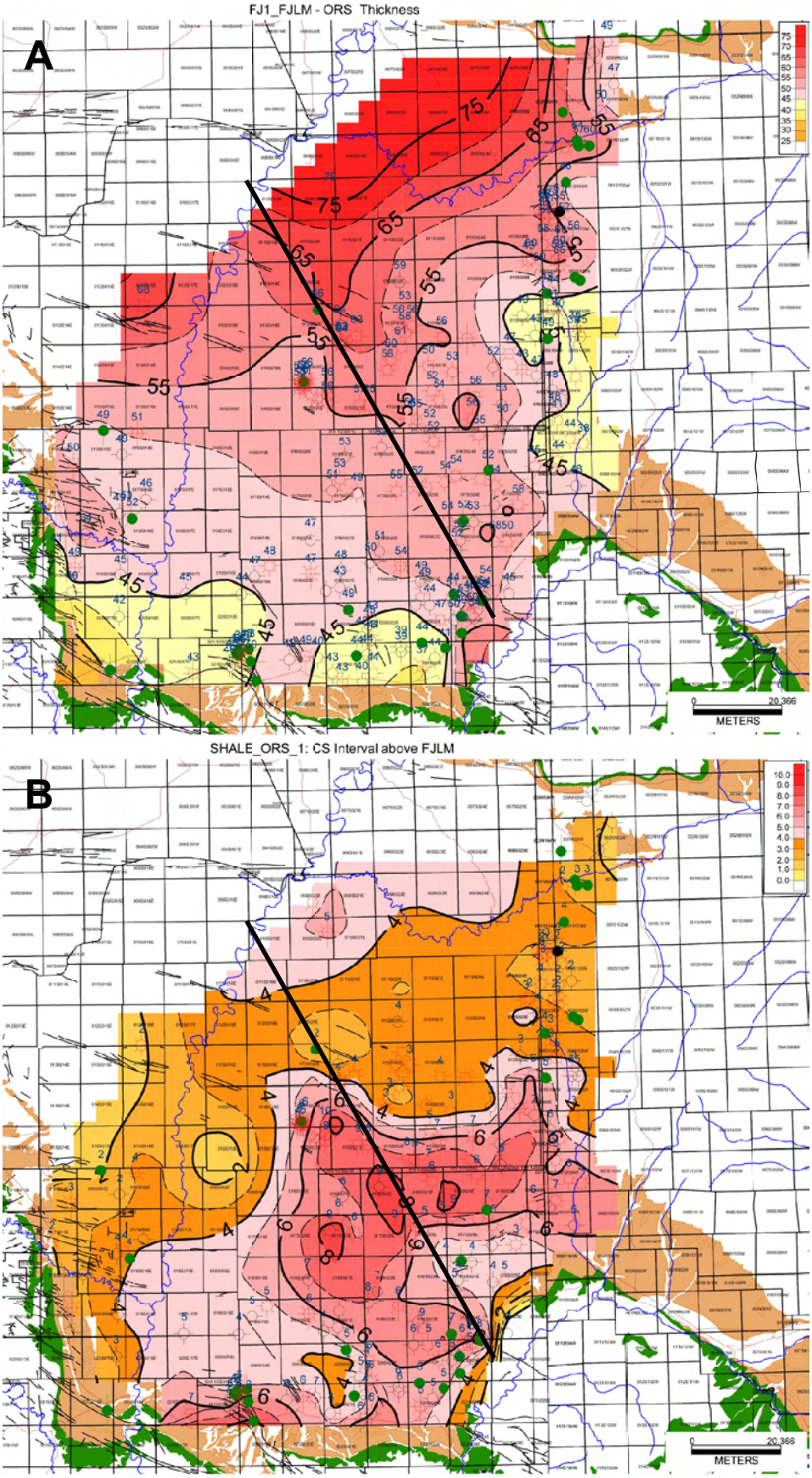

Figure 26. Isochore maps, annotation as in Fig. 24. A) Organic-rich interval FJ1_FJLM of lower HST? of sequence 4. B) Organic-rich shale of condensed interval in sequence 4, above FJLM marker.

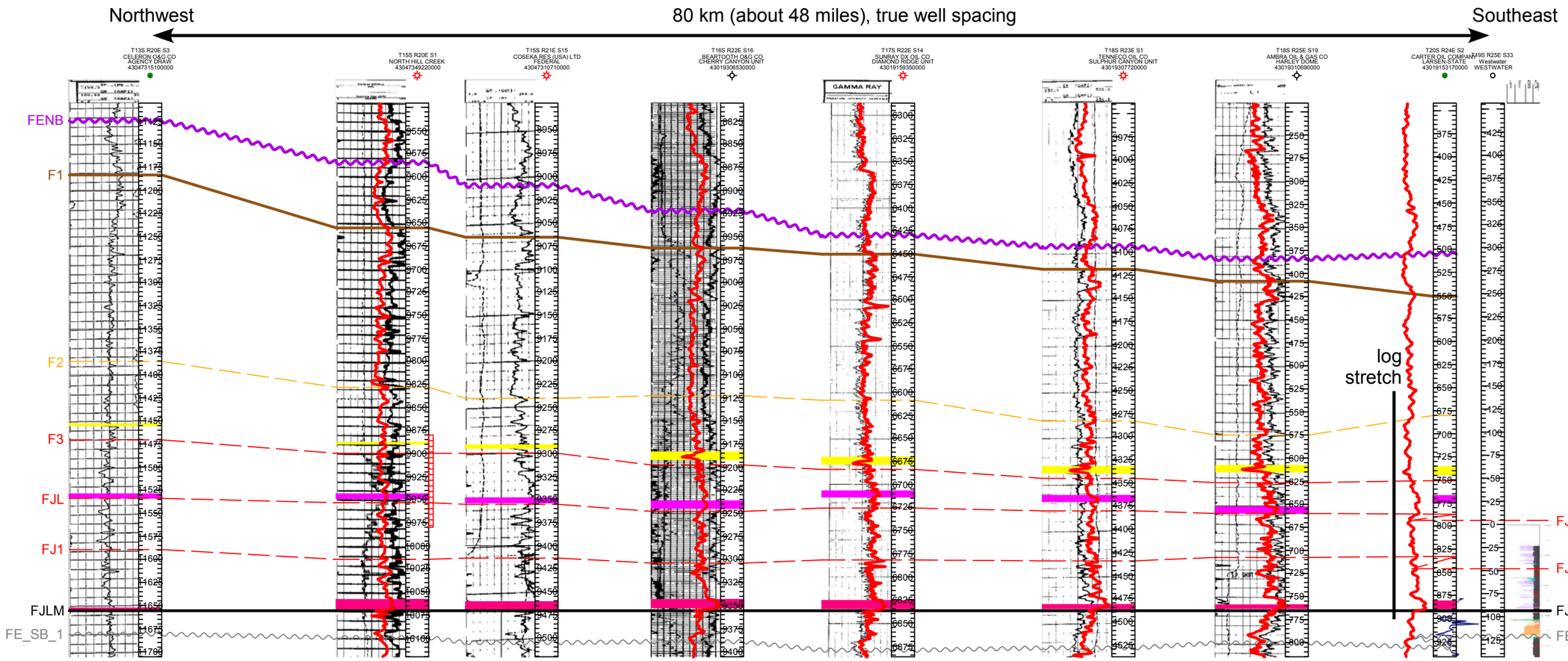

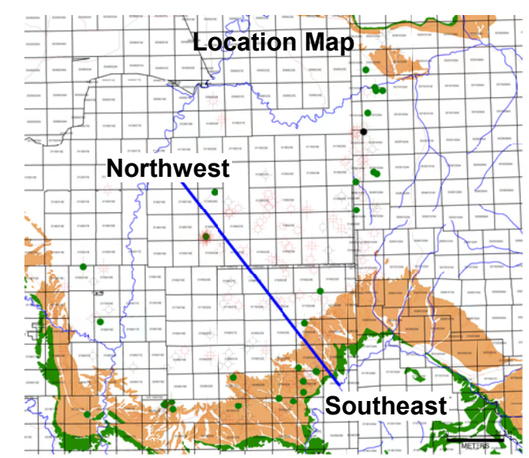

Figure 27. Northwest to southeast stratigraphic cross section of Ferron and younger intervals (Fe_SB_1 to FENB), showing correlation of markers interpreted for this study. The colored bars are the "net shale" (condensed organic rich intervals, red and purple) and "net sandstone" (yellow) intervals mapped in relevant figures and discussed in text. Inset map shows location of cross section: land grid is townships (6 x 6 miles). Gamma ray logs shown on left side of depth tracks. Isochore thicks in Larsen well (L) are due to log stretch discussed in text and shown on Figure 8.

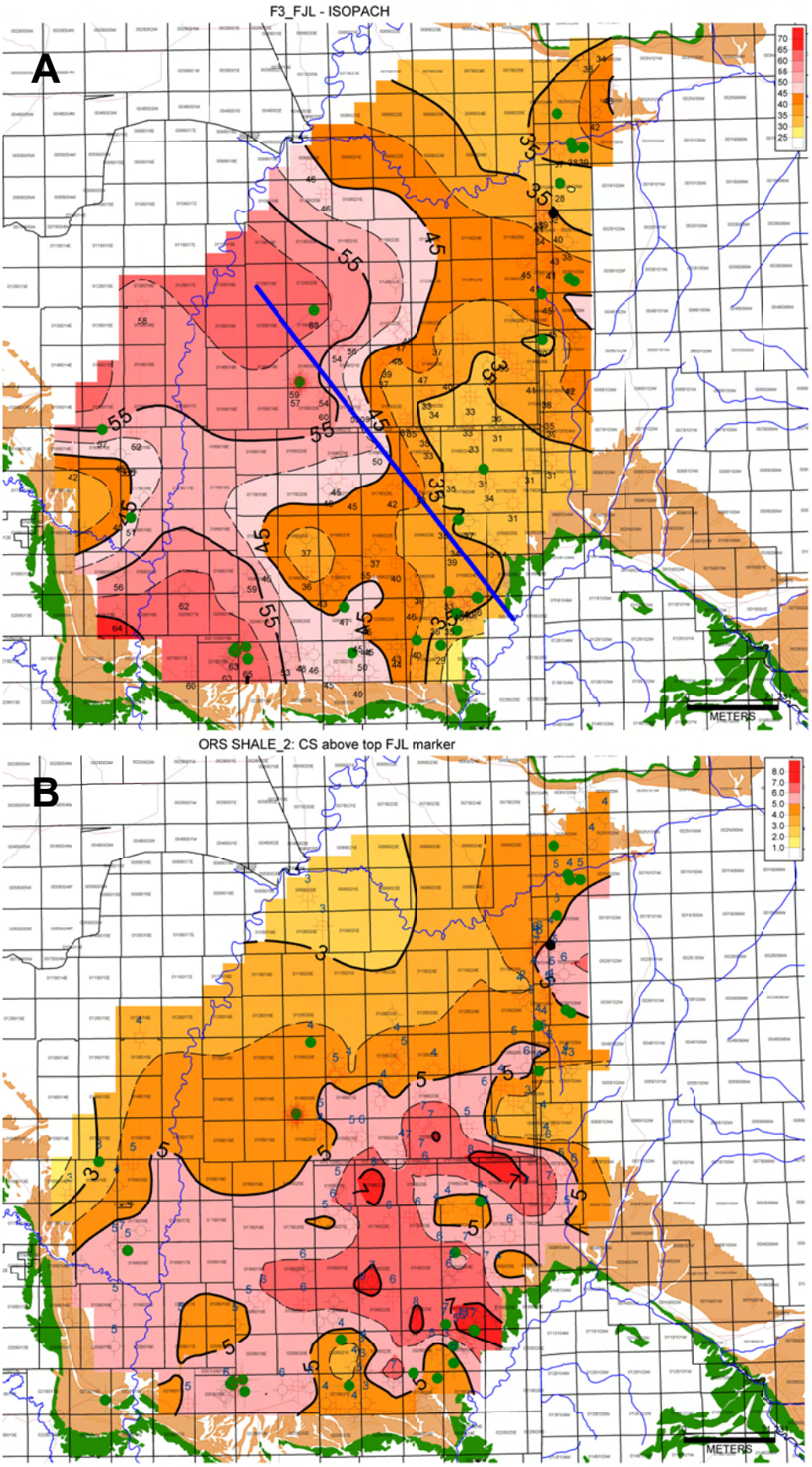

Figure 28. Isochore maps, annotation as in Fig. 24. A) Interval F3_FJL, B) Organic-rich shale of condensed interval, above FJL marker.

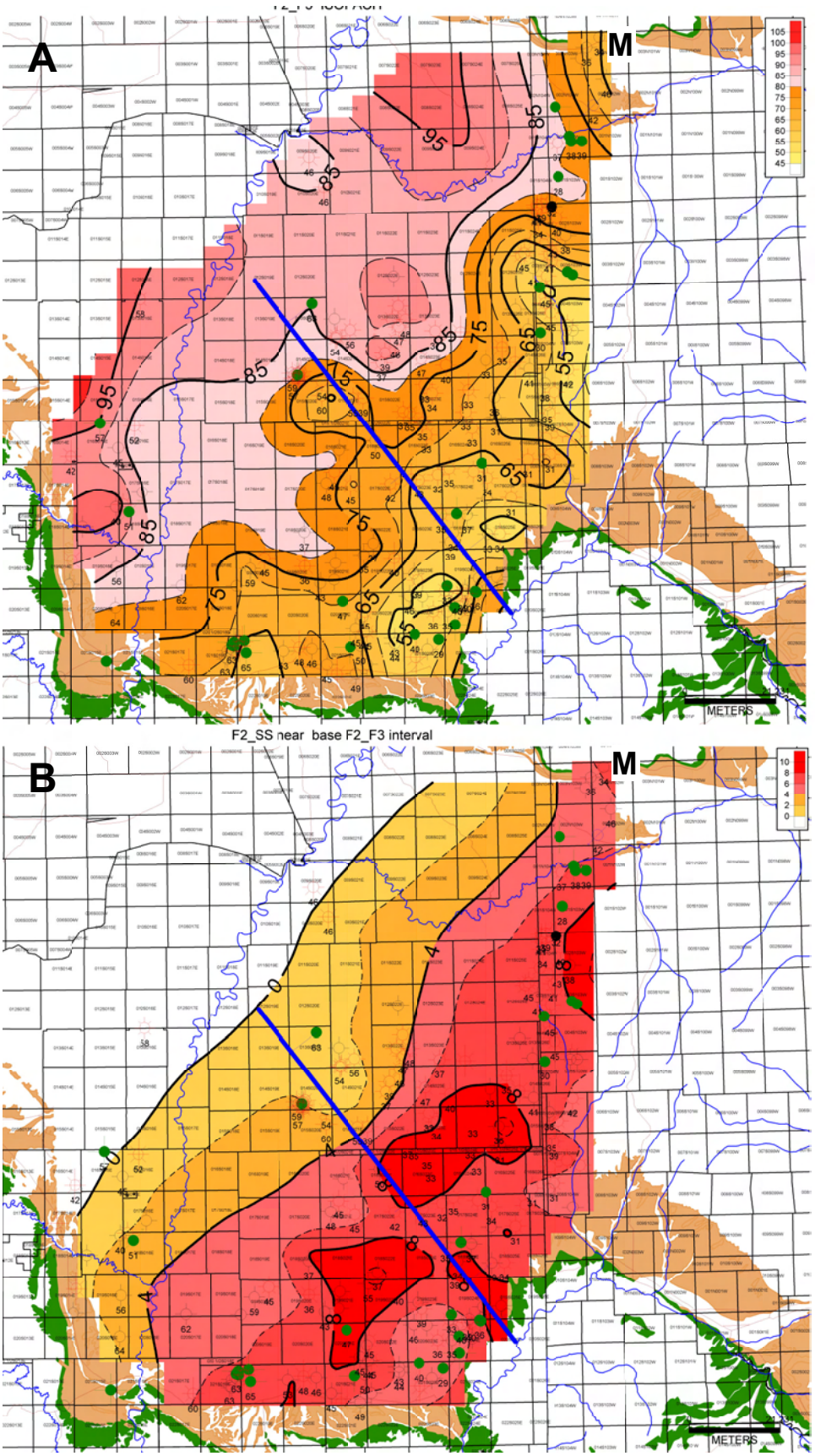

Figure 29. Isochore maps, annotation as in Fig. 24. A) Interval F2 to F3., which correlates to Frontier of Molenaar and Cobban (1991) north of Rangely (marked "M"). B) Widespread thin, turbidite (?) sandstone interval, above F3 marker and at base of F2-F3 interval. Possible turbidite origin discussed in text. Line of cross section shown for Figure 27.

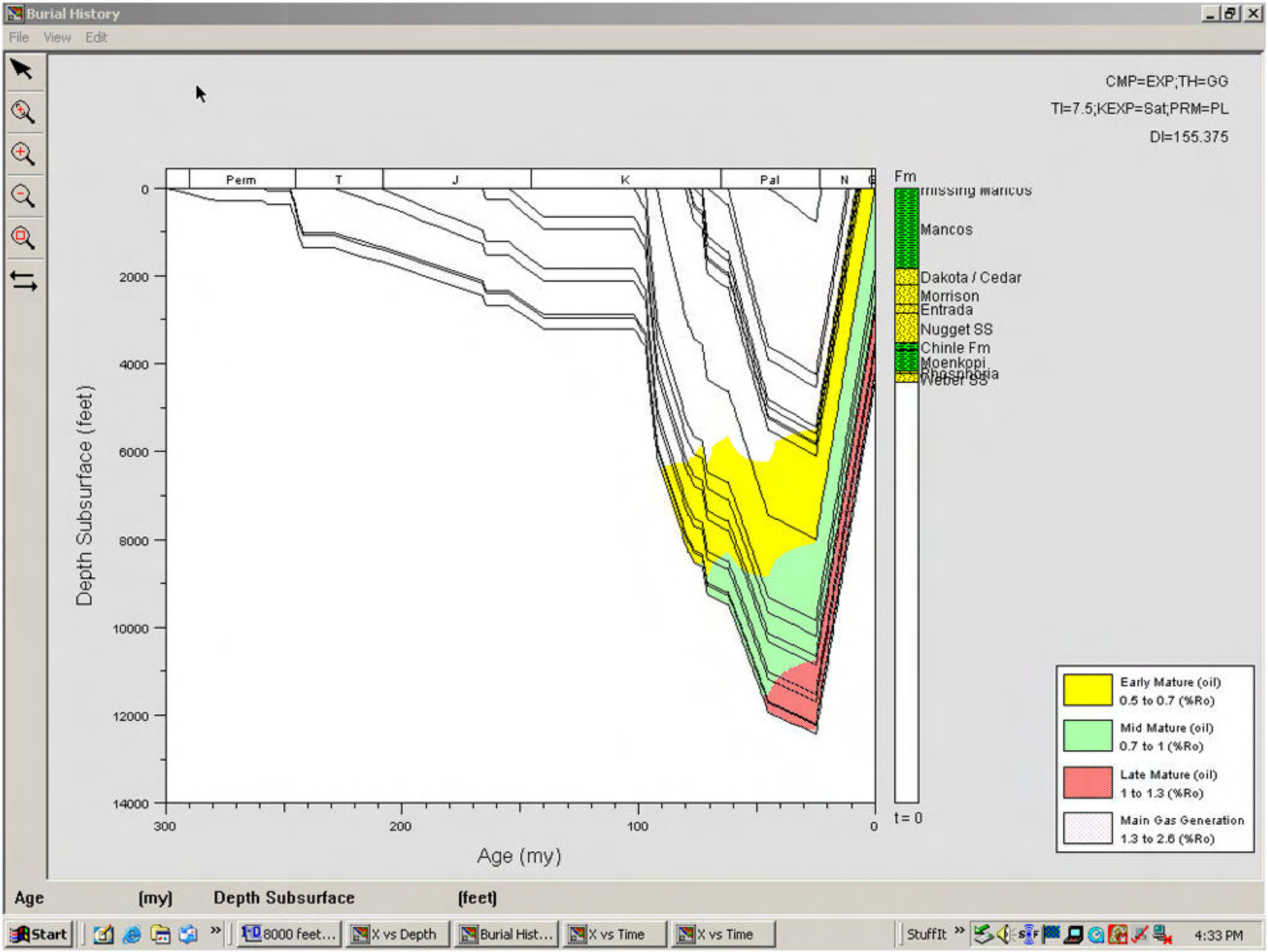

Figure 30. Burial history model for the Westwater Canyon / Larsen State-1 area.

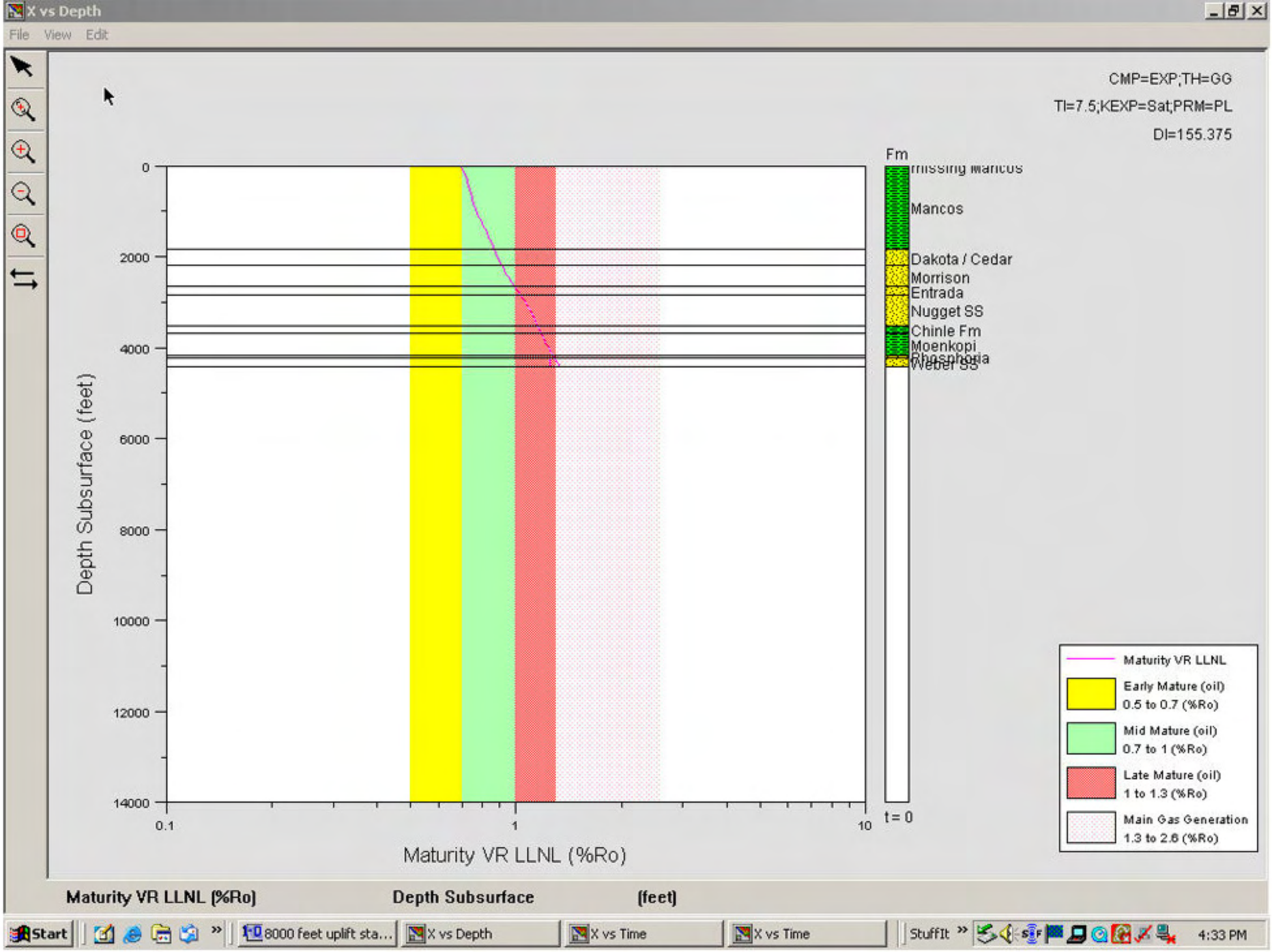

Figure 31. Maturation profile for the Westwater Canyon / Larsen State-1 area.

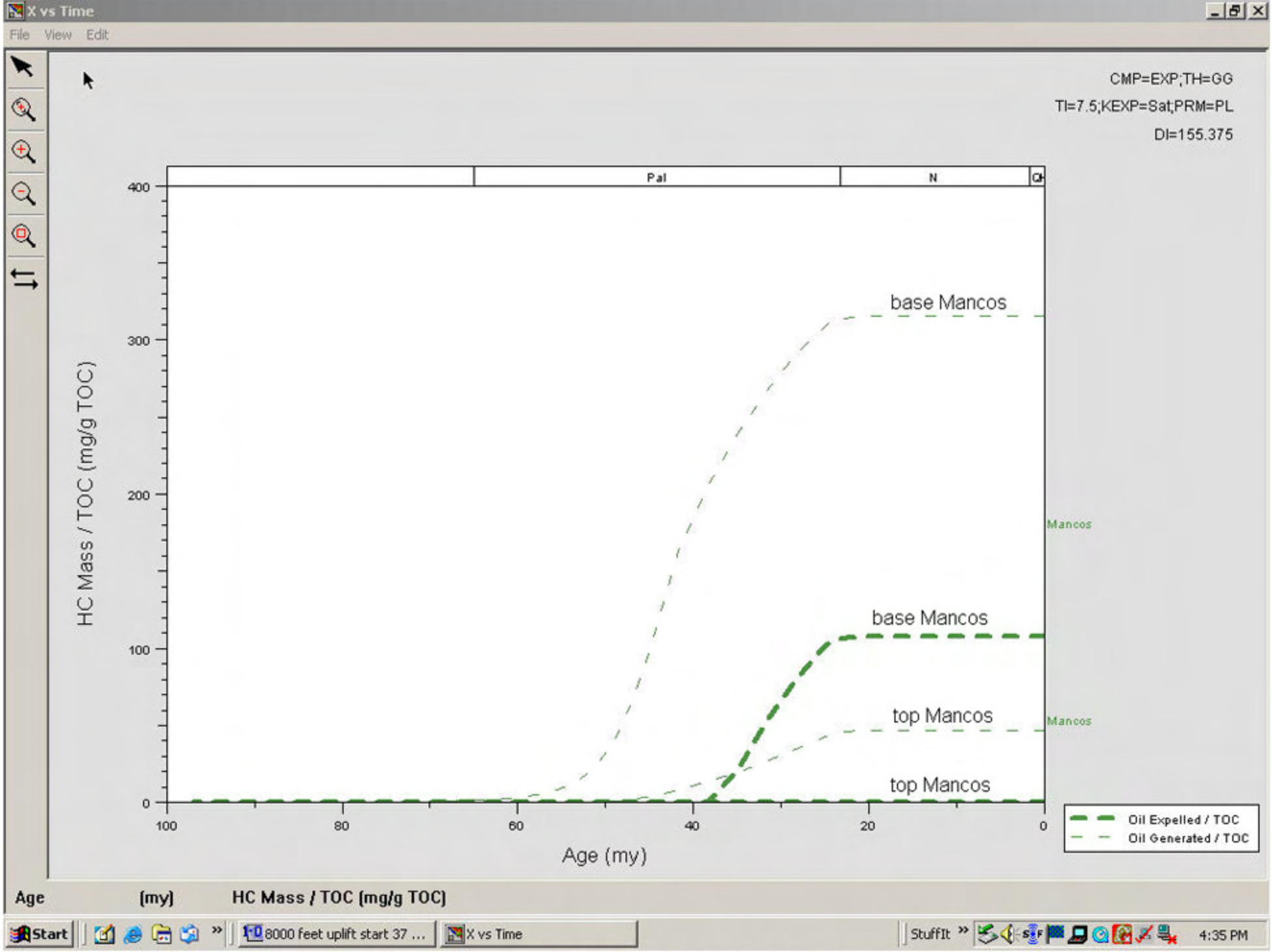

Figure 32. Modeled oil generation and expulsion history for the base Mancos and top Mancos horizons.

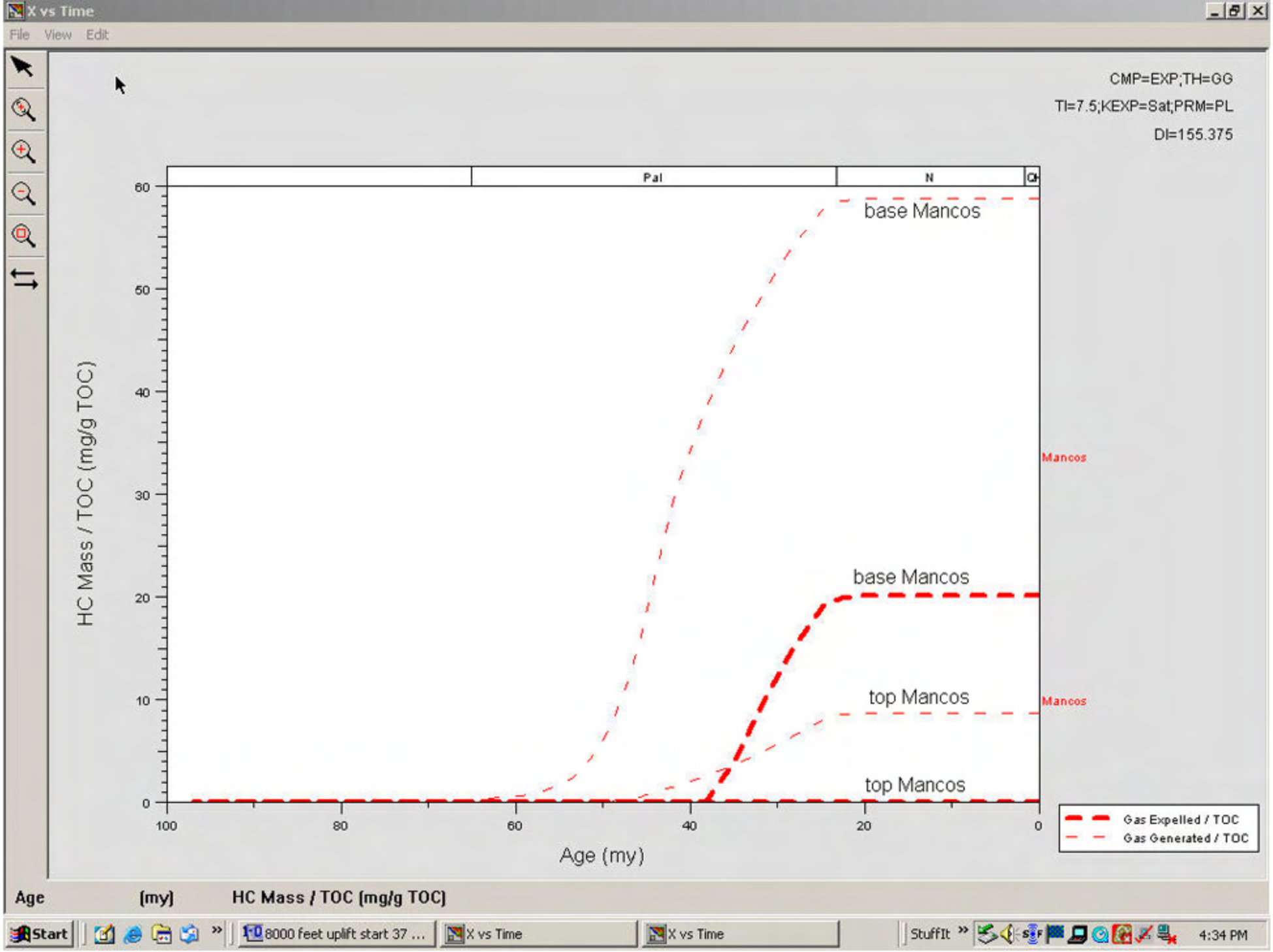

Figure 33. Modeled gas generation and expulsion history for base and top Mancos horizons.

Appendix A

Westwater Measured Section, Raw Log Sheets

And Raw GPS data

Westwater Measured Section

Logged By: DSA, LWA

Date: 3-26-05

Depth (m)	Texture, Ich-Fossils, Sedimentary Structures (Clay, Silt, Vf, fn)	Bioturb (0–100%)	HCl rxn (0–Hi)	color	Sample	Photo	Comments
90							@ 90m → traverse to SE.
							→ 116 = overview to NE
89	v. poor exposure	none	no HCl rxn	dk gray		(115)	← (top low hill) upper hill [traverse]
						124–128	thin ripple trains – discont. (formsets)
88						(114)	(fissile dk gray shale)
						122, 123	rippled zones clustered on ~0.5m intervals
87			conc.			(113)	87A, B, C, D [traverse along to West face of upper hill] concretion horizon.
86	gopher hole					112	discontinuous thk VAB
	Kahuna						20 cm VAB to N. ss ledge mappable to N.
85						111	traverse @ ledge to NE @ 85m [85A]
	laterally persistent VAB						
84						110	slope breaks back to next hill to N
					W@3.5	129 gully	
						129 – over view	Isolated (2cm long) starved ripples
83	VAB					109	2 VAB?
				dk gry			fiss blk shal
			conc.			108	discont. thin lags conc. <.5m – horizon
82	starved					107	(silty sh) isolated
			conc.	hel-brn ss		106 conc.	concretions <.5m
	sm conc. horizon		conc	dk gry sh			Inoc. + hash on ss bdg
			no HCl rxn			105 ripple (104)	micro HCS, corr ripples
81							

Westwater Measured Section

Logged By: DSA, RGF / DSA, LWA

Date: 10-16-05 / 3-26-06 (windy & cold)

cic = cone-in-cone
cfr = combined flow ripple

Depth (m)	Texture, Ich-Fossils, Sedimentary Structures (Clay, Silt, Vf, fn)	Bioturb (0–100%)	HCl rxn (0–Hi)	color	Sample	Photo	Comments
81	microHCS					104	103 overview 1m; Inocermaid (sample) in ss
80						102,	
79						101	
78	VAB			dk gray sh.		100	selenite wx in shale; rr starved ripples in vfu ss; traverse – to saddle next hill; ammonite rolling traces
77	thin VAB? (discont)		all non-calc.			099	in clusters, sep by sh; discontinuous lenses ss - vfu to fL - curr rippled sparse traces on bdg surf.
	VAB			dk gry sh.			
76	microHCS, cfr?				76.0	082	[Top of hill] start 3-26-06 end of 10-16-05 field session; Prionocyclus sp; 1cm on ss bedding planes
75					75.0	081	VAB
				dk gry			v. fissile, "paper" shale
74	ls - cic; cfr				74.0	080	limestone c-i-c
	microHCS w/ c.f.r.						
73	VAB			gray	73.0	078	laterally all ss lenses – fill scours? w/ low relief; horiz. burrows on bd tops
	c.f.r. SE, SW			yl-brn		079	lo < lam (modified SCS?); comb. flo ripples (SE) SW
72				dk-gry	(72.0)	(077)	fissile dk gry shale

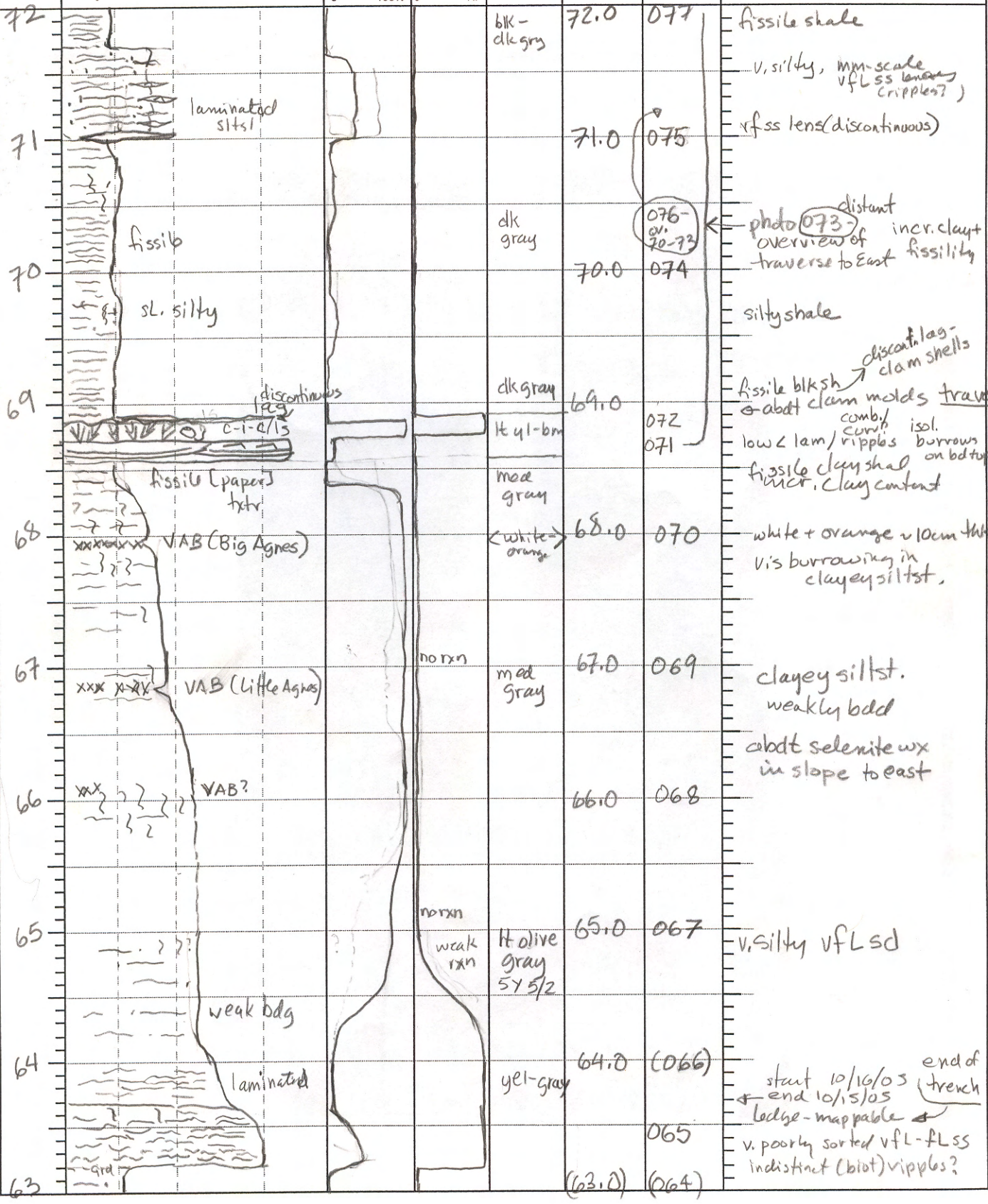
Depth (m)
Clay
Silt
Vf
fn
Bioturb
0
100%
rxn
0
Hi
color
Sample
Photo
Comments
72
71
70
69
68
67
66
65
64
63
laminated sltst
fissile
sL. silty
discontinuous lag
c-i-c/ls
fissile [paper] txtr
VAB (Big Agnes)
VAB (Little Agnes)
VAB?
weak bdg
laminated
grd
blk - dk gry
dk gray
dk gray
lt yl-brn
med gray
<white-orange>
no rxn
med gray
no rxn
weak rxn
lt olive gray 5Y 5/2
yel-gray
72.0
71.0
70.0
69.0
68.0
67.0
66.0
65.0
64.0
(63.0)
077
075
076-ov. 70-73
074
072
071
070
069
068
067
(066)
065
(064)
fissile shale
v. silty, mm-scale vfL ss lenses (ripples?)
vf ss lens (discontinuous)
photo 073 - distant overview of traverse to East
incr. clay + fissility
silty shale
fissile blk sh
discont. lag - clam shells
abdt clam molds trav
low < lam / comb./curv. ripples
isol. burrows on bd top
fissile clay shal incr. clay content
white + orange ~10cm thk
v. is burrowing in clayey siltst.
clayey siltst. weakly bdd
abdt selenite wx in slope to east
v. silty vfL sd
start 10/16/05
end 10/15/05
end of trench
ledge - mappable
v. poorly sorted vfL-fL ss
indistinct (biot) ripples?

Depth (m)	Clay Silt Vf fn	Bioturb 0 100%	HCl rxn 0 Hi	Color	Sample	Photo	Comments
63	$CaCO_3$			concretion	63.0	064	laterally = isolated concretion w/ cone-in-cone in limestone
62		n.o.		med. gray	62.0	063	
61					61.0	062	
60	VAB	n.o.			60.0	061	
59		n.o.	notice rxn		59.0	060	
58		n.o.		med. gray	58.0	059	↑ silty shale incr. in silt?
	← chg to blocky wx						↓
57		n.o.			57.0	058	fissile shale
56		n.o.		med-dk gry	56.0	057	
55		n.o.			55.0	056	
54					(54.0)	(055)	v. fissile shale

Westwater Measured Section

Logged By: DSA, RGF

Date: 10-15-05, edit 1-21-06

n.o. = not observable

Depth (m)	Texture, Ich-Fossils, Sedimentary Structures (Clay, Silt, Vf, fn)	Bioturb (0 – 100%)	HCl rxn (0 – Hi)	color	Sample	Photo	Comments
54					54.0	055	
		n.o.					
53					53.0	054	
		n.o.		med gry			clayey siltst.
	thin VAB						
52					52.0	053	incr clay/silt content
				yl-gry			
	VAB						white VAB
		n.o					
51					51.0	052	
50				yl-gry to gray	50.0	051	shale w/ vfL sand - friable. mod well sorted
		n.o.					
						050+ 049	overview of trench (highest wht bag @ 49.0)
49					49.0	048	v. friable
		n.o		- - - - -			sh mixed w/ fn sand? intbeddg inferred.
48		n.o.		blk - dk gry	48.0	047	
			no HCl rxn				fissile
47					47.0	046	
		n.o.		blk - dk gry			alt claysh + fn sd
				white	46.4	045	VAB - ~10cm thick
46					46.0	044	
					45.8 (sd)	043	friable shale chip
	VAB						v. fissile black sh.
	VAB	n.o.		black	(45.0)	(042)	
45							

Westwater Measured Section

Logged By: DSA, RGF

Date: 10-15-05, edited 1-21-05

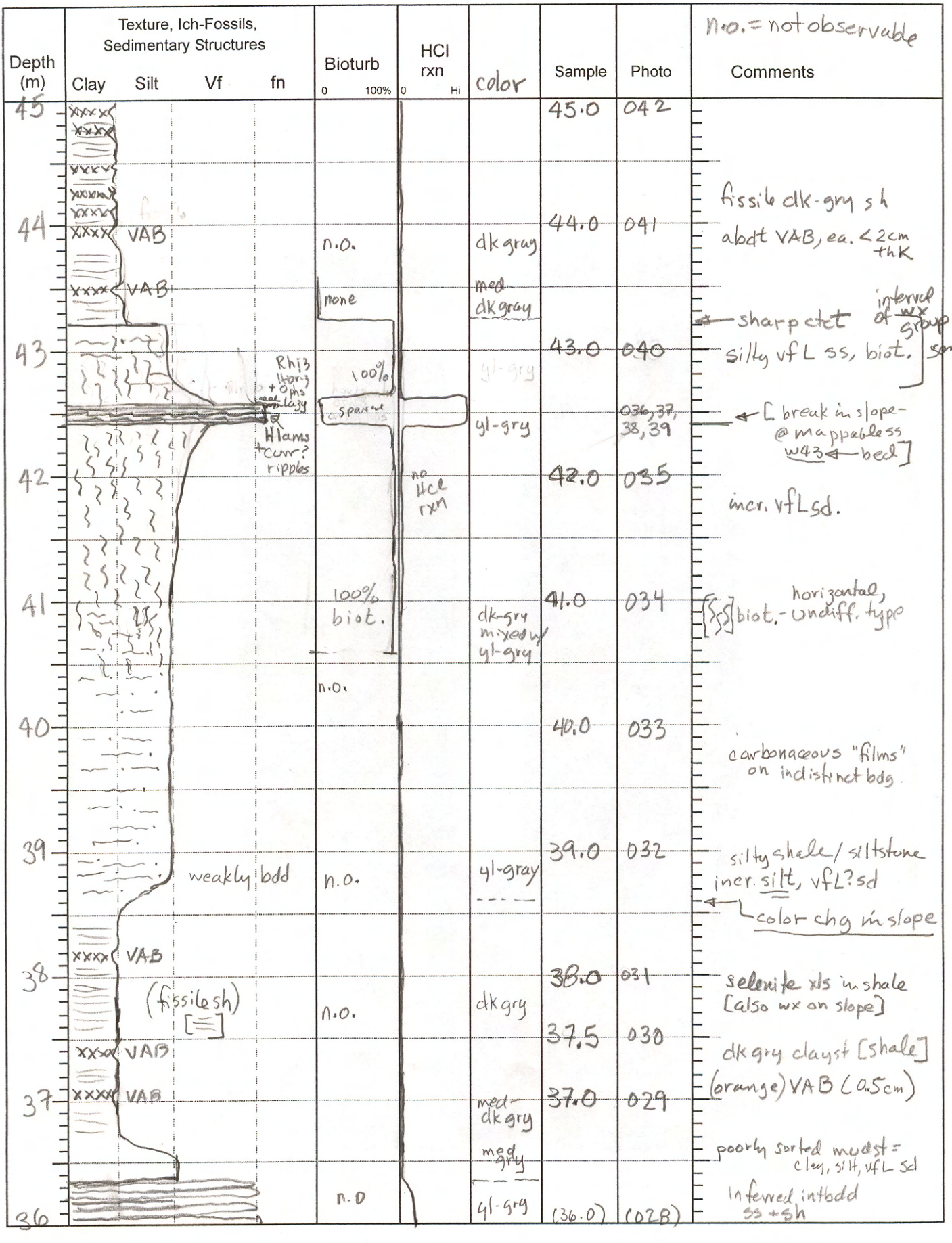

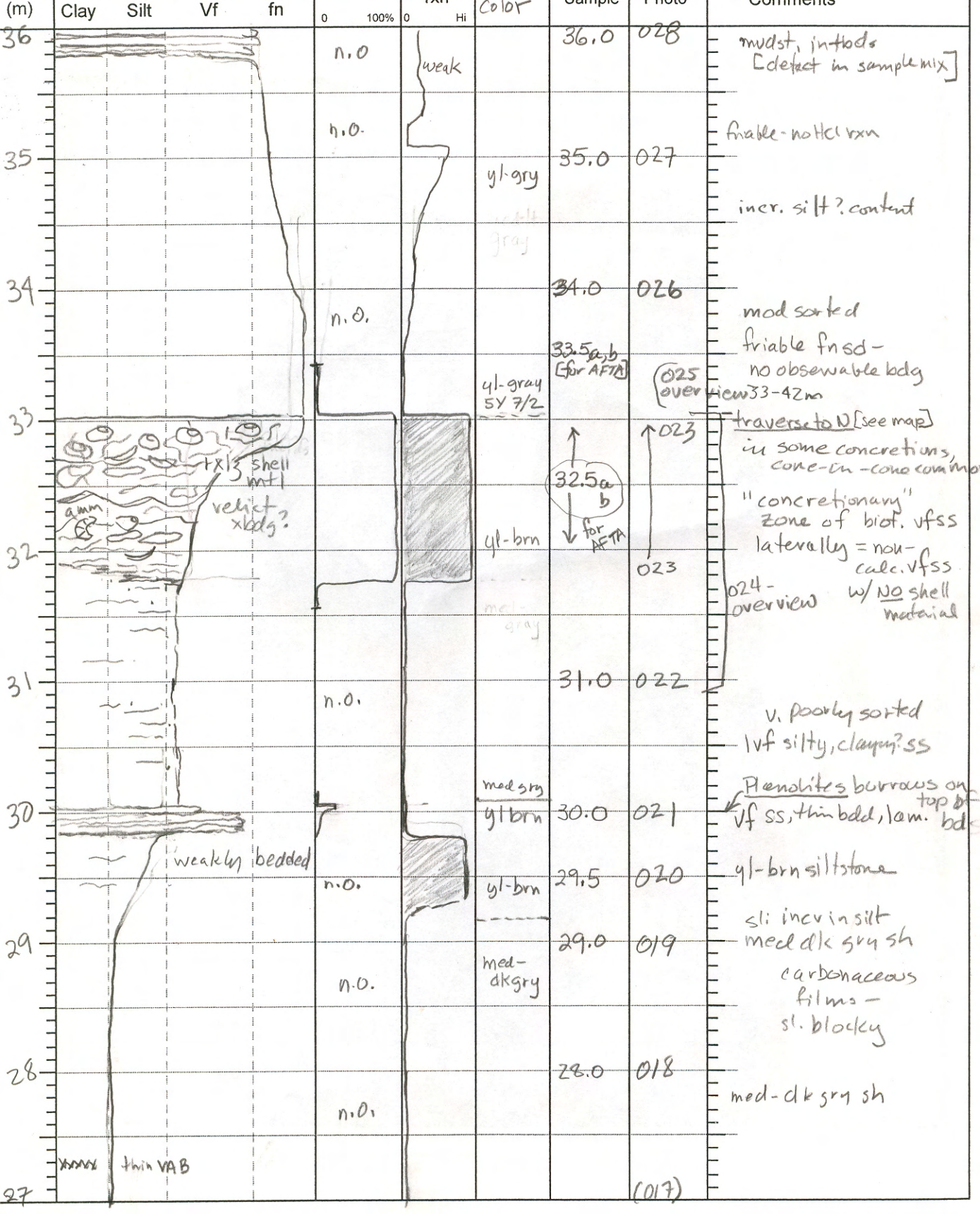
(m)
Clay
Silt
Vf
fn
0
100%
rxn
0
Hi
Color
Sample
Photo
Comments
36
35
34
33
32
31
30
29
28
27
n.o
n.o.
n.o.
n.o.
n.o.
n.o.
n.o.
weak
yl-gry
yl-gray 5Y 7/2
yl-brn
med gry
yl brn
yl-brn
med-dkgry
36.0
35.0
34.0
33.5a,b [for AFTA]
32.5a b
for AFTA
31.0
30.0
29.5
29.0
28.0
028
027
026
025 overview 33-42m
023
023
022
021
020
019
018
(017)
mudst, intbds [defect in sample mix]
friable-no HCl rxn
incr. silt? content
mod sorted
friable fn sd - no observable bdg
traverse to N [see map]
in some concretions, cone-in-cone common
"concretionary" zone of biot. vfss
laterally = non-calc. vfss w/ NO shell material
024 - overview
v. poorly sorted
lvf silty, clayey? ss
Planolites burrows on top of bds
vf ss, thin bdd, lam.
yl-brn siltstone
sl. incr in silt
med dk gry sh
carbonaceous films - sl. blocky
med-dk gry sh
rxlz shell mtl
relict xbdg?
amm
weakly bedded
thin VAB

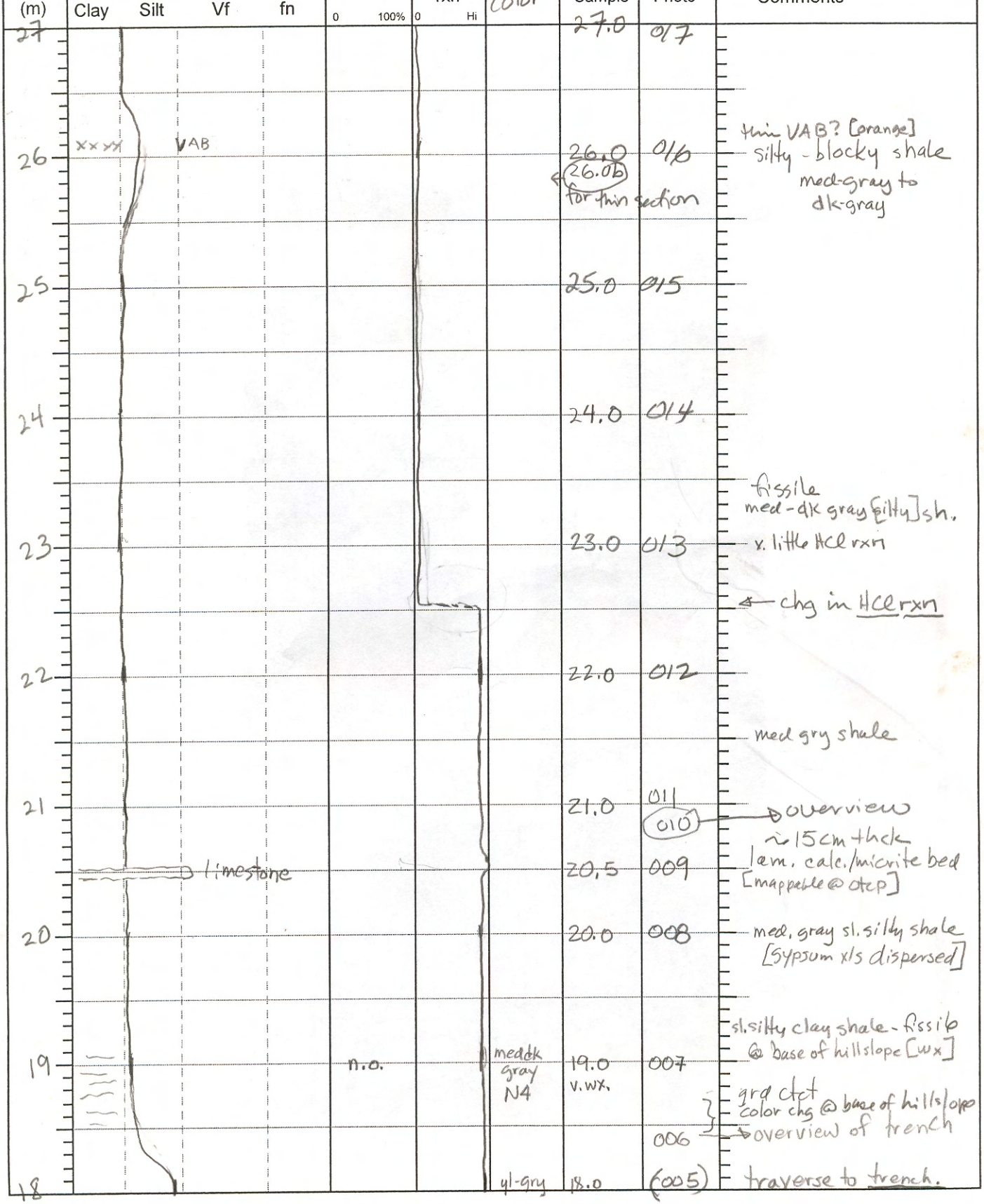
(m)
Clay
Silt
Vf
fn
0
100%
0
Hi
Color
Sample
Photo
Comments
27
26
25
24
23
22
21
20
19
18
xxxx
VAB
limestone
n.o.
med dk gray N4
yl-gry
27.0
26.0
26.0b
for thin section
25.0
24.0
23.0
22.0
21.0
20.5
20.0
19.0
v. wx.
18.0
017
016
015
014
013
012
011
010
009
008
007
006
(005)
thin VAB? [orange]
silty - blocky shale
med-gray to
dk-gray
fissile
med - dk gray [silty] sh.
v. little HCl rxn
chg in HCl rxn
med gry shale
overview
~15cm thck
lam. calc./micrite bed
[mappable @ otcp]
med. gray sl. silty shale
[Sypsum x/s dispersed]
sl. silty clay shale - fissile
@ base of hillslope [wx]
grd ctct
color chg @ base of hillslope
overview of trench
traverse to trench.

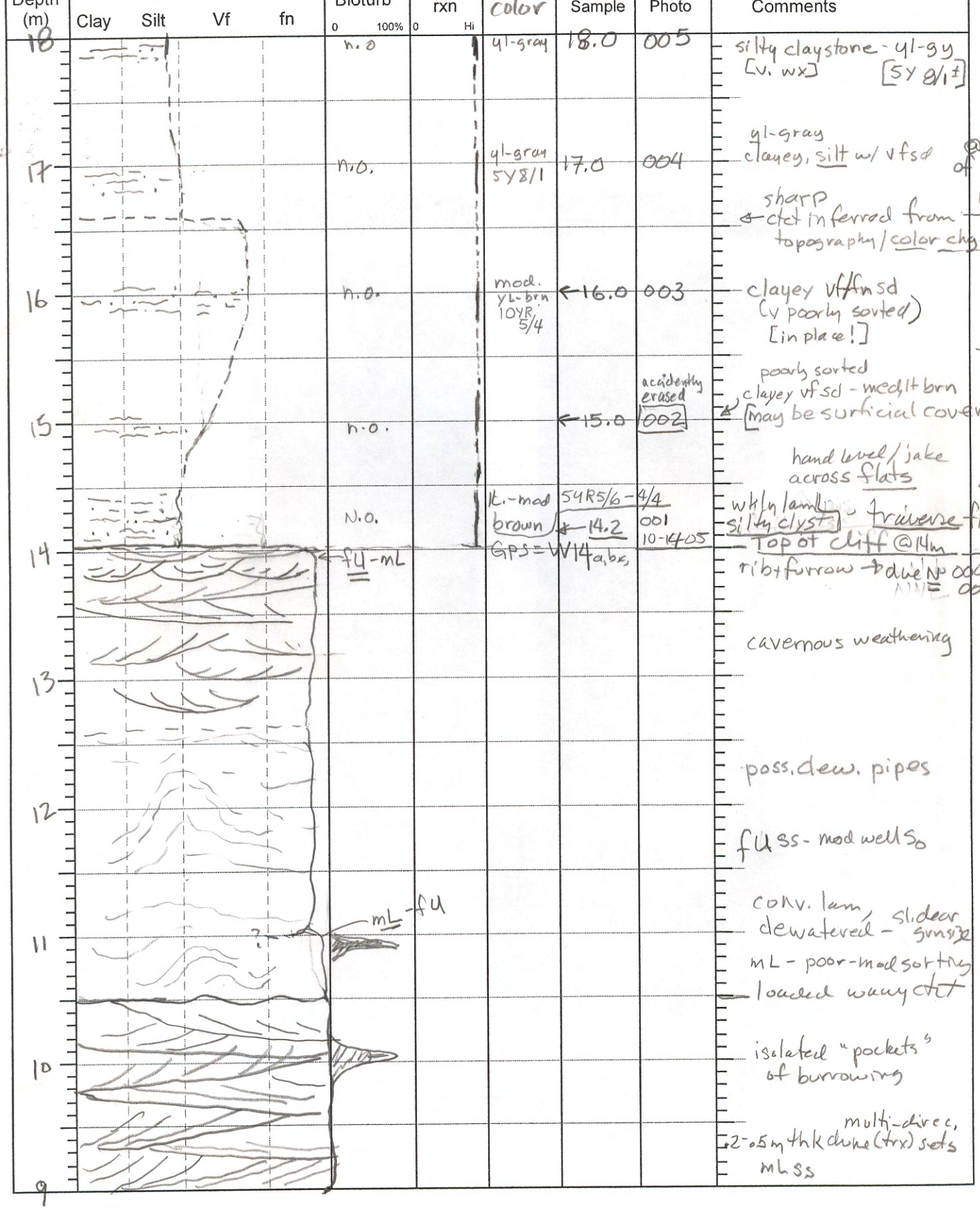
Depth (m)
Clay
Silt
Vf
fn
Bioturb
0
100%
rxn
0
Hi
Color
Sample
Photo
Comments
18
17
16
15
14
13
12
11
10
9
n.o
yl-gray
18.0
005
silty claystone - yl-gy
[v. wx]
[5Y 8/1 ±]
n.o.
yl-gray
5Y8/1
17.0
004
yl-gray
clayey, silt w/ vfsd
@base of phon pole will
sharp
ctct inferred from topography/color chg to yl-
n.o.
mod. yl-brn
10YR 5/4
16.0
003
clayey vf/fn sd
(v poorly sorted)
[in place!]
flats
poorly sorted
clayey vf sd - med lt brn
[may be surficial cover mi
accidently erased
15.0
002
n.o.
hand level/jake across flats
N.O.
lt.-mod brown
5YR5/6-4/4
14.2
001
10-1405
wkly lam
silty clyst
traverse flats
Top of cliff @14m
fU-mL
GPS=W14a,b,c,
rib+furrow → due N 000-001°
cavernous weathering
poss. dew. pipes
fU ss - mod well So
conv. lam, dewatered - sl. clear grn size
mL-fU
mL - poor-mod sorting
loaded wavy ctct
isolated "pockets" of burrowing
multi-direc, .2-.5m thk dune (trx) sets
mL ss

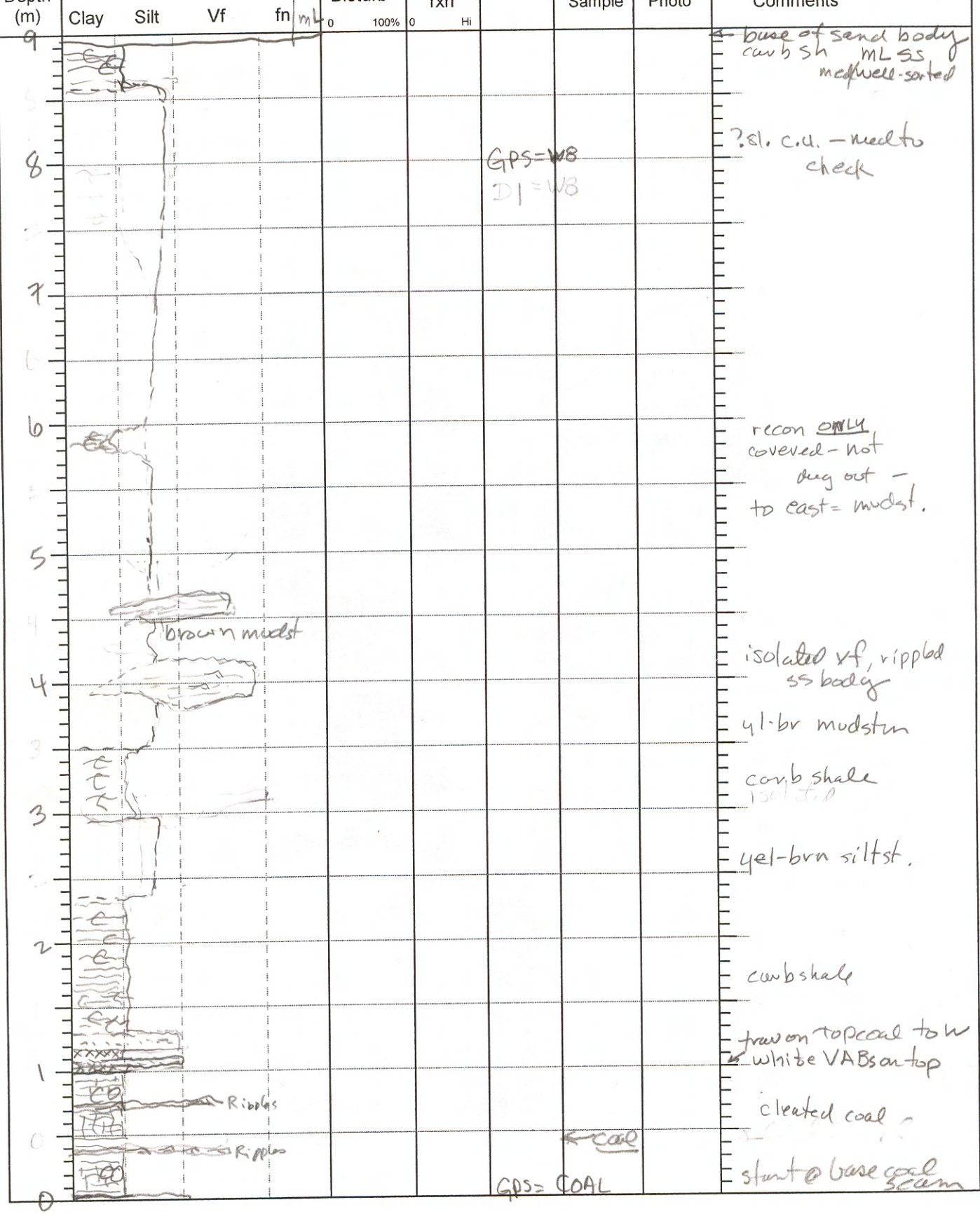
Depth (m)
Clay
Silt
Vf
fn
mL
Distance
0
100%
Txn
0
Hi
Sample
Photo
Comments
9
8
7
6
5
4
3
2
1
0
base of sand body
carb sh
mL ss
med/well-sorted
?sl. c.u. – need to check
GPS=W8
D1=W8
recon ONLY
covered – not dug out –
to east = mudst.
brown mudst
isolated vf, rippled ss body
yl-br mudstn
carb shale
yel-brn siltst.
carb shale
trav on top coal to W
white VABs on top
Ripples
cleated coal
Ripples
coal
GPS= COAL
start @ base coal seam

Westwater Measured Section

Logged By: DSA, LWA

Date: 3-26-05

Depth (m)	Texture, Ich-Fossils, Sedimentary Structures (Clay, Silt, Vf, fn)	Bioturb (0 – 100%)	HCl rxn (0 – Hi)	color	Sample	Photo	Comments
95							
94							
93	soft soil, deeply wx						Top of hill @ USBR benchmark (highest point in otop belt, and thickest strat section position until North of I 70.
92		bjot limited to bases of ripple formsets isolated rare traces - (horiz.)					
91	V. poor exp.						break in slope @ shale
90			none	yl-brn			

Grid	Lat/Lon hddd.ddddd°			
Datum	NAD27 CONUS			
GPS data for Westwater (W) measured section, numbers correspond to meters in section				
Header	Name	Description	Type	Position
Waypoint	WCOAL	10/13/2005 16:02	User Waypoint	N39.10505 W109.15344
Waypoint	W14	10/13/2005 16:42	User Waypoint	N39.10523 W109.15363
Waypoint	W14A	10/13/2005 17:14	User Waypoint	N39.10550 W109.15448
Waypoint	W14B	10/13/2005 17:18	User Waypoint	N39.10636 W109.15454
Waypoint	W14C	10/13/2005 17:20	User Waypoint	N39.10700 W109.15375
Waypoint	W14D	10/13/2005 17:22	User Waypoint	N39.10660 W109.15512
Waypoint	W14E	10/13/2005 17:24	User Waypoint	N39.10731 W109.15557
Waypoint	W14F	10/13/2005 17:26	User Waypoint	N39.10689 W109.15588
Waypoint	W14G	10/13/2005 18:46	User Waypoint	N39.10714 W109.15599
Waypoint	W15	10/13/2005 18:50	User Waypoint	N39.10753 W109.15601
Waypoint	W16	10/13/2005 18:54	User Waypoint	N39.10812 W109.15613
Waypoint	W17	10/13/2005 19:01	User Waypoint	N39.10928 W109.15668
Waypoint	W18A	10/13/2005 19:38	User Waypoint	N39.10936 W109.15672
Waypoint	W19	10/13/2005 20:57	User Waypoint	N39.10990 W109.15727
Waypoint	W21	10/13/2005 19:12	User Waypoint	N39.10952 W109.15674
Waypoint	W23	10/13/2005 20:55	User Waypoint	N39.10998 W109.15722
Waypoint	W26	10/13/2005 20:54	User Waypoint	N39.11003 W109.15719
Waypoint	W29	10/13/2005 20:54	User Waypoint	N39.11008 W109.15716
Waypoint	W30	10/13/2005 20:53	User Waypoint	N39.11009 W109.15715
Waypoint	W31	10/13/2005 20:53	User Waypoint	N39.11011 W109.15713
Waypoint	W32	10/13/2005 20:52	User Waypoint	N39.11015 W109.15710
Waypoint	W33	10/13/2005 20:52	User Waypoint	N39.11019 W109.15705
Waypoint	W33A	10/15/2005 15:06	User Waypoint	N39.11121 W109.15760
Waypoint	W34	10/15/2005 15:56	User Waypoint	N39.11123 W109.15760
Waypoint	W36	10/15/2005 15:55	User Waypoint	N39.11127 W109.15758
Waypoint	W38	10/15/2005 15:54	User Waypoint	N39.11130 W109.15756
Waypoint	W40	10/15/2005 15:54	User Waypoint	N39.11133 W109.15756
Waypoint	W42	10/15/2005 15:53	User Waypoint	N39.11135 W109.15754
Waypoint	W43	10/15/2005 18:57	User Waypoint	N39.11135 W109.15752
Waypoint	W44	10/15/2005 18:58	User Waypoint	N39.11138 W109.15752
Waypoint	W45	10/15/2005 19:00	User Waypoint	N39.11139 W109.15750
Waypoint	W46	10/15/2005 19:00	User Waypoint	N39.11142 W109.15749
Waypoint	W47	10/15/2005 19:01	User Waypoint	N39.11143 W109.15746
Waypoint	W48	10/15/2005 19:01	User Waypoint	N39.11146 W109.15746
Waypoint	W49	10/15/2005 19:02	User Waypoint	N39.11147 W109.15743
Waypoint	W50	10/15/2005 19:02	User Waypoint	N39.11150 W109.15743
Waypoint	W51	10/15/2005 19:03	User Waypoint	N39.11151 W109.15742
Waypoint	W52	10/15/2005 19:03	User Waypoint	N39.11152 W109.15740
Waypoint	W53	10/15/2005 19:04	User Waypoint	N39.11153 W109.15738
Waypoint	W54	10/15/2005 19:04	User Waypoint	N39.11155 W109.15736
Waypoint	W55	10/15/2005 19:05	User Waypoint	N39.11157 W109.15736
Waypoint	W56	10/15/2005 19:05	User Waypoint	N39.11159 W109.15734
Waypoint	W57	10/15/2005 19:06	User Waypoint	N39.11160 W109.15732
Waypoint	W58	10/15/2005 19:06	User Waypoint	N39.11161 W109.15731
Waypoint	W59	10/15/2005 19:07	User Waypoint	N39.11163 W109.15730
Waypoint	W60	10/15/2005 19:07	User Waypoint	N39.11165 W109.15729
Waypoint	W61	10/15/2005 19:08	User Waypoint	N39.11166 W109.15729
Waypoint	W62	10/15/2005 19:08	User Waypoint	N39.11167 W109.15728
Waypoint	W63	10/15/2005 19:09	User Waypoint	N39.11168 W109.15727
Waypoint	W64	10/16/2005 15:55	User Waypoint	N39.11172 W109.15726
Waypoint	W65	10/16/2005 15:55	User Waypoint	N39.11173 W109.15726
Waypoint	W66	10/16/2005 15:56	User Waypoint	N39.11173 W109.15725
Waypoint	W67	10/16/2005 15:56	User Waypoint	N39.11175 W109.15724
Waypoint	W68	10/16/2005 15:57	User Waypoint	N39.11175 W109.15724
Waypoint	W69	10/16/2005 15:57	User Waypoint	N39.11176 W109.15723
Waypoint	W70	10/16/2005 15:59	User Waypoint	N39.11173 W109.15680
Waypoint	W71	10/16/2005 15:59	User Waypoint	N39.11175 W109.15681

Waypoint	W72	10/16/2005 16:00	User Waypoint	N39.11177	W109.15682
Waypoint	W73	10/16/2005 16:00	User Waypoint	N39.11178	W109.15684
Waypoint	W74	10/16/2005 16:01	User Waypoint	N39.11180	W109.15685
Waypoint	W75	10/16/2005 16:01	User Waypoint	N39.11183	W109.15686
Waypoint	W76	10/16/2005 16:02	User Waypoint	N39.11188	W109.15689
Waypoint	W76A	3/26/2006 15:55	User Waypoint	N39.11186	W109.15685
Waypoint	W77	3/26/2006 16:01	User Waypoint	N39.11193	W109.15698
Waypoint	W78	3/26/2006 16:05	User Waypoint	N39.11242	W109.15690
Waypoint	W79	3/26/2006 16:22	User Waypoint	N39.11241	W109.15689
Waypoint	W8	10/13/2005 16:26	User Waypoint	N39.10511	W109.15354
Waypoint	W80	3/26/2006 16:25	User Waypoint	N39.11242	W109.15690
Waypoint	W81	3/26/2006 16:26	User Waypoint	N39.11245	W109.15689
Waypoint	W82	3/26/2006 16:28	User Waypoint	N39.11256	W109.15689
Waypoint	W83	3/26/2006 16:29	User Waypoint	N39.11258	W109.15687
Waypoint	W84	3/26/2006 16:33	User Waypoint	N39.11266	W109.15685
Waypoint	W85	3/26/2006 16:33	User Waypoint	N39.11268	W109.15683
Waypoint	W85A	3/26/2006 20:49	User Waypoint	N39.11310	W109.15618
Waypoint	W86	3/26/2006 16:34	User Waypoint	N39.11271	W109.15684
Waypoint	W86A	3/26/2006 20:54	User Waypoint	N39.11331	W109.15606
Waypoint	W87	3/26/2006 16:37	User Waypoint	N39.11277	W109.15687
Waypoint	W87A	3/26/2006 20:55	User Waypoint	N39.11342	W109.15605
Waypoint	W87B	3/26/2006 21:58	User Waypoint	N39.11345	W109.15636
Waypoint	W87C	3/26/2006 21:58	User Waypoint	N39.11351	W109.15648
Waypoint	W87D	3/26/2006 21:59	User Waypoint	N39.11358	W109.15657
Waypoint	W88	3/26/2006 16:38	User Waypoint	N39.11278	W109.15686
Waypoint	W88A	3/26/2006 21:05	User Waypoint	N39.11344	W109.15607
Waypoint	W88D	3/26/2006 21:59	User Waypoint	N39.11360	W109.15656
Waypoint	W89	3/26/2006 16:38	User Waypoint	N39.11279	W109.15687
Waypoint	W89A	3/26/2006 21:04	User Waypoint	N39.11345	W109.15609
Waypoint	W89D	3/26/2006 22:00	User Waypoint	N39.11361	W109.15654
Waypoint	W9	10/13/2005 16:32	User Waypoint	N39.10514	W109.15356
Waypoint	W90A	3/26/2006 21:04	User Waypoint	N39.11348	W109.15613
Waypoint	W90D	3/26/2006 22:00	User Waypoint	N39.11361	W109.15653
Waypoint	W91A	3/26/2006 21:03	User Waypoint	N39.11351	W109.15615
Waypoint	W92A	3/26/2006 21:03	User Waypoint	N39.11357	W109.15618
Waypoint	W93A	3/26/2006 21:02	User Waypoint	N39.11363	W109.15623
Waypoint	W93USBR	3/26/2006 22:01	User Waypoint	N39.11374	W109.15645

Appendix B

Westwater Measured Section

Outcrop Gamma Ray Raw Data

LAS File

Westwater Outcrop Gamma Ray Raw data

	cps1	cps2	cps3	cps4	cps5	AVG	m (depth)
	52	46	50	42	51	49	93.0
	49	44	60	53	59	54	92.5
	60	53	56	50	56	55	92.0
	66	62	73	69	54	66	91.5
	57	42	56	42	50	49	91.0
	50	60	53	59	75	57	90.5
	77	74	92	74	67	75	90.0
	76	67	56	76	60	68	89.5
	67	70	74	78	69	71	89.0
	71	70	67	78	73	71	88.5
	73	77	67	76	73	74	88.0
	71	69	76	69	68	70	87.5
	79	61	69	62	56	64	87.0
	42	45	38.0	43	41	42	86.5
	45	42	44	40	42	43	86.0
	47	40	45	51	52	48	85.5
	50	44	42	43	42	43	85.0
	48	45	39	43	45	44	84.5
	41	46	36	46	37	41	84.0
	41	43	44	32	39	41	83.5
	52	40	44	44	47	45	83.0
	51	48	53	56	47	51	82.5
	47	47	53	53	48	49	82.0
	57	63	49	54	57	56	81.5
	55	53	59	45	55	54	81.0
	74	78	77	70	81	76	80.5
	69	75	70	78	78	74	80.0
	84	80	82	81	93	82	79.5
	81	86	84	81	77	82	79.0
	80	83	73	84	81	81	78.5
	69	76	67	76	74	73	78.0
	71	69	70	77	80	73	77.5
	58	74	65	59	64	63	77.0
	64	67	61	67	79	66	76.5
	63	51	57	54	64	58	76.0
	85	82	71	79	80	80	75.9
	90	102	119	104	97	101	75.0
	91	84	81	82	76	82	74.0
	108	95	91	89	91	92	73.0
	95	104	97	87	94	95	72.0
	95	72	85	87	92	88	71.0
	92	86	93	81	86	88	70.0
	61	75	65	56	52	61	69.0
	120	110	113	117	119	116	68.0
	140	158	136	146	143	143	67.0
	77	87	80	82	79	80	66.0
	89	82	92	87	91	89	65.0
	66	70	68	76	71	70	64.0
	47	60	59	46	45	51	63.5
	80	85	87	82	91	85	63.0
	82	84	87	83	78	83	62.0

	73	70	80	74	75	74	61.0
	80	74	83	84	82	82	60.0
	86	79	70	81	80	80	59.0
	79	91	75	88	86	84	58.0
	108	104	99	100	95	101	57.0
	94	93	100	87	93	93	56.0
	87	107	105	94	107	102	55.0
	101	110	111	104	100	105	54.0
	107	125	135	134	124	128	53.0
	94	88	90	81	100	91	52.0
	99	91	101	96	92	96	51.0
	94	84	85	86	94	88	50.0
	94	82	88	71	82	84	49.0
	88	92	82	90	76	87	48.0
	89	88	90	100	81	89	47.0
	118	131	117	126	116	120	46.4
	102	104	112	103	95	103	46.0
	93	101	90	95	90	93	45.8
	110	111	98	104	108	107	45.0
	76	75	74	84	81	77	44.0
	47	67	69	70	74	69	43.0
	62	60	70	63	64	63	42.0
	78	88	80	74	85	81	41.0
	81	77	78	71	73	76	40.0
	81	79	82	85	90	83	39.0
	108	90	97	89	99	95	38.0
	101	107	101	105	101	102	37.5
	123	133	124	133	125	127	37.0
	82	93	101	94	85	91	36.0
	67	69	65	77	67	68	35.0
	87	68	69	763	83	80	34.0
	79	70	68	88	69	73	33.2
	45	42	43	49	36	43	33.0
	65	54	62	64	63	63	32.0
	80	73	77	72	71	74	31.0
	68	90	77	76	84	79	30.5
	89	75	78	77	78	78	30.0
	87	88	69	77	79	81	29.5
	99	107	106	108	103	105	29.0
	111	110	108	124	109	110	28.0
	111	133	143	119	137	130	27.0
	103	110	109	107	115	109	26.0
	104	106	101	100	105	103	25.0
	110	106	105	103	114	107	24.0
	100	98	94	107	118	102	23.0
	106	104	111	97	107	106	22.0
	71	59	63	65	57	62	21.5
	95	110	96	107	104	102	21.0
	90	86	92	88	90	89	20.0
	90	94	87	81	88	88	19.0
	74	82	85	84	78	81	18.8
	68	67	76	77	69	71	18.0

	69	64	80	70	77	72	17.0
	65	67	65	57	69	66	16.0
	72	58	62	67	61	63	15.0
	49	48	55	53	50	51	14.2
	18	20	23	31	29	24	14.0
	29	27	25	28	33	28	13.5
	25	31	30	31	24	29	13.0
	24	33	28	38	30	30	12.0
	33	27	29	32	39	31	11.0
	42	39	37	44	39	40	10.0
	45	57	50	53	45	49	9.0
	48	54	63	56	63	58	8.0
	37	39	62	68	56	52	7.0
	53	48	55	50	52	52	6.0
	63	80	62	60	79	68	5.0
	87	111	97	86	103	96	4.0
	129	105	129	113	112	118	3.0
	99	100	95	81	99	98	2.0
	92	91	82	84	95	89	1.2
	71	81	77	63	76	75	1.0
	71	81	77	63	76	75	0.5
	136	139	153	141	137	139	0.0

```
~Version Information
 VERS.                 2.0:
 WRAP.                  NO:
 END.               PETRA:GeoPLUS Corporation
~Well Information Block
#MNEM.UNIT       Data Type    Information
#---------    -------------   ---------------------------------
 STRT.F            80.0000:
 STOP.F           327.0000:
 STEP.F             1.0000:
 NULL.            -999.25:
 COMP.                        : COMPANY
 FLD.                        : FIELD
 LOC.                        : LOCATION
 DATE.      31-MAY-2006          : DATE
 WELL.      Westwater            : Well Name
 LABL.      019S025E33                    : Well Label
 APIN.      WESTWATER            : API Number
 UWI.       WESTWATER            : Unique Well Number
~Parameter Block
#MNEM.UNIT           VALUE            Description
#---------    --------------------   --------------------------------
 EKB.F                 4641.0 : KB Elevation
~Curve Information Block
#MNEM.UNIT      API CODE      Curve Description
#---------    -------------   ---------------------------------
 DEPT.F                 00 000 00 00: Depth (MD)
 GR.GAPI                 00 001 00 00: NATURAL GAMMA
~A       DEPT          GR
       80.000     100.804
       81.000      94.475
       82.000      94.003
       83.000      92.871
       84.000      84.399
       85.000      82.129
       86.000      85.894
       87.000      86.388
       88.000      86.571
       89.000      86.755
       90.000      87.522
       91.000      88.585
       92.000      88.576
       93.000      87.016
       94.000      82.731
       95.000      82.717
       96.000      82.717
       97.000      82.473
       98.000      81.812
       99.000      80.623
      100.000      71.087
      101.000      55.986
      102.000      56.359
```

103.000	71.696
104.000	106.811
105.000	87.304
106.000	98.761
107.000	129.481
108.000	113.383
109.000	82.309
110.000	78.766
111.000	75.452
112.000	75.039
113.000	77.621
114.000	81.562
115.000	74.123
116.000	68.411
117.000	62.666
118.000	55.449
119.000	50.076
120.000	68.844
121.000	78.882
122.000	78.629
123.000	77.823
124.000	77.180
125.000	76.537
126.000	74.042
127.000	69.783
128.000	73.207
129.000	76.632
130.000	76.598
131.000	76.506
132.000	76.151
133.000	75.404
134.000	75.024
135.000	76.057
136.000	77.091
137.000	78.124
138.000	79.373
139.000	82.997
140.000	90.574
141.000	91.670
142.000	88.826
143.000	87.985
144.000	87.847
145.000	89.572
146.000	93.016
147.000	95.718
148.000	97.202
149.000	98.029
150.000	99.717
151.000	103.758
152.000	107.799
153.000	113.492
154.000	112.722

155.000	88.742
156.000	86.380
157.000	85.599
158.000	87.983
159.000	88.500
160.000	88.897
161.000	87.308
162.000	85.718
163.000	84.129
164.000	82.588
165.000	81.183
166.000	79.778
167.000	79.092
168.000	79.769
169.000	80.445
170.000	81.119
171.000	81.780
172.000	82.442
173.000	85.219
174.000	97.914
175.000	106.940
176.000	106.081
177.000	92.158
178.000	90.162
179.000	96.472
180.000	99.641
181.000	98.537
182.000	84.935
183.000	70.401
184.000	67.921
185.000	65.623
186.000	63.852
187.000	62.150
188.000	60.704
189.000	59.257
190.000	59.932
191.000	61.841
192.000	70.107
193.000	74.395
194.000	76.280
195.000	75.802
196.000	72.165
197.000	70.538
198.000	72.755
199.000	77.794
200.000	81.227
201.000	84.660
202.000	88.094
203.000	91.360
204.000	94.430
205.000	100.008
206.000	117.140

207.000	97.994
208.000	86.697
209.000	85.974
210.000	81.331
211.000	63.763
212.000	63.267
213.000	64.164
214.000	65.345
215.000	67.441
216.000	69.650
217.000	68.469
218.000	67.289
219.000	48.855
220.000	41.249
221.000	43.953
222.000	57.178
223.000	61.439
224.000	64.820
225.000	68.202
226.000	71.047
227.000	73.665
228.000	73.107
229.000	72.383
230.000	74.059
231.000	77.228
232.000	89.533
233.000	98.286
234.000	99.801
235.000	101.814
236.000	102.974
237.000	102.974
238.000	105.349
239.000	120.640
240.000	111.290
241.000	103.579
242.000	102.063
243.000	100.179
244.000	98.325
245.000	97.361
246.000	97.380
247.000	98.143
248.000	98.906
249.000	99.669
250.000	98.484
251.000	96.739
252.000	95.438
253.000	96.641
254.000	97.843
255.000	99.045
256.000	80.334
257.000	58.119
258.000	71.410

259.000	91.804
260.000	84.502
261.000	82.425
262.000	82.700
263.000	82.927
264.000	82.431
265.000	82.435
266.000	81.029
267.000	71.694
268.000	68.388
269.000	66.285
270.000	65.413
271.000	66.377
272.000	66.585
273.000	65.116
274.000	63.647
275.000	60.354
276.000	59.360
277.000	59.106
278.000	58.851
279.000	58.523
280.000	53.747
281.000	48.971
282.000	21.922
283.000	24.126
284.000	25.727
285.000	26.199
286.000	26.559
287.000	26.662
288.000	26.766
289.000	28.095
290.000	27.785
291.000	27.671
292.000	30.977
293.000	36.900
294.000	37.176
295.000	37.451
296.000	39.024
297.000	42.661
298.000	46.183
299.000	50.041
300.000	53.537
301.000	53.537
302.000	52.244
303.000	50.709
304.000	49.520
305.000	48.465
306.000	48.315
307.000	48.165
308.000	48.014
309.000	49.181
310.000	50.598

311.000	59.565
312.000	70.286
313.000	77.725
314.000	85.164
315.000	89.760
316.000	90.448
317.000	96.931
318.000	106.259
319.000	97.957
320.000	92.239
321.000	90.187
322.000	87.707
323.000	85.228
324.000	77.087
325.000	70.961
326.000	71.473
327.000	113.462

Appendix C

Palynological Report

Larsen State-1 well

Dr. Gerald Waanders

Consulting Palynologist

Gerald Waanders
Consulting Palynologist

1475 Rancho Encinitas Drive
Encinitas, California 92024-7031
Phone: (858) 759-0180
FAX: (858) 759-9028
Email: waanpaly@adelphia.net

May 16, 2006

TO: Mr. Craig D. Morgan
Utah Geological Survey,
P.O.Box 146100
Salt Lake City, UT 84114

Ms. Donna S. Anderson, Ph.D.
Dept. Geology & Geological Engineering
Colorado School of Mines
Golden, CO 80401

RE: Palynology and Thermal Maturation Analysis of 12 composite samples from the Linn Brothers, Larsen State #1 Well, Sec. 2, T20S-R24E, Grand Co., Utah. The interval examined ranges from 473-1105' .

PALYNOLOGY AND THERMAL MATURATION REPORT

The data generated from the analysis of these samples is presented in the attached Figures 1 and 2 and summarized in the following paragraphs.

473-804'

Age: **Coniacian**

Environment: **Nearshore Open Marine**

T.A.I.: **0.4-0.5% Estimated R_0**

This interval is represented by a diverse assemblage of dinoflagellate cysts. Frequent to common occurrences of *Hystrichodinium pulchrum, Palaeohystrichophora infusorioides, Odontochitina costata* and *Surculosphaeridium longifurcatum* suggest a Coniacian age. The high diversities of dinoflagellate species indicate an open marine paleoenvironment for the interval. The kerogens, however, are mixed with fairly high concentrations of land derived, woody materials along with moderate diversities of spores and pollen suggesting nearshore conditions.

The late Cretaceous aged palynomorphs in these samples are light brown in color and estimated to be at a maturation level of 0.4-0.5 R_0 or at the threshold of peak oil generation. The recycled palynomorphs (Late Devonian to Mississippian) in the interval may be of a slightly higher maturation level. The organic recoveries for the samples in this interval were all very good and worthy of checking for source rock potential. The kerogens were mixed and indicate potential for both oil and gas generation.

804-880'

Age:	**Coniacian**
Environment:	**Restricted Marine or Lacustrine**
T.A.I.:	**0.4-0.4% Estimated R_0**

When compared to the interval described above, this unit shows a distinct drop in species diversities, a shift to higher relative concentrations of amorphous kerogens and probably a somewhat higher total organic recovery in the samples. Higher organic recoveries coupled with increased concentrations of amorphous kerogens suggest quieter water (possibly deeper) with reducing conditions. The reduction in microplankton diversity, however, indicates a restricted marine or possibly basinal lacustrine paleoenvironment.

Thermal alteration values are unchanged from above. The overall kerogen content is mostly amorphous or oil generating.

900-1087'

Age:	**Coniacian**
Environment:	**Nearshore Open Marine**
T.A.I.:	**0.4-0.5 Estimated R_0**

The paleoenvironment for this interval is the same as noted higher in the well at 473-804' where open marine conditions are suggested by higher dinoflagellate diversities and a nearshore conditions are indicated by increased amounts of terrestrial kerogens and higher numbers of spores and pollen.

The late Cretaceous aged palynomorphs in these samples are light brown in color and estimated to be at a maturation level of 0.4-0.5 R_0 or at the threshold of peak oil generation. The recycled palynomorphs in the interval may be of a slightly higher maturation level. The organic recoveries for the samples in this interval were good to very good and worthy of checking for source rock potential. The kerogens were mixed and indicate potential for both oil and gas generation.

1100-1105'

Age:	**Turonian?**
Environment:	**Deltaic/ Estuarine**
T.A.I.:	**0.4-0.5 Estimated R_0**

There was a gap in samples from 1087-1100' and this deepest interval is represented by only one 5' sample. It contains the first occurrences of *Appendicisporites matesovae* and *Trilobosporites marylandensis* and they would normally suggest an age at least as old as Turonian. However, the age of the sample is problematic because it also contains several recycled Late Devonian to Mississippian aged spores and we are left wondering whether or not these older Cretaceous taxa might be recycled as well. Increased spore/pollen diversities and decreased microplankton diversities suggest a paleoenvironment that is somewhat shallower than the interval above. The thermal maturation, kerogen quality and total organic recovery for this sample are all similar to the interval above.

Analysis By:

_____

Gerald Waanders

Gerald Waanders
Consulting Palynologist

Figure 1

5/17/2006

Spores

Age	Depth	Araucariacites australis	Cicatricosisporites dorogensis	Cingulatisporites spp.	Deltoidospora spp.	Exesipollenites tumulus	Gleicheniidites senonicus	Matonisporites equiexinus	Taxodiaceae	Undifferentiated Bisaccates	Acanthotriletes varispinosus	Cicatricosisporites australiensis	Densosporites sp. (reworked)	Leptolepidites verrucosus	Lycopodiumsporites spp.	Quadripollis krempii	Tsugaepollenites sp.	Appendicisporites potomacensis	Classopollis classoides	Punctatosporites scabratus	Taurocusporites segmentatus	Tricolpites sagax
Coniacian	473-522	**C**	R	R	R	R	R	R	**F**	R												
	522-530	R			R			R	R	R	R	R	R*	R	R	R	R					
	575-642	F	R		R	R	R		**A**	R		R				R	R	R	R	R	R	R
	642-725	R	R	R	R	R			**A**	R			R*		R		R			R		
	733-804	R			R		R		**A**	R			R*			R			R			
	804-841								R			R								R		
	841-880	R				R																
	900-954	R										R							R			
	954-1007	R			R				R	R	R	R					R		R			
	1007-1053	R								R									R			
	1053-1087						R			R			R*						R			
Turonian?	1100-1105				R					R		R										

Depth	Camarozonosporites spp.	Nevesisporites semiscalaris	Stereisporites spp.	Cicatricosisporites crassiterminatus	Foraminisporis dailyi	Gabonisporis sp.	Klukisporites sp.	Perotrilites sp.	Stereisporites congruens	Cicatricosisporites venustus	Foveotriletes sp.	Rugubivesiculites reductus	Punctatisporites spp. (reworked)	Tripartites vetustus (reworked)	Dictyotriletes sp. (reworked)	Aequitriradites ornatus	Appendicisporites matesovae	Calamospora sp. (reworked)	Knoxisporites sp. (reworked)	Schulzospora rara (reworked)	Trilobosporites marylandensis
473-522																					
522-530																					
575-642																					
642-725	R	R	R																		
733-804	R			R	R	R	R	R	R												
804-841																					
841-880	R									R	R										
900-954									R			R									
954-1007	R		R																		
1007-1053													R*	R*							
1053-1087	R												R*		R*						
1100-1105	R		R										R*			R	R	R*	R*	R*	R

Marine Taxa

Depth	Canningia sp.	Chatangiella victoriensis	Chlamydophorella nyei	Coronifera oceanica	Exochosphaeridium bifidum	Exochosphaeridium spp.	Foveosphaera sp. A	Florentinia stellata	Glaphrocysta retiintexta	Hystrichodinium pulchrum	Hystrichosphaeridium tubiferum	Impletosphaeridium spp.	Isabelidinium acuminatum	Palaeohystrichophora infusorioides	Palaeoperidinium pyrophorum	Odontochitina costata	Oligosphaeridium complex	Senoniasphaera protrusa	Spiniferites cingulatus	Spiniferites ramosus
473-522	R	**F**	R	R	R	**F**	R	R	**F**	**F**	R	**F**	R	**F**	R	**F**	**F**	R	R	**C**
522-530	R	R	R	R	R	**F**		R	**F**	R		**C**	R	**F**	**F**	**F**	R	R		**C**
575-642	R	**F**		R		**F**						**F**		**F**	**F**	**F**	R	R		R
642-725		**F**				R		R		R			R	R	R	**C**	R	R		R
733-804		R				R				R		R				**F**				R
804-841																R				
841-880												R								
900-954						R						R	R	R			R			R
954-1007						R						**F**	R	R			R	R		R
1007-1053										R		**F**	R				R			**F**
1053-1087						**F**		R		R		**F**		R			R		**F**	**F**
1100-1105						R									R		R			R

Depth	Spiniferites scabrosus	Surculosphaeridium longifurcatum	Tasmanaceae (reworked?)	Adnatosphaeridium reticulense	Cyclonephelium distinctum	Florentinia cooksoniae	Microforaminifera linings	Cribroperidinium edwardsi	Michrystridium spp. (reworked?)	Coronifera striolatum	Polysphaeridium sp.	Scolecodont sp. (reworked)	Cordosphaeridium sp.	Lanterna sp.	Baltisphaeridium sp. (reworked?)	Spinidinium echinoideum	Cannosphaeropsis sp.	Cyclonephelium vannophorum	Trichodinium castanea
473-522	**F**	**C**	R*																
522-530		**F**	R*	**F**	R	R	R												
575-642		**C**		**A**	R		R	R	R*										
642-725		R	R*	**A**		R	R		R*	R	R	R*							
733-804		R		**A**	R	R	R						R	R					
804-841			R*				R												
841-880			R*																
900-954		R		R	R		R	R							R*	R			
954-1007		R			**C**	R	R	**F**									R	R	R
1007-1053		**F**		R	R	R	R	R											
1053-1087		R	R*		R		R	R											
1100-1105				R			R												R

Linn Brothers Oil & Gas Inc
Larsen State 1
API 4301915317
nenw section 2, T. 20 S., R. 24 E., 660 FNL 1980 FWL
Grand Co., Utah
Greater Cisco Field, Morrison oil well
UTM 652956, 4329364
Lat/Long 39.10188, -109.23116

R = Rare, less than 6 specimens/slide
F = Frequent, 6-15 specimens/slide
C = Common, 16-30 specimens/slide
A = Abundant, over 30 specimens/slide

* = Recycled palynomorph

1475 Rancho Encinitas Drive, Encinitas, CA 92024
(858) 759-0180, FAX: (858) 759-9028, waanpaly@adelphia.net

Gerald Waanders
Consulting Palynologist

Figure 2

5/17/2006

Age	Depth	HCl Reaction	T.A.I.	Kerogen Distribution: Amorphous	Cuticular	Woody/Inertinite	Organic Recovery	Kerogen Content	Taxa Distribution: Spores	Marine taxa	Species Diversity	Paleoenvironment
								0% 20% 40% 60% 80% 100%			0 10 20 30	
Coniacian	473-522	Strong	0.3-0.4	30%	20%	50%	Very Good		9	22		Nearshore Open Marine Shelf
	522-530	Strong	0.3-0.4	50%	20%	30%	Very Good		11	22		
	575-642	Strong	0.3-0.4	40%	20%	40%	Very Good		15	16		
	642-725	Strong	0.3-0.4	60%	10%	30%	Very Good		13	17		
	733-804	Strong	0.4-0.5	65%	10%	25%	Very Good		14	13		
	804-841	Strong	0.4-0.5	80%	10%	10%	Very Good		3	2		Restricted Marine/ Lacustrine
	841-880	Weak	0.4-0.5	80%	10%	10%	Very Good		5	1		
	900-954	Weak	0.4-0.5	70%	15%	15%	Very Good		5	12		Nearshore Open Marine Shelf
	954-1007	Weak	0.4-0.5	50%	20%	30%	Very Good		10	15		
	1007-1053	Weak	0.4-0.5	35%	15%	50%	Good		3	11		
	1053-1087	Strong	0.4-0.5	35%	15%	50%	Good		4	12		
Turonian?	1100-1105	Strong	0.4-0.5	40%	20%	40%	Very Good		8	7		Estuarine/Deltaic

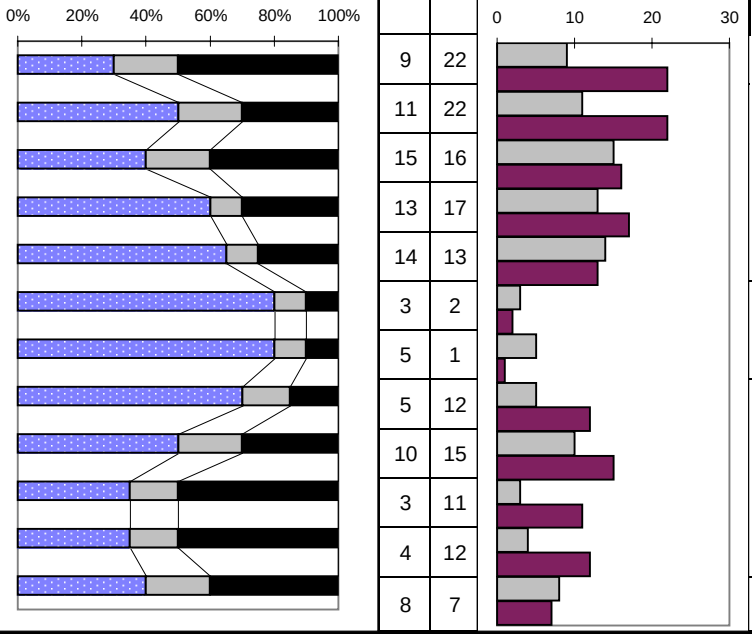

Linn Brothers Oil & Gas Inc
Larsen State 1
API 4301915317
nenw section 2, T. 20 S., R. 24 E., 660 FNL 1980 FWL
Grand County Co., Utah
Greater Cisco Field, Morrison oil well
UTM 652956, 4329364
Lat/Long 39.10188, -109.23116

1475 Rancho Encinitas Drive, Encinitas, CA 92024
(858) 759-0180, FAX: (858) 759-9028, waanpaly@adelphia.net

Appendix D

Digital Tops and “Pay zones” Database (on CD)

						FMTOPS	FMTOPS	FMTOPS	FMTOPS	FMTOPS	FMTOPS
UWI (APINum)	Surf Lat	Surf Lon	Section	Township	Range	F1	F2	F3	FJL	FJ1	FJLM
43047301110000	40.015890	-109.659200	22	9S	20E	14993	15207	15290	15336	15401	
43047301450000	39.953660	-109.620330	13	10S	20E	14362	14576	14661	14707	14768	14847
43007300490001	39.723920	-110.124640	33	12S	16E	12510	12673	12768	12826	12881	12949
43047303570000	39.764600	-109.434810	22	12S	22E	10825	11045		11203	11265	11324
43047316740000	39.807860	-109.079380	2	12S	25E	7356	7613	7672	7716	7766	7827
43047156720000	39.802710	-109.088130	2	12S	25E	7482	7705		7830	7890	7939
43047315970000	39.776510	-109.056780	13	12S	25E	6814	7072	7128	7169	7222	7272
43047315100000	39.710230	-109.656960	3	13S	20E	11183	11386	11470	11534	11589	11656
43047301700000	39.677560	-109.597290	20	13S	21E	10447	10660		10806	10865	10929
43047301430000	39.653980	-109.554700	27	13S	21E	9056	9268	9354	9409	9467	9530
43047334480000	39.637460	-109.592540	32	13S	21E	10048	10245		10359	10416	10470
43047334450000	39.641840	-109.592120	32	13S	21E	10108	10312		10452	10515	10569
43047334470000	39.638350	-109.596490	32	13S	21E	10092	10294	10382	10436	10496	10549
43047301650000	39.702490	-109.424030	11	13S	22E	10121	10347		10502	10559	10612
43047301660000	39.674740	-109.441740	22	13S	22E	9285	9492		9642	9697	9753
43047301680000	39.673940	-109.405060	24	13S	22E	9567	9773	9867	9915	9977	10033
43047302760000	39.658870	-109.423450	26	13S	22E	9224	9442	9526	9573	9629	9687
43047303860000	39.648700	-109.324260	34	13S	23E	8961	9182	9272	9310	9373	9429
43047307730000	39.645130	-109.256310	32	13S	24E	8622	8861				
43047312310000	39.690610	-109.106290	15	13S	25E	7653	7901		8000	8053	8109
43047307880000	39.648630	-109.073360	36	13S	25E	7273	7489		7587	7651	7694
43047335950000	39.568510	-109.689620	28	14S	20E	10109	10269		10425	10483	10539
43047336160000	39.565010	-109.699310	29	14S	20E	9990	10151		10302	10358	10412
43047336170000	39.564870	-109.694310	29	14S	20E						
43047335960000	39.565390	-109.712320	30	14S	20E	9986	10156	10239	10298	10355	10407
43047336180000	39.561200	-109.698560	32	14S	20E						
43047335570000	39.560970	-109.694200	32	14S	20E						
43047333370000	39.557620	-109.699060	32	14S	20E	9964			10276		10385
43047336190000	39.557800	-109.694570	32	14S	20E						
43047333330000	39.561230	-109.708360	32	14S	20E	9943	10095		10253	10309	10362
43047335580000	39.553980	-109.708960	32	14S	20E						
43047336210000	39.553990	-109.703720	32	14S	20E	9898	10037		10202	10260	10316
43047105770001	39.553990	-109.694410	32	14S	20E						
43047336200000	39.553990	-109.699100	32	14S	20E						
43047340980000	39.550360	-109.694460	32	14S	20E	9897	10040		10208	10262	10313

UWI (APINum)	Surf Lat	Surf Lon	Section	Township	Range	F1	F2	F3	FJL	FJ1	FJLM
43047301350000	39.630890	-109.433460	3	14S	22E	8961	9176	9266	9312	9367	9428
43047309600000	39.604780	-109.461490	16	14S	22E	8271	8466	8560	8598	8653	8713
43047310630000	39.583870	-109.471040	20	14S	22E	7601	7782	7879	7915	7976	8032
43047302710000	39.590910	-109.363450	20	14S	23E	8357	8569	8651	8698	8760	8810
43047309780000	39.576480	-109.297560	25	14S	23E	8161	8346	8422	8462	8516	8569
43047309760000	39.585080	-109.189310	23	14S	24E	7721	7937	8009	8043	8105	8157
43047106920000	39.612560	-109.143670	8	14S	25E	6442	6657	6732	6767	6827	6874
43047050290000	39.580170	-109.110520	22	14S	25E	6144	6374		6468	6528	6571
43047318940000	39.565860	-109.072370	25	14S	25E	6913	7120	7178	7219	7279	7326
43047311370000	39.511260	-109.522120	13	15S	21E	8926	9093	9174	9213	9268	9323
43047310710000	39.510850	-109.548980	15	15S	21E	9066	9241	9300	9355	9414	9471
43047314960000	39.478360	-109.398070	25	15S	22E	7900	8069	8148	8184	8239	8294
43047161980000	39.480920	-109.415820	26	15S	22E	7589	7760	7810	7848	7902	7959
43047310430000	39.537390	-109.355090	4	15S	23E	7775	7959	8030	8064	8123	8175
43047306180000	39.518700	-109.335480	15	15S	23E	7552	7730	7801	7835	7891	7945
43047304480000	39.524050	-109.238240	9	15S	24E	7818	8009	8079	8112	8168	8224
43047302480000	39.478050	-109.246480	29	15S	24E	7077	7266	7336	7369	7422	7478
43047310120000	39.507380	-109.167140	18	15S	25E	7696	7899	7962	7998	8062	8115
43019100890000	39.465730	-109.164840	31	15S	25E	6904	7091	7156	7187	7245	7295
43015103740000	39.396450	-110.316040	25	16S	14E	4119	4276	4366	4408	4461	4511
43015300220000	39.465150	-110.236150	3	16S	15E	7704	7867	7964	8021	8072	8121
43015300800000	39.413500	-110.188440	24	16S	15E	6671	6841	6927	6971	7032	7081
43015301980000	39.458970	-110.145060	4	16S	16E	11583	11754	11836	11888	11942	11993
43019108060000	39.402960	-109.590790	22	16S	21E	9070	9230	9313	9349	9402	9455
43019306530000	39.421550	-109.491470	16	16S	22E	8963	9123	9198	9248	9304	9356
43019311480000	39.431720	-109.352690	11	16S	23E	7499	7664	7738	7771	7822	7874
43019302400000	39.443470	-109.230220	2	16S	24E	6797	6983	7052	7085	7139	7193
43019307040000	39.370260	-109.206030	31	16S	25E	4639	4817	4881	4912	4964	5016
43019313180000	39.376200	-109.081170	31	16S	26E	3274	3445	3513	3545	3599	3645
43015109280000	39.316100	-110.367100	29	17S	14E						386
43015108000000	39.319830	-110.124470	27	17S	16E	4124	4252		4390	4446	4493
43019156730000	39.357340	-109.604260	4	17S	21E	9059	9212	9295	9340	9395	9448
43019307060000	39.327250	-109.560270	14	17S	21E	8794	8937	9005	9050	9105	9154
43019306820000	39.334190	-109.626070	17	17S	21E	9035	9169	9247	9295	9349	9400
43019159350000	39.330780	-109.453370	14	17S	22E	6451	6609	6684	6726	6782	6837
43019159330000	39.339660	-109.397760	8	17S	23E	5260	5420		5518	5575	5627

UWI (APINum)	Surf Lat	Surf Lon	Section	Township	Range	F1	F2	F3	FJL	FJ1	FJLM
43019307080000	39.337310	-109.375070	9	17S	23E	4766	4950	5010	5053		5119
43019308950000	39.348030	-109.324360	12	17S	23E	4310	4485	4547	4579	4633	4686
43019305710000	39.353140	-109.229340	2	17S	24E						
43019201540000	39.360490	-109.293990	6	17S	24E	5571	5763	5827	5862	5917	5971
43019307730000	39.338960	-109.191170	7	17S	25E	3650	3827	3891	3924	3976	4030
43019150220000	39.341120	-109.100250	12	17S	25E	2366			2632		2732
43019310140000	39.296530	-109.128390	27	17S	25E	2003	2160	2223	2254	2300	2357
43019104630000	39.296200	-109.193350	30	17S	25E						
43015301990000	39.289850	-110.195850	1	18S	15E	5578	5718	5817	5857	5899	5947
43015052110000	39.248920	-110.285600	19	18S	15E	2428	2550		2701	2752	2806
43015301130000	39.294860	-110.176620	6	18S	16E	5331			5629	5681	5731
43015300140000	39.279150	-110.161230	8	18S	16E	5357	5481	5568	5619	5665	5716
43019303980000	39.232040	-109.686750	23	18S	20E	8201	8334	8415	8452	8506	8554
43019055910000	39.206110	-109.501590	29	18S	22E	4897	5052	5127	5165	5209	5260
43019307720000	39.263930	-109.317650	1	18S	23E	4119	4283	4345	4380	4435	4489
43019304930000	39.265150	-109.276180	5	18S	24E	3128	3297		3374	3429	3481
43019114330000	39.261920	-109.248760	10	18S	24E	2335	2506	2567	2604	2650	2703
43019310690000	39.221570	-109.193250	19	18S	25E	408	575	627	660	708	765
43019310720000	39.221590	-109.160130	21	18S	25E	429	589	638	672	718	769
43015300010000	39.179000	-110.314690	11	19S	14E	1347	1478		1612	1659	1708
43015105030000	39.128220	-110.323300	35	19S	14E	258	367		517	565	605
43015300210000	39.164380	-110.195880	14	19S	15E	3858	3989	4074	4129	4184	4229
43019308350000	39.124030	-110.021210	33	19S	17E	3994	4133	4214	4276	4319	4364
43019110130000	39.121490	-109.872900	36	19S	18E	4745	4887		5029	5074	5117
43019308090000	39.178550	-109.795700	2	19S	19E	6436	6592	6671	6716	6757	6805
43019308040000	39.157470	-109.835940	16	19S	19E	5506	5659	5727	5786	5828	5874
43019307340000	39.161080	-109.686760	14	19S	20E	6597	6741	6821	6858	6901	6948
43019100840000	39.166880	-109.604860	9	19S	21E	5687	5850		5963	6006	6054
43019301940000	39.131980	-109.609050	21	19S	21E	3868	4013		4126	4173	4216
43019307450000	39.125160	-109.646220	30	19S	21E	3892	4030	4098	4141	4191	4224
43019303230000	39.182020	-109.527290	6	19S	22E	5455	5606	5688	5743	5797	5853
43019307320000	39.174870	-109.446270	11	19S	22E	3564	3713	3784	3824	3868	3922
43019303860000	39.141630	-109.394440	20	19S	23E	2028	2206		2287	2330	2379
43019302550000	39.128050	-109.384840	28	19S	23E	2011	2170	2225	2264	2307	2356
43019305640000	39.129690	-109.221000	26	19S	24E	959	1103		1199	1247	1301
43019307560000	39.114680	-109.305420	31	19S	24E	1503	1656	1707	1739	1792	1836

UWI (APINum)	Surf Lat	Surf Lon	Section	Township	Range	F1	F2	F3	FJL	FJ1	FJLM
43019307680000	39.104560	-109.310770	31	19S	24E	1388	1539		1624	1668	1719
43019308680000	39.104950	-109.257930	33	19S	24E	736	873		964	1018	1058
43019115770000	39.106540	-109.224790	35	19S	24E	587	725		828	877	932
43019100430000	39.130770	-109.170160	29	19S	25E						137
43015301290000	39.078690	-110.199680	14	20S	15E	1911	2031	2110	2175	2214	2256
43019311990000	39.086380	-109.587500	10	20S	21E	2155	2297	2370	2417	2462	2512
43019308550000	39.028760	-109.552250	36	20S	21E	1776	1912	1979	2024	2064	2106
43019308750000	39.063500	-109.526860	18	20S	22E	1676	1813	1876	1921	1963	2006
43019308960000	39.053620	-109.533310	19	20S	22E	1480	1620		1727	1762	1806
43019308760000	39.021820	-109.522460	31	20S	22E	1788	1913	1978	2023	2065	2106
43019308770000	39.021040	-109.530500	31	20S	22E	1567	1709	1774	1817	1858	1904
43019310610000	39.093350	-109.371520	4	20S	23E	1386	1515		1591	1629	1673
43019310640000	39.095070	-109.407640	6	20S	23E	2477	2638	2692	2738		2832
43019311350000	39.062210	-109.343560	14	20S	23E	723	857	918	954	997	1044
43019107120000	39.101080	-109.230210	2	20S	24E	505	649		744	794	847
43019153170000	39.102280	-109.230810	2	20S	24E	551	680	751	787	833	892
43019300650000	39.100300	-109.227910	2	20S	24E	444	588		685	735	787
43019309160000	39.097170	-109.253610	3	20S	24E	535	667	722	762	809	855
43019309350000	39.098460	-109.263360	4	20S	24E	698	834	888	926	977	1026
43019311130000	39.092150	-109.279150	5	20S	24E	823	971	1024	1064	1109	1162
43019306300000	39.083100	-109.301160	7	20S	24E	899	1047		1134	1184	1239
43019055960000	39.064350	-109.251220	15	20S	24E	103	227		321	366	420
43019304100000	39.073050	-109.258160	16	20S	24E	346	472		562	611	660
43019302780000	39.069450	-109.286010	17	20S	24E	509	635		722	777	826
43019308940000	39.061350	-109.305720	18	20S	24E	526	679	730	765	810	860
43019104580000	39.033220	-109.286000	29	20S	24E		67		139	186	245
43015111820000	38.966710	-110.224880	24	21S	15E						
43019300290000	38.957330	-110.004526	26	21S	17E	781	922	993	1053	1095	1129
43019302440000	39.002730	-109.881570	12	21S	18E	2789			3087		3166
43019310630000	39.002200	-109.876690	12	21S	18E	3115	3273		3385	3425	3462
43019312000000	38.995130	-109.881230	12	21S	18E	3152	3311		3436	3479	3515
43019302070000	38.997200	-109.887100	12	21S	18E	3017	3159	3232	3295	3335	3377
43019312210000	38.984440	-109.876050	13	21S	18E	2791	2940		3074	3119	3156
43019312450000	38.985750	-109.898730	14	21S	18E	2505	2630		2750	2788	2835
43019303120000	38.972330	-109.905470	23	21S	18E	2222	2351	2420	2483	2525	2571
43019102190000	38.968900	-109.899410	23	21S	18E	1897			2151		2234

UWI (APINum)	Surf Lat	Surf Lon	Section	Township	Range	F1	F2	F3	FJL	FJ1	FJLM
43019102300000	39.005950	-109.854110	7	21S	19E	3034	3162		3293	3330	3379
43019107900000	39.003990	-109.859260	7	21S	19E	2877	3044		3149	3190	3235
43019107890000	38.995130	-109.867630	7	21S	19E	2518			2763		2851
43019106100000	38.995650	-109.867070	7	21S	19E	2508	2642		2773	2817	2861
43019302150000	38.981170	-109.849230	17	21S	19E	2437	2560	2621	2686	2721	2771
43019305420000	38.987560	-109.671120	14	21S	20E	2241	2357	2429	2476	2515	2555
43019305010000	38.990820	-109.704550	16	21S	20E	2249	2384	2462	2510	2545	2594
43019300700000	38.983600	-109.746940	18	21S	20E	2219	2349	2416	2469	2504	2553
43019110830000	38.989740	-109.567830	11	21S	21E	2014	2146		2262	2304	2348
43019310220000	38.991870	-109.540070	12	21S	21E	1868	2001	2071	2121	2164	2208
43019308630000	38.954550	-109.631620	30	21S	21E	1058	1181	1249	1294	1333	1376
43019051280000	38.934500	-109.606080	33	21S	21E	537	678		772	809	852
43019300820000	39.006890	-109.449360	2	21S	22E	1028	1159	1206	1249	1294	1333
43019303280000	38.996020	-109.448560	11	21S	22E	1009	1155	1206	1251	1296	1335
43019309180000	38.953440	-109.523570	30	21S	22E	1241	1363		1476	1523	1567
43019302660000	39.002420	-109.330280	1	21S	23E	268	414	472	501	551	592
43019303250000	39.014060	-109.394210	5	21S	23E	626	760	818	858	904	947
43019302710000	38.982550	-109.360380	15	21S	23E	81	225		315	361	405
43019115500000	38.966570	-109.393870	20	21S	23E	291			493	544	581
05103070900000	40.050590	-108.948970	15	1N	103W	7213	7419		7530	7592	7645
05103090220000	40.037090	-108.981960	20	1N	103W	7757	7984	8072	8109	8170	8214
05103089200000	40.039500	-108.944090	22	1N	103W	7066	7300	7374	7411	7471	7518
05103088640000	40.039310	-108.915550	23	1N	103W	7095	7323	7400	7439	7500	7546
05103058400000	40.167070	-108.845220	4	2N	102W	4013	4227	4292	4337	4396	4445
05103091780000	40.113520	-108.882870	30	2N	102W	2453	2672	2743	2785	2848	2891
05103082010000	40.112130	-108.986090	29	2N	103W	10021					10307
05081060390000	40.235500	-108.897010	13	3N	103W	5511		5767	5803		5941
05103059250000	40.213120	-108.912300	24	3N	103W	4839					
05103075130000	39.966220	-108.982010	17	1S	103W	6357	6616	6699	6727	6782	6828
05103092790000	39.920540	-109.001080	31	1S	103W	6994	7250	7320	7352	7406	7457
05103092680000	39.910730	-109.030930	35	1S	104W	6136	6380	6460	6500	6556	6610
05103092590000	39.903940	-109.001840	6	2S	103W				6738	6789	6844
05103098000000	39.842530	-108.965410	28	2S	103W	5679	5917	5993	6031	6082	6161
05103100180000	39.834540	-109.000730	31	2S	103W	6832	7083	7149	7192	7241	7296
05103099850000	39.908690	-109.042380	2	2S	104W	6357	6599	6678	6713	6764	6821
05103100090000	39.899610	-109.031830	2	2S	104W	6114	6356		6478	6524	6585

UWI (APINum)	Surf Lat	Surf Lon	Section	Township	Range	F1	F2	F3	FJL	FJ1	FJLM
05103092760000	39.902360	-109.041850	2	2S	104W	5905	6148	6232	6273	6323	6374
05103096230000	39.892430	-109.041820	11	2S	104W	6227	6462		6578	6632	6687
05103096240000	39.876420	-109.040010	14	2S	104W	6396	6632	6714	6748	6797	6857
05103092130000	39.838020	-109.048130	27	2S	104W	7526			7891	7937	7996
05103099920000	39.810490	-109.003620	6	3S	103W	6283	6552		6646	6689	6749
05103100250000	39.791580	-109.003700	18	3S	103W	6347	6601		6695	6743	6798
05103087830000	39.767030	-108.962400	21	3S	103W				5776		5874
05103080150000	39.760620	-108.948750	27	3S	103W	5360			5678		5779
05103094620000	39.804510	-109.012570	12	3S	104W	6332	6580	6645	6686	6735	6794
05103081990000	39.759150	-109.020390	25	3S	104W	6177	6450		6528	6577	6641
05103089180000	39.735530	-109.039910	2	4S	104W	6223	6482		6576	6634	6682
05103088260000	39.731030	-109.024580	12	4S	104W	5960	6211	6265	6310	6357	6401
05103087150000	39.701840	-109.026700	24	4S	104W	5794	6033		6131	6189	6230
05103089330000	39.681860	-109.011500	25	4S	104W	5852	6091	6146	6191	6251	6291
05045062970000	39.655280	-108.966090	4	5S	103W	5328	5583		5666	5728	5763
05045064510000	39.644230	-108.969950	9	5S	103W	6006	6235		6324	6386	6425
05045063940000	39.643870	-108.951490	10	5S	103W	5344	5576		5671	5736	5780
05045063710000	39.640910	-109.040700	11	5S	104W	7047	7265	7329	7359	7420	7470
05045063090000	39.561910	-108.966290	3	6S	104W	6212	6420	6473	6515	6579	6623
05045061250000	39.534670	-109.031660	18	6S	104W	5598	5795	5855	5893	5956	6003
05045060370000	39.515580	-109.006840	29	6S	104W	4768			5063		5155
05045063560000	39.489250	-109.025940	31	6S	104W	6288	6489	6547	6582	6639	6686
05045071870000	39.472580	-109.020360	8	7S	104W	6159	6356	6412	6451	6509	6550
05045061210000	39.432540	-108.985280	21	7S	104W	3603	3817		3892	3953	3999
05045069470000	39.421380	-108.950500	26	7S	104W	3936	4138		4215	4274	4312
05045061390000	39.419600	-109.031120	30	7S	104W	3490	3693		3775	3829	3876
05045061520000	39.385860	-109.021640	7	8S	104W	3079	3247	3319	3351	3405	3450
05077085150000	39.334620	-108.972380	27	8S	104W	1851	2032		2121	2174	2221
43019950050000	38.934500	-109.553800	35	21S	21E	1120	1248	1319	1368	1414	1454
05103103430000	39.879665	-108.989800	18	2S	103W	6593	6824	6897	6937	6988	7041
43019307310000	39.226190	-109.286080	11	18S	25E	2992	3150	3212	3246	3295	3348
43019307840000	39.206500	-109.294610	30	18S	24E	2971	3125	3187	3226	3273	3324
43047349220000	39.547000	-109.634000	1	15S	20E	9656	9828	9900	9953	10015	10070
43047351400000	39.547750	-109.709940	5	15S	20E	10088	10255	10336	10393	10450	10503
43047350540000	39.517710	-109.634220	13	15S	20E	9404	9582	9643	9703	9761	9817
43019313970000	39.457950	-109.362650	34	15.5S	23E	6987	7157	7210	7245	7303	7354

UWI (APINum)	Surf Lat	Surf Lon	Section	Township	Range	F1	F2	F3	FJL	FJ1	FJLM
WESTWATER	39.113660	-109.156440	33	19S	25E				-4	48	93
SKCKMOLENAAR	40.256232	-108.861684	5	3N	102W	-116	108	173	208	269	318
I70SECITON	38.935030	-110.350960	2	22S	14E				-21	34	61

	FMTOPS	FMTOPS	FMTOPS	FMTOPS	FMTOPS	FMTOPS	FMTOPS	FMTOPS
UWI (APINum)	FE_SB_1	BENT_57	BENT_46	CW_SB_2	BENT_38	CW_SB_1	BENT_27	MTUNC
43047301110000	15494		15520		15523			15547
43047301450000	14888		14918		14921			14943
43007300490001	12983		13016		13025		13093	13130
43047303570000	11338	11358	11376		11379			11438
43047316740000					7883			7903
43047156720000	7984				8008			8031
43047315970000					7330			7353
43047315100000	11681	11695	11712		11715		11777	11819
43047301700000		10971			10989		11051	11056
43047301430000	9553	9567	9587		9588		9649	9653
43047334480000	10503	10514	10529		10531		10584	10600
43047334450000	10604	10614	10632		10636			10702
43047334470000	10580	10591	10610		10610		10674	10677
43047301650000	10633	10659			10679			10728
43047301660000	9786	9813			9823			9872
43047301680000	10058	10088	10098		10101			10147
43047302760000	9724	9744			9754			9807
43047303860000	9463	9478	9492		9494			9535
43047307730000								8990
43047312310000	8146	8168	8180		8180			8218
43047307880000		7752	7764		7767			7801
43047335950000	10569	10583			10608		10671	10689
43047336160000		10453			10478		10542	10576
43047336170000								10623
43047335960000		10456	10468		10478		10538	10574
43047336180000								10568
43047335570000								10582
43047333370000								10552
43047336190000								10564
43047333330000		10409			10436		10502	10531
43047335580000								10453
43047336210000		10367			10387		10457	10486
43047105770001								10506
43047336200000								10510
43047340980000		10359			10385		10451	10482

UWI (APINum)	FE_SB_1	BENT_57	BENT_46	CW_SB_2	BENT_38	CW_SB_1	BENT_27	MTUNC
43047301350000	9452	9484			9497			9542
43047309600000	8746	8764	8777		8779			8828
43047310630000	8061	8085	8097		8100		8150	8162
43047302710000								8943
43047309780000	8601	8617	8631		8642		8686	8697
43047309760000		8201	8218		8225		8273	8275
43047106920000		6936			6948			6993
43047050290000		6622			6647			6689
43047318940000	7359	7374	7390		7398			7444
43047311370000	9354	9372	9384		9400		9467	9472
43047310710000	9505	9516	9536		9548		9603	9619
43047314960000	8325	8341	8355		8368		8422	8451
43047161980000	7987	7999	8014		8024		8085	8108
43047310430000	8208	8230	8240		8245		8300	8319
43047306180000	7976	7989	8005		8019		8061	8068
43047304480000	8256	8268	8285		8296		8339	8350
43047302480000	7504	7524	7539		7547		7600	7607
43047310120000	8147	8166	8176		8187		8222	8226
43019100890000	7328	7345	7363		7371		7408	7411
43015103740000	4554	4589	4614		4628		4708	4777
43015300220000	8166	8201	8224		8236		8309	8366
43015300800000	7121	7163	7181		7197		7282	7353
43015301980000	12036	12067	12089		12100		12178	12242
43019108060000	9494	9508	9530		9548		9604	9630
43019306530000	9389	9410	9421		9437		9495	9505
43019311480000	7907	7928	7937		7950		8006	8036
43019302400000	7221	7243	7256		7268		7310	7327
43019307040000	5050	5073	5088		5098		5147	5154
43019313180000	3676	3703	3719		3726		3764	3773
43015109280000	438	463	489		517		618	724
43015108000000	4524	4566	4584		4602		4690	4766
43019156730000	9489	9502	9527		9544		9602	9628
43019307060000	9191	9209	9229		9250		9302	9334
43019306820000	9443	9458	9482		9502		9564	9606
43019159350000	6880	6891	6910		6930		6978	7013
43019159330000	5681	5694	5710		5731		5786	5804

UWI (APINum)	FE_SB_1	BENT_57	BENT_46	CW_SB_2	BENT_38	CW_SB_1	BENT_27	MTUNC
43019307080000	5159	5177	5188		5202		5248	5292
43019308950000	4722	4740	4753		4770		4836	4855
43019305710000								5672
43019201540000	6011	6026	6043		6058		6119	6154
43019307730000	4064	4085	4100		4114		4169	4203
43019150220000								2879
43019310140000	2394	2414	2430		2444		2490	2505
43019104630000								4950
43015301990000	6003	6023	6052		6071		6161	6239
43015052110000	2856	2905	2931		2946		3026	3142
43015301130000	5770	5811	5833		5850		5941	6011
43015300140000	5764	5786	5814		5831		5925	6006
43019303980000	8601	8622	8654		8668		8729	8764
43019055910000	5315	5327	5343		5369		5430	5463
43019307720000	4529	4548	4560		4577		4626	4655
43019304930000		3545	3552		3579		3621	3653
43019114330000	2749	2765	2782		2805		2854	2882
43019310690000	800	826	843	857	860	878	906	927
43019310720000	797	828	847	855	862	876	916	936
43015300010000	1770	1804	1830		1848		1946	2028
43015105030000	657	686	712		731		836	921
43015300210000	4288	4323	4349		4363		4469	4558
43019308350000	4408	4441	4469		4489		4587	4661
43019110130000	5157	5200	5217		5246		5334	5395
43019308090000	6837	6872	6897		6921		6995	7048
43019308040000	5912	5951	5972		5998		6073	6134
43019307340000	6985	7017	7042		7068		7124	7169
43019100840000	6114	6125	6146		6174		6236	6284
43019301940000	4270	4287	4307		4334		4396	4433
43019307450000	4262	4293	4315		4347		4411	4450
43019303230000	5918	5928	5953		5985		6055	6094
43019307320000	3974	3989	4004		4031		4091	4118
43019303860000		2450	2466		2488		2545	2572
43019302550000		2425	2441		2468		2518	2546
43019305640000	1333	1367	1382	1397	1409	1432	1455	1490
43019307560000	1876	1909	1923		1953		1997	2031

UWI (APINum)	FE_SB_1	BENT_57	BENT_46	CW_SB_2	BENT_38	CW_SB_1	BENT_27	MTUNC
43019307680000	1759	1791	1807		1840		1884	1920
43019308680000	1101	1125	1145	1163	1174	1187	1216	1247
43019115770000	971	1002	1018	1033	1048	1065	1096	1132
43019100430000							312	319
43015301290000	2308	2346	2372		2388		2504	2571
43019311990000	2563	2590	2614		2651		2715	2757
43019308550000	2163	2189	2206		2243		2290	2333
43019308750000	2061	2087	2104		2140		2197	2229
43019308960000	1859	1888	1906		1941		1997	2031
43019308760000	2162	2188	2206		2244		2300	2336
43019308770000	1960	1987	2008		2047		2105	2139
43019310610000	1709	1743	1759		1787		1836	1871
43019310640000	2873	2907	2926		2962		3005	3045
43019311350000	1087	1116	1134		1168		1211	1245
43019107120000	888	922	941	954	969	989	1020	1049
43019153170000	932	963	978	996	1009	1023	1054	1090
43019300650000	827	859	878	891	905	929	955	984
43019309160000	895	930	946	960	976	986	1017	1053
43019309350000	1065	1102	1118		1149	1162	1196	1227
43019311130000	1204	1238	1254		1286	1299	1332	1364
43019306300000	1279	1329	1326		1358		1415	1448
43019055960000	460	510	512		541		588	628
43019304100000	702	737	751		782		827	860
43019302780000	866		924		955		1002	1033
43019308940000	903	935	955		990		1035	1068
43019104580000	316	324	347		377		413	460
43015111820000								67
43019300290000	1194	1224	1241		1270		1382	1452
43019302440000								3466
43019310630000	3507	3552	3571		3604		3696	3758
43019312000000	3561	3605	3631		3666			3763
43019302070000	3423	3465	3487		3528		3621	3694
43019312210000	3201	3246	3270		3304		3398	3463
43019312450000	2879	2921	2948		2981		3079	3150
43019303120000	2618	2659	2686		2722		2818	2886
43019102190000								2556

UWI (APINum)	FE_SB_1	BENT_57	BENT_46	CW_SB_2	BENT_38	CW_SB_1	BENT_27	MTUNC
43019102300000	3425	3495	3491		3525		3611	3680
43019107900000	3287		3355		3384		3475	3542
43019107890000								3142
43019106100000	2903	2946	2971		3000		3089	3152
43019302150000	2825	2859	2890		2927		3008	3076
43019305420000	2616	2679	2699		2729		2779	2826
43019305010000	2654	2682	2705		2748		2814	2862
43019300700000	2613	2644	2668		2711		2780	2836
43019110830000	2415	2445	2467		2505		2554	2607
43019310220000	2269	2302	2320		2364		2423	2460
43019308630000	1436	1464	1486		1528			1638
43019051280000	918	951	977		1018		1075	1116
43019300820000	1384	1415	1432		1474		1519	1555
43019303280000	1385	1417	1435		1478		1521	1559
43019309180000	1624	1657	1683		1728		1779	1822
43019302660000	634	672	691		733		778	812
43019303250000	994	1030	1047		1087		1133	1171
43019302710000	452	490	508		552		599	632
43019115500000	633	668	687		729		772	805
05103070900000								7705
05103090220000								8275
05103089200000								7582
05103088640000								7608
05103058400000								4505
05103091780000								2955
05103082010000								10378
05081060390000								5993
05103059250000								
05103075130000								6891
05103092790000								7511
05103092680000					6675			6675
05103092590000					6900			6902
05103098000000					6215			6225
05103100180000					7357			7364
05103099850000								6881
05103100090000					6643			6650

UWI (APINum)	FE_SB_1	BENT_57	BENT_46	CW_SB_2	BENT_38	CW_SB_1	BENT_27	MTUNC
05103092760000								6439
05103096230000								6749
05103096240000					6916			6921
05103092130000					8059			8066
05103099920000					6813			6823
05103100250000					6863			6875
05103087830000								5947
05103080150000								5863
05103094620000					6855			6867
05103081990000								6717
05103089180000	6711				6740			6769
05103088260000	6440		6466		6469			6505
05103087150000	6265		6290		6292			6331
05103089330000		6343			6355			6393
05045062970000		5816			5828			5866
05045064510000		6485			6494			6532
05045063940000		5833			5843			5881
05045063710000		7520	7540		7542			7582
05045063090000		6670	6689		6697			6735
05045061250000	6045	6058	6072		6083			6123
05045060370000								5273
05045063560000	6716	6731	6751		6756			6793
05045071870000	6587	6605	6629		6629			6672
05045061210000	4035	4051	4077		4077		4118	4119
05045069470000	4348	4365	4387		4391		4426	4428
05045061390000	3917	3933			3957			3993
05045061520000	3493	3506	3522		3532		3574	3577
05077085150000	2267	2275	2297		2312		2353	2356
43019950050000	1507	1547	1570		1618		1679	1728
05103103430000					7099			7103
43019307310000	3378	3410	3425		3447		3492	3519
43019307840000	3359	3390	3407		3429		3483	3505
43047349220000	10099	10112	10129		10140		10202	10219
43047351400000	10535	10551	10568		10576		10644	10673
43047350540000	9849	9866	9882		9891		9957	9975
43019313970000	7387	7403	7419		7430		7480	7513

UWI (APINum)	FE_SB_1	BENT_57	BENT_46	CW_SB_2	BENT_38	CW_SB_1	BENT_27	MTUNC
WESTWATER	121	154	175	190	204	226	239	267
SKCKMOLENAAR								366
I70SECITON	128		200		217		358	447

APINUM	PAY NAME	TOPMD	BASEMD
43007300490001	COONSPG_SS	13026.09	13032.655
43047303570000	COONSPG_SS	11383.53	11387.323
43047303570000	COONSPG_SS	11395.383	11400.124
43047315100000	COONSPG_SS	11718.402	11729.564
43047301430000	COONSPG_SS	9592.207	9606.199
43047334470000	COONSPG_SS	10612.798	10627.723
43047301680000	COONSPG_SS	10104.095	10108.362
43047303860000	COONSPG_SS	9498.768	9504.655
43047312310000	COONSPG_SS	8183.643	8190.427
43047307880000	COONSPG_SS	7772.068	7778.236
43047335950000	COONSPG_SS	10611.772	10629.271
43047336160000	COONSPG_SS	10482.989	10504.44
43047336210000	COONSPG_SS	10390.508	10411.394
43047340980000	COONSPG_SS	10387.824	10409.839
43047309600000	COONSPG_SS	8783.505	8790.653
43047310630000	COONSPG_SS	8098.784	8107.179
43047309780000	COONSPG_SS	8646.998	8655.311
43047309760000	COONSPG_SS	8227.693	8234.447
43047318940000	COONSPG_SS	7402.001	7404.428
43047318940000	COONSPG_SS	7405.642	7409.283
43047311370000	COONSPG_SS	9404.352	9421.794
43047310710000	COONSPG_SS	9551.411	9570.792
43047314960000	COONSPG_SS	8371.741	8386.199
43047161980000	COONSPG_SS	8027.93	8042.387
43047310430000	COONSPG_SS	8248.666	8260.413
43047306180000	COONSPG_SS	8020.636	8032.585
43047304480000	COONSPG_SS	8298.795	8310.224
43047310120000	COONSPG_SS	8194.032	8200.786
43019100890000	COONSPG_SS	7376.618	7383.892
43015103740000	COONSPG_SS	4632.23	4657.844
43015300220000	COONSPG_SS	8238.256	8261.169
43015300800000	COONSPG_SS	7200.644	7230.019
43015301980000	COONSPG_SS	12105.27	12125.524
43019108060000	COONSPG_SS	9552.102	9566.96
43019108060000	COONSPG_SS	9569.544	9579.88
43019306530000	COONSPG_SS	9440.271	9460.298
43019311480000	COONSPG_SS	7955.09	7970.947
43019302400000	COONSPG_SS	7267.553	7278.463
43019307040000	COONSPG_SS	5102.417	5119.759
43019313180000	COONSPG_SS	3735.299	3743.794
43015109280000	COONSPG_SS	516.667	532.365
43019156730000	COONSPG_SS	9551.106	9571.758
43019307060000	COONSPG_SS	9252.363	9278.204
43019306820000	COONSPG_SS	9504.649	9539.615
43019159350000	COONSPG_SS	6932.812	6959.613
43019307080000	COONSPG_SS	5204.638	5228.812
43019308950000	COONSPG_SS	4774.214	4797.336
43019201540000	COONSPG_SS	6068.866	6082.004
43019307730000	COONSPG_SS	4116.653	4137.674
43019310140000	COONSPG_SS	2446.895	2452.15
43019310140000	COONSPG_SS	2455.828	2462.66

APINUM	PAY NAME	TOPMD	BASEMD
43015301990000	COONSPG_SS	6075.605	6106.879
43015301130000	COONSPG_SS	5855.874	5881.725
43015300140000	COONSPG_SS	5837.452	5864.477
43019303980000	COONSPG_SS	8669.363	8689.534
43019055910000	COONSPG_SS	5371.973	5384.142
43019307720000	COONSPG_SS	4583.145	4592.549
43019307720000	COONSPG_SS	4601.577	4603.834
43019114330000	COONSPG_SS	2809.576	2816.896
43019310690000	COONSPG_SS	864.397	875.065
43019310720000	COONSPG_SS	865.888	875.301
43015105030000	COONSPG_SS	740.752	761.09
43015300210000	COONSPG_SS	4374.298	4397.058
43019308350000	COONSPG_SS	4492.48	4529.082
43019110130000	COONSPG_SS	5251.569	5282.942
43019308090000	COONSPG_SS	6922.266	6948.496
43019308040000	COONSPG_SS	5999.843	6021.389
43019307340000	COONSPG_SS	7071.626	7088.43
43019100840000	COONSPG_SS	6177.983	6191.023
43019307450000	COONSPG_SS	4346.418	4364.96
43019303230000	COONSPG_SS	5988.345	6003.41
43019307320000	COONSPG_SS	4033.286	4048.352
43019302550000	COONSPG_SS	2471.667	2478.151
43019307560000	COONSPG_SS	1955.715	1962.698
43019308680000	COONSPG_SS	1176.727	1184.25
43019308680000	COONSPG_SS	1190.269	1195.159
43015301290000	COONSPG_SS	2394.618	2431.044
43019311990000	COONSPG_SS	2652.718	2660.831
43019308550000	COONSPG_SS	2243.811	2252.633
43019308750000	COONSPG_SS	2143.235	2150.585
43019308960000	COONSPG_SS	1944.07	1951.157
43019308760000	COONSPG_SS	2245.11	2253.379
43019308770000	COONSPG_SS	2049.546	2057.463
43019310610000	COONSPG_SS	1792.687	1800.169
43019310640000	COONSPG_SS	2961.88	2969.303
43019311350000	COONSPG_SS	1170.387	1177.278
43019153170000	COONSPG_SS	1013.376	1019.947
43019309160000	COONSPG_SS	979.089	985.313
43019309350000	COONSPG_SS	1153.023	1160.17
43019309350000	COONSPG_SS	1169.198	1173.336
43019311130000	COONSPG_SS	1288.433	1296.155
43019304100000	COONSPG_SS	786.582	795.61
43019304100000	COONSPG_SS	800.876	805.39
43019308940000	COONSPG_SS	992.007	999.987
43019104580000	COONSPG_SS	382.013	390.877
43019104580000	COONSPG_SS	393.832	400.111
43019300290000	COONSPG_SS	1278.921	1307.389
43019310630000	COONSPG_SS	3610.416	3632.393
43019312000000	COONSPG_SS	3671.497	3685.771
43019302070000	COONSPG_SS	3531.413	3558.273
43019312210000	COONSPG_SS	3310.311	3337.171
43019312450000	COONSPG_SS	2987.202	3011.603

APINUM	PAY NAME	TOPMD	BASEMD
43019303120000	COONSPG_SS	2726.245	2752.291
43019302150000	COONSPG_SS	2932.378	2943.417
43019305420000	COONSPG_SS	2734.345	2741.839
43019305010000	COONSPG_SS	2750.075	2764.126
43019300700000	COONSPG_SS	2714.23	2721.724
43019310220000	COONSPG_SS	2366.168	2375.578
43019300820000	COONSPG_SS	1472.995	1482.405
43019303280000	COONSPG_SS	1479.278	1488.891
43019309180000	COONSPG_SS	1732.547	1740.78
43019302660000	COONSPG_SS	735.215	745.19
43019303250000	COONSPG_SS	1089.632	1099.608
43019302710000	COONSPG_SS	555.761	565.072
43019115500000	COONSPG_SS	731.806	739.121
05103088260000	COONSPG_SS	6470.399	6472.251
05103087150000	COONSPG_SS	6295.272	6300.206
05103089330000	COONSPG_SS	6357.453	6363.003
05045062970000	COONSPG_SS	5830.256	5833.48
05045064510000	COONSPG_SS	6496.096	6499.32
05045063940000	COONSPG_SS	5847.115	5849.802
05045063710000	COONSPG_SS	7544.479	7549.315
05045063090000	COONSPG_SS	6699.353	6701.502
05045061250000	COONSPG_SS	6086.167	6089.808
05045061250000	COONSPG_SS	6091.426	6096.686
05045063560000	COONSPG_SS	6758.809	6762.854
05045071870000	COONSPG_SS	6632.743	6640.025
05045061210000	COONSPG_SS	4083.322	4092.626
05045069470000	COONSPG_SS	4393.703	4402.735
05045061520000	COONSPG_SS	3537.151	3546.861
05077085150000	COONSPG_SS	2318.139	2328.657
43019950050000	COONSPG_SS	1621.035	1629.016
4301930731	COONSPG_SS	3449.842	3458.869
4301930731	COONSPG_SS	3469.402	3473.163
4301930784	COONSPG_SS	3433.187	3439.582
4301930784	COONSPG_SS	3456.509	3461.399
43047349220000	COONSPG_SS	10144.432	10165.318
43047351400000	COONSPG_SS	10579.141	10601.156
43047350540000	COONSPG_SS	9894.672	9919.509
4301931397	COONSPG_SS	7433.605	7448.996
I70SECITON	COONSPG_SS	219.607	260.523
43047301450000	F2_SS	14643.04	14644.438
43007300490001	F2_SS	12746	12746
43047316740000	F2_SS	7661.333	7667.913
43047315970000	F2_SS	7113.846	7122.071
43047315100000	F2_SS	11453.15	11455.113
43047334470000	F2_SS	10375.978	10377.656
43047301680000	F2_SS	9840.665	9844.676
43047303860000	F2_SS	9250.611	9256.548
43047335960000	F2_SS	10229.723	10231.81
43047309600000	F2_SS	8535.817	8538.637
43047310630000	F2_SS	7854.9	7857.72
43047309780000	F2_SS	8397.962	8406.859

APINUM	PAY NAME	TOPMD	BASEMD
43047309760000	F2_SS	7985.568	7993.492
43047106920000	F2_SS	6713.608	6721.532
43047318940000	F2_SS	7163.79	7169.073
43047311370000	F2_SS	9149.912	9152.502
43047310710000	F2_SS	9290.96	9294.521
43047314960000	F2_SS	8125.941	8133.819
43047161980000	F2_SS	7783.969	7793.816
43047310430000	F2_SS	8008.215	8015.629
43047306180000	F2_SS	7775.379	7782.793
43047304480000	F2_SS	8056.132	8065.979
43047310120000	F2_SS	7942.051	7953.867
43019100890000	F2_SS	7133.654	7143.501
43015300800000	F2_SS	6903.497	6904.871
43019108060000	F2_SS	9287.158	9293.355
43019306530000	F2_SS	9183.588	9191.85
43019311480000	F2_SS	7715.114	7724.962
43019302400000	F2_SS	7026.803	7032.711
43019307040000	F2_SS	4861.328	4868.557
43019313180000	F2_SS	3497.567	3502.988
43019156730000	F2_SS	9278.024	9283.006
43019307060000	F2_SS	8992.985	8997.633
43019306820000	F2_SS	9234.678	9239.326
43019159350000	F2_SS	6670.41	6678.157
43019307080000	F2_SS	4990.006	4997.753
43019308950000	F2_SS	4526.836	4533.721
43019201540000	F2_SS	5805.245	5812.992
43019307730000	F2_SS	3875.344	3882.573
43019310140000	F2_SS	2201.775	2210.811
43015301990000	F2_SS	5792.928	5794.917
43015300140000	F2_SS	5547.026	5549.016
43019303980000	F2_SS	8397.11	8406.077
43019055910000	F2_SS	5106.738	5119.388
43019307720000	F2_SS	4332.361	4339.246
43019114330000	F2_SS	2548.797	2555.682
43019310690000	F2_SS	607.926	614.811
43019310720000	F2_SS	623.88	630.765
43015300210000	F2_SS	4059.155	4062.47
43019308350000	F2_SS	4201.663	4207.455
43019308090000	F2_SS	6656.501	6661.134
43019308040000	F2_SS	5716.178	5722.156
43019307340000	F2_SS	6805.626	6811.419
43019307450000	F2_SS	4083.418	4090.369
43019303230000	F2_SS	5670.678	5679.946
43019307320000	F2_SS	3771.75	3780.786
43019302550000	F2_SS	2214.88	2220.302
43019307560000	F2_SS	1694.856	1699.768
43019308680000	F2_SS	916.757	923.986
43015301290000	F2_SS	2090.419	2092.704
43019311990000	F2_SS	2357.82	2367.088
43019308550000	F2_SS	1967.043	1975.337
43019308750000	F2_SS	1866.354	1873.305

APINUM	PAY NAME	TOPMD	BASEMD
43019308760000	F2_SS	1966.958	1975.252
43019308770000	F2_SS	1763.946	1770.167
43019310640000	F2_SS	2681.873	2686.855
43019311350000	F2_SS	908.269	912.254
43019153170000	F2_SS	735.961	744.148
43019309160000	F2_SS	713.183	717.817
43019309350000	F2_SS	878.569	885.119
43019311130000	F2_SS	1013.834	1018.468
43019308940000	F2_SS	721.9	726.534
43019300290000	F2_SS	980.104	985.896
43019302070000	F2_SS	3218.457	3223.091
43019303120000	F2_SS	2409.928	2418.037
43019302150000	F2_SS	2610.879	2617.1
43019305420000	F2_SS	2418.113	2422.26
43019305010000	F2_SS	2446.153	2455.398
43019300700000	F2_SS	2399.901	2408.195
43019310220000	F2_SS	2064.254	2070.857
43019308630000	F2_SS	1237.066	1244.99
43019300820000	F2_SS	1194.612	1200.404
43019303280000	F2_SS	1193.934	1200.155
43019302660000	F2_SS	460.903	466.087
43019303250000	F2_SS	809.219	814.2
05103090220000	F2_SS	8058.727	8064.566
05103089200000	F2_SS	7358.952	7365.625
05103088640000	F2_SS	7385.297	7391.97
05103058400000	F2_SS	4281.625	4287.221
05103091780000	F2_SS	2732.163	2736.668
05103075130000	F2_SS	6684.024	6690.697
05103092790000	F2_SS	7304.915	7311.588
05103092680000	F2_SS	6446.307	6452.887
05103098000000	F2_SS	5979.818	5989.688
05103100180000	F2_SS	7135.707	7141.546
05103099850000	F2_SS	6665.14	6671.053
05103092760000	F2_SS	6217.838	6227.708
05103096240000	F2_SS	6699.986	6706.566
05103094620000	F2_SS	6636.509	6643.483
05103088260000	F2_SS	6253.82	6259.798
05103089330000	F2_SS	6135.554	6142.528
05045063710000	F2_SS	7313.863	7320.837
05045063090000	F2_SS	6458.747	6464.168
05045061250000	F2_SS	5832.517	5840.441
05045063560000	F2_SS	6531.74	6537.162
05045071870000	F2_SS	6398.645	6405.874
05045061520000	F2_SS	3305.474	3310.895
43019950050000	F2_SS	1309.49	1314.773
05103103430000	F2_SS	6884.791	6891.464
4301930731	F2_SS	3193.932	3202.968
4301930784	F2_SS	3169.664	3178.7
43047349220000	F2_SS	9887.958	9889.697
43047351400000	F2_SS	10329.119	10331.58
43047350540000	F2_SS	9637.853	9639.904

APINUM	PAY NAME	TOPMD	BASEMD
4301931397	F2_SS	7185.743	7195.59
SKCKMOLENAAR	F2_SS	164.992	171.388
43047301450000	SHALE_ORS_1	14839.602	14845.064
43007300490001	SHALE_ORS_1	12945.071	12946.871
43047303570000	SHALE_ORS_1	11320.041	11321.62
43047316740000	SHALE_ORS_1	7822.87	7825.344
43047156720000	SHALE_ORS_1	7932.997	7935.543
43047315970000	SHALE_ORS_1	7262.531	7266.998
43047315100000	SHALE_ORS_1	11652.87	11654.67
43047301430000	SHALE_ORS_1	9521.411	9525.413
43047334470000	SHALE_ORS_1	10543.916	10547.432
43047301680000	SHALE_ORS_1	10023.971	10027.29
43047303860000	SHALE_ORS_1	9419.775	9423.7
43047312310000	SHALE_ORS_1	8105.432	8108.444
43047307880000	SHALE_ORS_1	7684.749	7691.197
43047335950000	SHALE_ORS_1	10533.437	10539.174
43047336160000	SHALE_ORS_1	10405.444	10411.308
43047333370000	SHALE_ORS_1	10376.883	10383.398
43047336210000	SHALE_ORS_1	10310.883	10315.444
43047340980000	SHALE_ORS_1	10306.385	10310.921
43047309600000	SHALE_ORS_1	8710	8712
43047310630000	SHALE_ORS_1	8022.011	8024.541
43047309780000	SHALE_ORS_1	8564.721	8567.766
43047309760000	SHALE_ORS_1	8152.882	8155.89
43047318940000	SHALE_ORS_1	7315.378	7319.04
43047318940000	SHALE_ORS_1	7320.414	7323.619
43047311370000	SHALE_ORS_1	9316.263	9321.246
43047310710000	SHALE_ORS_1	9465.509	9469.479
43047310710000	SHALE_ORS_1	9461.042	9470.471
43047314960000	SHALE_ORS_1	8283.068	8288.366
43047314960000	SHALE_ORS_1	8290.132	8293.076
43047161980000	SHALE_ORS_1	7949.051	7956.704
43047310430000	SHALE_ORS_1	8165.537	8167.796
43047310430000	SHALE_ORS_1	8170.055	8172.765
43047306180000	SHALE_ORS_1	7934.827	7937.184
43047306180000	SHALE_ORS_1	7938.598	7942.841
43047304480000	SHALE_ORS_1	8214.496	8218.739
43047304480000	SHALE_ORS_1	8220.154	8222.511
43047310120000	SHALE_ORS_1	8104.635	8109.349
43047310120000	SHALE_ORS_1	8111.707	8114.064
43019100890000	SHALE_ORS_1	7286.037	7289.809
43019100890000	SHALE_ORS_1	7291.223	7295.466
43015103740000	SHALE_ORS_1	4508.295	4511.186
43015300220000	SHALE_ORS_1	8117.818	8119.58
43015300800000	SHALE_ORS_1	7077.855	7080.205
43015301980000	SHALE_ORS_1	11987.87	11991.395
43019108060000	SHALE_ORS_1	9446.612	9453.063
43019306530000	SHALE_ORS_1	9343.538	9352.334
43019311480000	SHALE_ORS_1	7865.385	7869.506
43019311480000	SHALE_ORS_1	7870.683	7873.038
43019302400000	SHALE_ORS_1	7180.474	7186.603

APINUM	PAY NAME	TOPMD	BASEMD
43019307040000	SHALE_ORS_1	5006.906	5011.029
43019307040000	SHALE_ORS_1	5012.404	5015.611
43019313180000	SHALE_ORS_1	3637.317	3643.269
43019156730000	SHALE_ORS_1	9439.241	9445.265
43019307060000	SHALE_ORS_1	9143.823	9150.273
43019306820000	SHALE_ORS_1	9389.171	9398.554
43019159350000	SHALE_ORS_1	6825.885	6834.59
43019307080000	SHALE_ORS_1	5112.265	5117.763
43019308950000	SHALE_ORS_1	4678.418	4683.916
43019201540000	SHALE_ORS_1	5958.963	5968.127
43019307730000	SHALE_ORS_1	4019.457	4022.206
43019307730000	SHALE_ORS_1	4024.497	4027.246
43019310140000	SHALE_ORS_1	2351.952	2355.425
43015301990000	SHALE_ORS_1	5941.801	5945.459
43015301130000	SHALE_ORS_1	5727.211	5730.736
43015300140000	SHALE_ORS_1	5710.55	5714.663
43019303980000	SHALE_ORS_1	8545.473	8552.426
43019055910000	SHALE_ORS_1	5252.029	5258.982
43019307720000	SHALE_ORS_1	4481.884	4486.279
43019114330000	SHALE_ORS_1	2695.387	2699.779
43019310690000	SHALE_ORS_1	759.068	762.731
43019310720000	SHALE_ORS_1	757.868	763.235
43015300210000	SHALE_ORS_1	4222.651	4226.678
43019308350000	SHALE_ORS_1	4359.14	4364.068
43019110130000	SHALE_ORS_1	5111.551	5115.618
43019308090000	SHALE_ORS_1	6792.99	6797.674
43019308040000	SHALE_ORS_1	5867.756	5872.44
43019307340000	SHALE_ORS_1	6941.252	6947.046
43019307450000	SHALE_ORS_1	4218.361	4222.417
43019303230000	SHALE_ORS_1	5845.802	5853.335
43019307320000	SHALE_ORS_1	3911.603	3917.398
43019302550000	SHALE_ORS_1	2345.472	2354.45
43019307560000	SHALE_ORS_1	1827.525	1835.007
43019307680000	SHALE_ORS_1	1709.753	1717.067
43019308680000	SHALE_ORS_1	1049.592	1054.555
43015301290000	SHALE_ORS_1	2250.679	2253.617
43019311990000	SHALE_ORS_1	2504.96	2510.175
43019308550000	SHALE_ORS_1	2100.896	2105.601
43019308750000	SHALE_ORS_1	1999.61	2005.264
43019308960000	SHALE_ORS_1	1801.418	1804.946
43019308760000	SHALE_ORS_1	2100.699	2106.58
43019308770000	SHALE_ORS_1	1897.439	1902.528
43019310610000	SHALE_ORS_1	1666.492	1671.48
43019310640000	SHALE_ORS_1	2821.901	2827.734
43019311350000	SHALE_ORS_1	1037.809	1043.556
43019153170000	SHALE_ORS_1	881.121	889.207
43019309160000	SHALE_ORS_1	846.812	849.924
43019309160000	SHALE_ORS_1	851.999	853.555
43019309350000	SHALE_ORS_1	1015.81	1019.781
43019309350000	SHALE_ORS_1	1022.262	1025.24
43019311130000	SHALE_ORS_1	1150.887	1156.678

APINUM	PAY NAME	TOPMD	BASEMD
43019304100000	SHALE_ORS_1	652.42	654.902
43019304100000	SHALE_ORS_1	656.887	659.368
43019308940000	SHALE_ORS_1	852.345	857.832
43019104580000	SHALE_ORS_1	240.067	244.768
43019300290000	SHALE_ORS_1	1121.562	1128.46
43019310630000	SHALE_ORS_1	3455.766	3460.65
43019312000000	SHALE_ORS_1	3512.254	3514.485
43019302070000	SHALE_ORS_1	3368.623	3372.693
43019312210000	SHALE_ORS_1	3149.149	3154.846
43019312450000	SHALE_ORS_1	2826.997	2832.91
43019303120000	SHALE_ORS_1	2562.641	2569.967
43019302150000	SHALE_ORS_1	2759.245	2767.128
43019305420000	SHALE_ORS_1	2546.54	2553.144
43019305010000	SHALE_ORS_1	2586.137	2591.758
43019300700000	SHALE_ORS_1	2544.672	2550.292
43019310220000	SHALE_ORS_1	2203.844	2207.373
43019308630000	SHALE_ORS_1	1371.813	1375.667
43019300820000	SHALE_ORS_1	1326.551	1332.432
43019303280000	SHALE_ORS_1	1326.606	1332.26
43019309180000	SHALE_ORS_1	1559.637	1566.106
43019302660000	SHALE_ORS_1	585.078	590.565
43019303250000	SHALE_ORS_1	942.128	947.915
43019302710000	SHALE_ORS_1	398.669	403.93
43019115500000	SHALE_ORS_1	574.406	579.667
05103089200000	SHALE_ORS_1	7513.514	7516.519
05103088640000	SHALE_ORS_1	7544.237	7546.782
05103058400000	SHALE_ORS_1	4493.166	4496.702
05103091780000	SHALE_ORS_1	2885.008	2886.921
05103075130000	SHALE_ORS_1	6821.322	6825.398
05103092790000	SHALE_ORS_1	7453	7456
05103092680000	SHALE_ORS_1	6605.835	6608.814
05103092590000	SHALE_ORS_1	6841.35	6843.35
05103098000000	SHALE_ORS_1	6158.452	6160.543
05103100180000	SHALE_ORS_1	7290.596	7292.687
05103099850000	SHALE_ORS_1	6814.958	6818.048
05103100090000	SHALE_ORS_1	6578.23	6580.758
05103092760000	SHALE_ORS_1	6370.387	6372.635
05103096230000	SHALE_ORS_1	6681.52	6684.329
05103096240000	SHALE_ORS_1	6852.909	6855.418
05103092130000	SHALE_ORS_1	7990.808	7994.891
05103099920000	SHALE_ORS_1	6744.61	6746.873
05103100250000	SHALE_ORS_1	6792.198	6795.439
05103094620000	SHALE_ORS_1	6790.974	6793.238
05103089180000	SHALE_ORS_1	6673.629	6677.333
05103088260000	SHALE_ORS_1	6393.527	6396.305
05103087150000	SHALE_ORS_1	6225.124	6228.1
05103089330000	SHALE_ORS_1	6285.938	6289.616
05045062970000	SHALE_ORS_1	5758.359	5761.776
05045064510000	SHALE_ORS_1	6414.943	6420.408
05045063940000	SHALE_ORS_1	5769.898	5774.615
05045063710000	SHALE_ORS_1	7460.87	7465.823

APINUM	PAY NAME	TOPMD	BASEMD
05045063090000	SHALE_ORS_1	6619.347	6622.276
05045061250000	SHALE_ORS_1	5994.04	5999.993
05045063560000	SHALE_ORS_1	6673.537	6676.284
05045063560000	SHALE_ORS_1	6680.405	6684.526
05045071870000	SHALE_ORS_1	6542.853	6545.6
05045071870000	SHALE_ORS_1	6546.973	6549.263
05045061210000	SHALE_ORS_1	3988.15	3996.391
05045069470000	SHALE_ORS_1	4303.859	4306.102
05045069470000	SHALE_ORS_1	4307.447	4309.689
05045061520000	SHALE_ORS_1	3439.201	3446.527
05077085150000	SHALE_ORS_1	2211.799	2218.209
43019950050000	SHALE_ORS_1	1444.659	1451.128
05103103430000	SHALE_ORS_1	7037	7039
4301930731	SHALE_ORS_1	3341.067	3345.462
4301930784	SHALE_ORS_1	3317.321	3322.78
43047349220000	SHALE_ORS_1	10058.291	10068.342
43047351400000	SHALE_ORS_1	10495.915	10499.489
43047350540000	SHALE_ORS_1	9813.036	9816.099
43047350540000	SHALE_ORS_1	9811.504	9816.099
4301931397	SHALE_ORS_1	7346.477	7353.541
43047301110000	SHALE_PAY_2	15331.366	15334.165
43047301450000	SHALE_PAY_2	14700.87	14703.668
43007300490001	SHALE_PAY_2	12820.195	12824.021
43047316740000	SHALE_PAY_2	7711.895	7714.239
43047156720000	SHALE_PAY_2	7821.934	7826.336
43047315970000	SHALE_PAY_2	7157.455	7162.591
43047315100000	SHALE_PAY_2	11529.139	11533.552
43047301430000	SHALE_PAY_2	9403.604	9407.282
43047334450000	SHALE_PAY_2	10445.069	10450.218
43047301650000	SHALE_PAY_2	10487.83	10492.15
43047301680000	SHALE_PAY_2	9901.81	9906.747
43047303860000	SHALE_PAY_2	9303.985	9308.401
43047312310000	SHALE_PAY_2	7983.606	7988.547
43047307880000	SHALE_PAY_2	7576.671	7582.663
43047309600000	SHALE_PAY_2	8592.531	8596.851
43047310630000	SHALE_PAY_2	7906.412	7912.584
43047309760000	SHALE_PAY_2	8032.72	8038.842
43047106920000	SHALE_PAY_2	6760.915	6765.064
43047318940000	SHALE_PAY_2	7213.739	7216.965
43047311370000	SHALE_PAY_2	9203.461	9209.627
43047310710000	SHALE_PAY_2	9348.447	9353.731
43047314960000	SHALE_PAY_2	8175.438	8182.029
43047161980000	SHALE_PAY_2	7840.839	7845.233
43047310430000	SHALE_PAY_2	8053.891	8061.298
43047306180000	SHALE_PAY_2	7813.735	7815.894
43047306180000	SHALE_PAY_2	7825.393	7830.574
43047304480000	SHALE_PAY_2	8090.247	8095.443
43047310120000	SHALE_PAY_2	7990.733	7994.42
43019100890000	SHALE_PAY_2	7180.523	7184.743
43019100890000	SHALE_PAY_2	7170.639	7174.434
43015103740000	SHALE_PAY_2	4398.183	4400.887

APINUM	PAY NAME	TOPMD	BASEMD
43015300220000	SHALE_PAY_2	8013.192	8016.254
43015300800000	SHALE_PAY_2	6961.642	6965.751
43015301980000	SHALE_PAY_2	11873.058	11878.009
43019108060000	SHALE_PAY_2	9339.824	9345.109
43019306530000	SHALE_PAY_2	9236.745	9244.672
43019311480000	SHALE_PAY_2	7763.374	7769.233
43019302400000	SHALE_PAY_2	7074.094	7079.721
43019302400000	SHALE_PAY_2	7066.001	7068.761
43019307040000	SHALE_PAY_2	4902.933	4907.327
43019313180000	SHALE_PAY_2	3536.62	3543.426
43019156730000	SHALE_PAY_2	9329.654	9336.026
43019307060000	SHALE_PAY_2	9041.31	9046.772
43019306820000	SHALE_PAY_2	9284.281	9288.833
43019159350000	SHALE_PAY_2	6707.172	6713.545
43019307080000	SHALE_PAY_2	5041.797	5048.17
43019308950000	SHALE_PAY_2	4570.72	4575.114
43019201540000	SHALE_PAY_2	5855.939	5860.333
43019307730000	SHALE_PAY_2	3918.072	3922.466
43019310140000	SHALE_PAY_2	2244.306	2250.139
43015301990000	SHALE_PAY_2	5851.054	5855.637
43015301130000	SHALE_PAY_2	5618.048	5624.896
43015300140000	SHALE_PAY_2	5605.904	5610.698
43019303980000	SHALE_PAY_2	8433.572	8439.944
43019055910000	SHALE_PAY_2	5154.31	5161.177
43019307720000	SHALE_PAY_2	4363.75	4370.123
43019114330000	SHALE_PAY_2	2595.619	2602.535
43019310690000	SHALE_PAY_2	652.762	659.678
43019310720000	SHALE_PAY_2	664.937	668.826
43015300210000	SHALE_PAY_2	4122.185	4127.663
43019308350000	SHALE_PAY_2	4266	4271
43019110130000	SHALE_PAY_2	5016.302	5020.92
43019308090000	SHALE_PAY_2	6703.23	6709.387
43019308040000	SHALE_PAY_2	5774	5779
43019307340000	SHALE_PAY_2	6842.327	6848.484
43019303230000	SHALE_PAY_2	5733.7	5742.283
43019307320000	SHALE_PAY_2	3813.901	3819.909
43019302550000	SHALE_PAY_2	2241.001	2249.402
43019307560000	SHALE_PAY_2	1720.885	1727.464
43019307680000	SHALE_PAY_2	1608.479	1615.201
43019308680000	SHALE_PAY_2	943.238	954.133
43015301290000	SHALE_PAY_2	2167.957	2173.435
43019311990000	SHALE_PAY_2	2409.051	2413.49
43019308550000	SHALE_PAY_2	2016.306	2020.005
43019308750000	SHALE_PAY_2	1909.703	1913.661
43019308960000	SHALE_PAY_2	1720.985	1723.944
43019308770000	SHALE_PAY_2	1803.009	1809.229
43019311350000	SHALE_PAY_2	937.252	941.857
43019153170000	SHALE_PAY_2	767.327	774.59
43019309160000	SHALE_PAY_2	743.542	750.806
43019309350000	SHALE_PAY_2	915.246	921.148
43019311130000	SHALE_PAY_2	1047.651	1052.191

APINUM	PAY NAME	TOPMD	BASEMD
43019308940000	SHALE_PAY_2	745.129	748.418
43019104580000	SHALE_PAY_2	127.995	132.6
43019300290000	SHALE_PAY_2	1045	1050
43019312450000	SHALE_PAY_2	2738.808	2744.544
43019302150000	SHALE_PAY_2	2674.235	2679.017
43019305420000	SHALE_PAY_2	2467.629	2473.606
43019305010000	SHALE_PAY_2	2502.139	2506.92
43019300700000	SHALE_PAY_2	2458.347	2464.324
43019310220000	SHALE_PAY_2	2112.233	2117.015
43019308630000	SHALE_PAY_2	1285.884	1289.737
43019303280000	SHALE_PAY_2	1236.133	1242.919
43019309180000	SHALE_PAY_2	1469.624	1472.583
05103090220000	SHALE_PAY_2	8096.227	8101.038
05103089200000	SHALE_PAY_2	7400.645	7404.922
05103088640000	SHALE_PAY_2	7429.192	7434.004
05103058400000	SHALE_PAY_2	4328.706	4332.926
05103091780000	SHALE_PAY_2	2772.778	2776.998
05103075130000	SHALE_PAY_2	6719.62	6724.364
05103092790000	SHALE_PAY_2	7332.951	7337.018
05103092680000	SHALE_PAY_2	6484.157	6490.487
05103098000000	SHALE_PAY_2	6029.784	6035.653
05103100180000	SHALE_PAY_2	7175.733	7180.868
05103099850000	SHALE_PAY_2	6701.177	6706.803
05103100090000	SHALE_PAY_2	6463.2	6468.623
05103092760000	SHALE_PAY_2	6263.663	6267.179
05103096230000	SHALE_PAY_2	6567.986	6571.375
05103096240000	SHALE_PAY_2	6736.521	6743.977
05103092130000	SHALE_PAY_2	7884.71	7888.331
05103099920000	SHALE_PAY_2	6631.357	6635.759
05103100250000	SHALE_PAY_2	6676.688	6681.824
05103094620000	SHALE_PAY_2	6678.094	6683.23
05103089180000	SHALE_PAY_2	6563.061	6567.285
05103088260000	SHALE_PAY_2	6304.47	6308.091
05103087150000	SHALE_PAY_2	6119.876	6124.817
05103089330000	SHALE_PAY_2	6183.018	6188.665
05045062970000	SHALE_PAY_2	5659.612	5663.847
05045064510000	SHALE_PAY_2	6318.605	6322.84
05045063940000	SHALE_PAY_2	5654.648	5657.751
05045063710000	SHALE_PAY_2	7350.319	7354.006
05045061250000	SHALE_PAY_2	5882.218	5886.366
05045063560000	SHALE_PAY_2	6574.066	6577.687
05045071870000	SHALE_PAY_2	6431.441	6437.068
05045061210000	SHALE_PAY_2	3879.7	3884.624
05045069470000	SHALE_PAY_2	4196.884	4202.511
05045061520000	SHALE_PAY_2	3342.72	3349.526
05077085150000	SHALE_PAY_2	2113.978	2118.839
43019950050000	SHALE_PAY_2	1360.122	1364.561
05103103430000	SHALE_PAY_2	6923.932	6928.677
43019307310000	SHALE_PAY_2	3240.565	3245.944
43019307840000	SHALE_PAY_2	3214.533	3220.68
43047349220000	SHALE_PAY_2	9943.934	9949.083

APINUM	PAY NAME	TOPMD	BASEMD
43047350540000	SHALE_PAY_2	9686.241	9690.654
43019313970000	SHALE_PAY_2	7235.745	7242.336
43019159350000	UPPER_CS_46	6919.297	6923.849
43019307080000	UPPER_CS_46	5193.894	5198.446
43019055910000	UPPER_CS_46	5352.577	5359.443
43019307720000	UPPER_CS_46	4568.592	4572.234
43019114330000	UPPER_CS_46	2786.964	2791.575
43019310690000	UPPER_CS_46	850.255	855.634
43019100840000	UPPER_CS_46	6157.519	6164.933
43019307320000	UPPER_CS_46	4011.309	4019.892
43019153170000	UPPER_CS_46	990.158	996.291
43019305420000	UPPER_CS_46	2704.307	2715.066
43019300700000	UPPER_CS_46	2684.267	2689.048
43019310220000	UPPER_CS_46	2330.981	2340.544
43019307310000	UPPER_CS_46	3435.753	3441.132
43019307840000	UPPER_CS_46	3415.868	3420.479